universität wien

MASTERARBEIT

Titel der Masterarbeit

„Characterization of immune cell populations in ascites from patients with serous epithelial ovarian cancer“

verfasst von

Nyamdelger Sukhbaatar, BSc

angestrebter akademischer Grad

Master of Science (MSc)

Wien, 2015

Studienkennzahl lt. Studienblatt:	A 066834
Studienrichtung lt. Studienblatt:	Masterstudium Molekulare Biologie
Betreut von:	Univ.-Prof. Robert Zeillinger, Ph.D

I dedicate my master thesis to my parents, my husband and to my beloved daughter Amanda.

Table of Contents

Table of figures

Part I

Part II

List of tables

Abbreviations

APC	Antigen presenting cells
BCA-1	B cell attracting chemokine 1
BRCA (1, 2)	breast cancer (1, 2)
BSA	bovine serum albumin
CA125	cancer antigen 125
CAF	cancer-associated fibroblasts
CK	cytokeratin
CLPs	common lymphoid progenitors
CMP	common myeloid progenitors
CSF-1	colony-stimulating factor
CTACK	cutaneous T-cell-attracting chemokine
CTL	cytotoxic T lymphocytes
DCs	dendritic cells
ddPCR	digital droplet PCR
DMEM	Dulbecco’s modified eagle medium
DMSO	dimethylsulfoxide
DTT	dithiothreitol
ENA-78	epithelial-derived neutrophil-activating peptide 78
EDTA	ethylenediaminetetraacetic acid
EGF	epithelial growth factor
EGFR	epidermal growth factor receptor
EOC	epithelial ovarian cancers
EpCAM	epithelial cell surface marker
FACS	fluorescence-activated cell sorting
FCS	fetal calf serum
FDR	false discovery rate
FFPE	formalin-fixed paraffin-embedded
FGF-basic	basic fibroblast growth factor
FIGO	International Federation of Gynecologists and Obstetricians
G-CSF	granulocyte-colony stimulating factor
GCP-2	granulocyte chemotactic protein 2
GM-CSF	granulocyte-macrophage colony-stimulating factor

GMPs	granulocyte-macrophage progenitors
GSEA	gene set enrichment analysis
HEPES	4-(2-hydroxyethyl)-1-piperazineethanesulfonic acid
HER2	human epidermal growth factor receptor 2
HGF	hepatocyte growth factor
HGSOC	high grade serious ovarian cancers
HIER	heat-induced epitope retrieval
HIF-1	hypoxia-inducible factor 1
HLA-DR	human leukocyte antigens DR
HSCs	hematopoietic stem cells
IARC	International Agency for Research on Cancer
ICAM-1	intercellular adhesion molecule 1
IF	immunofluorescence
IFN-γ	interferon γ
IGF-2	insulin-like growth factor 2
IHC	immunohistochemistry
IL (2, 4, 6, 8, 10, 16)	interleukin (2, 4, 6, 8, 10, 16)
IP-10	Interferon gamma-induced protein 10
I-TAC	interferon-inducible T-cell alpha chemoattractant
MCP (1-4)	monocyte chemoattractant protein (1-4)
M-CSF	macrophage colony-stimulating factor
MDC	macrophage-derived chemokine
mDC	myeloid DCs
MEPs	megakaryocyte/erythrocyte progenitors
MIF	macrophage migration inhibitory factor
MIG	monocyte/macrophage-activating IFN-γ-inducible protein
MIP (1α, 1β, 3α, 3β)	macrophage inflammatory protein (1α, 1β, 3α, 3β)
MPIF-1	myeloid progenitor inhibitory factor 1
MPPs	multipotent progenitors
NK	natural killer cells
NKT	natural killer T cells
PBS	phosphate-buffered saline
PBS-T	phosphate-buffered saline with 0.1% Tween
PCA	principal component analysis

pDC	plasmacytoid DCs
PDGF	platelet derived growth factor
PECAM-1	platelet endothelial cell adhesion molecule 1
PMN	polymorphonuclear leukocytes
QuSAGE	quantitative set analysis of gene expression
RO	reactive oxygens
RT	room temperature
SCF	stem cell factor
SCYB16	small inducible cytokine subfamily B member 16
SDF-1α+β	stromal cell-derived factor 1
sIL-6Rα	soluble interleukin-6 receptor α
SOC	serous ovarian carcinoma
sTIE-2	soluble angiopoietin receptor 2
sVEGFR (1, 2)	soluble vascular endothelial growth factor receptor (1, 2)
TAMs	tumor-associated macrophages
TARC	thymus and activation regulated chemokine
TECK	thymus-expressed chemokine
TILs	tumor infiltrating lymphocytes
TLR	toll-like receptor
TNF-α	tumor necrosis factor α
TP53	tumor protein 53
Treg	regulatory T cells
VEGF	vascular endothelial growth factor
VCAM-1	vascular adhesion molecule 1
6Ckine	secondary lymphoid chemokine

Introduction

Among all cancers in women, ovarian cancer is the seventh most common cancer with estimated 238,719 incidences worldwide and the eighth leading cause of death with a high mortality rate of 4.3% per 100,000 women, according to the statistics of 2012 [1-4].

The risks of developing ovarian cancer increase with advanced age, number of ovulatory cycles, and family history of ovarian, breast or colon cancer. Also, germ line mutations of breast cancer 1 (BRCA1), breast cancer 2 (BRCA2) and tumor protein 53 (TP53) genes were shown to be common causes for hereditary ovarian cancers [5, 6].

Diagnosis of ovarian cancer relies on pelvic examination, transvaginal ultrasound analysis and serum cancer antigen 125 (CA125) concentration, which is increased in 80% of ovarian cancers [5-7]. However, it is not a reliable marker, because in low stage ovarian cancers CA125 concentration is shown not to be raised sufficiently for detection and therefore the sensitivity and specificity is low [6, 8].

The first line standard therapy of ovarian cancer consists of a combination of surgery and platinium based chemotherapy with carboplatin and/or paclitaxel [9, 10]. New therapy options with different chemotherapeutic agents, targeted drugs against BRCA and novel agents against molecular pathways involved in ovarian cancer, such as human epidermal growth factor receptor 2 **(**HER2) signaling, have been investigated [11, 12]. However, current clinical trials and new screening methods did not deliver sufficient success or failed [6, 8]. In addition, more than 75% of the patients are diagnosed at an advanced stage of the disease and in about 80% of the cases, tumor relapse occur, which is also associated with high platinum resistance [6, 13]. Thereby, reliable molecular markers for early detection would be beneficial for the cure from this malignancy.

The distinct feature of ovarian cancer is that metastatic spread of ovarian cancer is mostly restricted to the peritoneal cavity accompanied mostly by formation of excessive ascitic fluid in the peritoneal cavity. Formation of ascites is highly associated with disease progression and poor patient prognosis [6]. Ascites creates a very unique tumor microenvironment, which represents a “homing site” for disseminated tumor cells in the peritoneal cavity. Hence, it is supposed to enable not only an efficient and fast tumor spread, but also provides an appropriate milieu for

tumor cells to escape the immune system. Ascites is known to contain various immune cells and immune-modulating agents, such as cytokines and growth factors that create cancer associated inflammatory networks [5, 14].

Ovarian cancer

Ovarian cancer and its classification

Based on grade of differentiation, benign, borderline and malignant tumors are distinguished [11]. Borderline tumors of low-malignancy contain morphologically and molecular partially transformed epithelial cells [6]. During malignancy, epithelial cells differentiate into various structure types with more complex characteristics, which is the basis for different histologically and other classifications [10].

According to histological features and molecular and genetic profiles, different subtypes of ovarian cancer can be differentiated: i) serious ovarian cancer, which resembles epithelial cells from the normal fallopian tube, ii) endometrioid resembles endometrium, iii) mucinous resembles mucin-secreting endocervical glands and iv) clear carcinoma, which resembles vaginal clear cells [2, 6, 11, 15].

Approximately 90% of malignant ovarian tumors are of epithelial origin [6]. 80% of epithelial ovarian cancers are diagnosed as high grade serious ovarian cancers (HGSOC), which is the most common ovarian cancer type [10, 11]. Furthermore, serious ovarian cancers are also classified into low grade serous ovarian cancer (LGSOC), which differ from HGSOC, due to differences in epidemiology, pattern of spread, response to chemotherapy and prognosis [11].

Based on histological grade, as well as molecular phenotype and genotype, comprising genetic stability and mutational frequencies, two groups of epithelial ovarian cancers (EOC) can be distinguished [16, 17]. Type I low grade cancers comprises all low grade histological subtypes and can be characterized by low growth and wild-type TP53 and BRCA1/2. Type II high grade cancers show aggressive growth, mutations of TP53 in high frequency (over 90%) and are mostly high grade cancers of serous, endometrioid or undifferentiated histotypes [6]. 10-15% of ovarian cancers show germline BRCA1/2 mutation, whereas 23% of high grade serous cancers show somatic BRCA1/2 mutations. However, this classification is regarded as too simplified [18].

According to the International Federation of Gynecologists and Obstetricians (FIGO) a four staging system is developed based on tumor spread [2]. The main stages and their features are summarized in table 1 [19].

Stage	Definition
I	Tumor l to ovaries or fallopian tube(s).
IA	Tumor limited to one ovary (capsule intact) or fallopian tube; no tumor on ovarian or fallopian tube surface; no malignant cells in the ascites or peritoneal washings.
IB	Tumor limited to both ovaries (capsules intact) or fallopian tubes; no tumor on ovarian or fallopian tube surface; no malignant cells in the ascites or peritoneal washings.
IC	Tumor limited to one or both ovaries or fallopian tubes, with any of the following:
	IC1: Surgical spill intraoperatively.
	IC2: Capsule ruptured before surgery or tumor on ovarian or fallopian tube surface.
	IC3: Malignant cells present in the ascites or peritoneal washings.
II	Tumor involves one or both ovaries or fallopian tubes with pelvic extension (below pelvic brim) or peritoneal cancer (Tp).
IIA	Extension and/or implants on the uterus and/or fallopian tubes and/or ovaries.
IIB	Extension to other pelvic intraperitoneal tissues.
III	Tumor involves one or both ovaries, or fallopian tubes, or primary peritoneal cancer, with cytologically or histologically confirmed spread to the peritoneum outside of the pelvis and/or metastasis to the retroperitoneal lymph nodes.
IIIA	Metastasis to the retroperitoneal lymph nodes with or without microscopic peritoneal involvement beyond the pelvis.
IIIAi	Positive retroperitoneal lymph nodes only (cytologically or histologically proven).
IIIAii	Metastasis >10 mm in greatest dimension.
IIIA2	Microscopic extrapelvic (above the pelvic brim) peritoneal involvement with or without positive retroperitoneal lymph nodes.
IIIB	Macroscopic peritoneal metastases beyond the pelvic brim ≤2 cm in greatest dimension, with or without metastasis to the retroperitoneal lymph nodes.
IIIC	Macroscopic peritoneal metastases beyond the pelvic brim >2 cm in greatest dimension, with or without metastases to the retroperitoneal nodes
IV	Distant metastasis excluding peritoneal metastases.
IVA	Pleural effusion with positive cytology.
IVB	Metastases to extra-abdominal organs (including inguinal lymph nodes and lymph nodes outside of the abdominal cavity

Table 1: FIGO staging according to data from 2014 (Table is adapted from [19]).

In addition, ovarian tumors are classified according to grade: well differentiated (grade I), moderately differentiated (grade II) and poorly differentiated (grade III) [20]. Several molecular subtyping attempts have been published [21-23]. Among them were: i) two different molecular subgroups of high-grade serous ovarian cancers could be identified based on gene expression profiling reflecting ovarian tumor progression and prognosis [21]. ii) mRNA and miRNA expression analysis provided differentiation of four serous ovarian carcinoma subtypes; referred to as “immunoreactive”, “differentiated”, “proliferative” and “mesenchymal” subtypes [22].

Although a considerable effort was made to classify, and thereby to obtain better prognosis, prediction and therapy options for ovarian cancer, it is still a challenge to understand distinct features and mechanisms of this disease.

Origin of epithelial ovarian cancer

The origin of EOC is discussed controversially [24, 25]. Normal ovary consists of three major cell types; i) germ cells, which proliferate and differentiate into oocytes, ii) endocrine or intestinal cells, which produce estrogen and progesterone and iii) columnar ovarian surface epithelial cells also called ovarian mesothelium [10]. Inclusion cysts lined with epithelial cells lie immediately beneath the ovarian surface. Inclusion cysts are suggested to be separated from the ovarian epithelium at the time of ovulation near ruptured follicles [10]. Because epithelial cells are exposed to repetitive ovulations with iterative rupture and repair, they have more potential to be affected by genetic aberrations than other cell types. Therefore, EOC types are thought to be derived from flattened ovarian surface epithelial cells [6]. Interestingly, they show both epithelial and mesenchymal characteristics, including classical epithelial features such as desmosomes and keratin expression, but also are able to produce mesenchymal typical intermediate filaments such as vimentin and N-cadherin [10, 26]. However, the ovarian epithelium does not show features of typical epithelial differentiation, such as expression of E-cadherin and CA125 [26]. Furthermore, distal fallopian tube is also considered as the origin of serious ovarian cancer [24, 27]. Fallopian tube is the connection between ovaries and uterus. SOC is supposed to arise from pre-malignant lesions (called Serous Tubal Intraepithelial Carcinoma, STIC) in the epithelium of distal fallopian tube (Fig. 1) [26, 28].

Metastatic spread of epithelial ovarian cancer

Most of EOC patients are diagnosed at a very late stage of the disease, which is characterized by high metastatic tumor load, mostly restricted to the peritoneal cavity (Fig. 1). This suggests that EOC tumors spread out rapidly to metastasize primarily on the peritoneum [14].

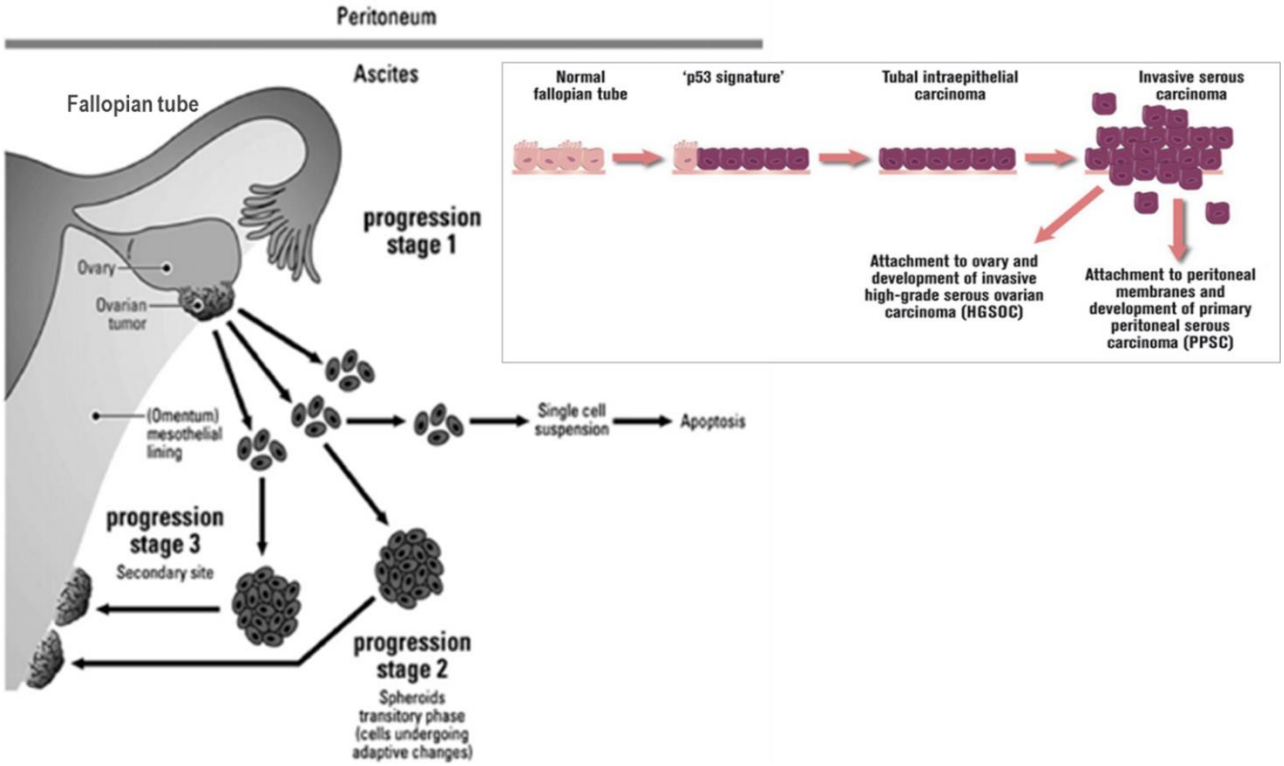

Figure 1: Model of epithelial ovarian cancer development and progression. High grade ovarian cancers originate from the epithelium of ovary and/or fallopian tube epithelium. An illustration of stepwise HGSOC development from fallopian tube is illustrated in the small box above. Spheroids and single tumor cells in ascites are able to spread to the peritoneum to metastasize. (Images are adapted from [29, 30]).

The peritoneum is a large continuous transparent membrane covering abdominal organs. The membrane consists of five layers; i) the outer endothelial cells, which are rich of tight junctions, ii) endothelial basement membrane, iii) a loose connective tissue in interstitial space, iv) submesothelial basement membrane and v) the inner mesothelium [6]. The mesothelium is a single layer epithelium, which is primarily responsible for absorption and secretion from and into the peritoneal cavity [31]. However, mesothelial cells are also able to produce adhesion molecules, such as intercellular adhesion molecule 1 (ICAM-1) and vascular adhesion molecule 1 (VCAM-1), when needed to form anti-adhesive surface, in order to attach leukocytes during inflammation in the peritoneal cavity. Additionally, these cells are considered as an important source of inflammatory cytokines and chemokines. Thus, the mesothelium can provide an effective protection in case of damages and injuries in the peritoneal cavity [6, 31].

Dissemination of tumor cells has been observed to spread mostly either via intra-abdominal or the lymphatic route for metastasizing into the peritoneal cavity [32]. Early peritoneal dissemination of ovarian tumor cells was associated with adhesion of

tumor cells to the mesothelium. Ovarian tumor cells can be characterized by expression of CD44, β-integrins and CA125 on their surface [32, 33]. CD44 is a transmembrane proteoglycan and variety of isoforms are expressed on many different cell types including epithelial cells and lymphocytes [33, 34]. Its expression on epithelial cells mediates cell adhesion and motility [34]. CD44H (hematopoietic) isoform and hyaluronic acid mediated attachment of tumor cells on mesothelium was reported [33]. Mesothelial cells express hyaluronic acid, which serves as binding partner for CD44H facilitating the interaction of tumor cells with mesothelial cells [33]. Once attached to the mesothelium tumor cells are able to proliferate and to invade into the mesothelium [32, 35]. Moreover, CD44 expression on lymphocytes is known to regulate lymphocyte homing [33].

In the peritoneal cavity, omentum, diaphragm and pelvis are the primary metastatic sites of HGSOC [5]. Part of the peritoneal membrane covering the abdominal organs, called omentum consists of a triple-layer comprising mesothelium, a loose network of connective tissue and endothelium. The omentum is rich in lymphatic tissues. The main function of the omentum is regulating fluid transport, sustaining immunity in the peritoneal cavity, storing and supplying lipids [36]. A large part of the omentum consists of adipose tissues, which are abundant with blood and lymph vessels and milky spots. Milky spots on omentum are responsible for immune defense in the peritoneal cavity [37]. They consist mainly of stromal cells and facilitate transmigration of immune cells to maintain immune protection in the peritoneal cavity [36]. Normally, in resting condition, few milky spots are present. However, the number of milky spots in adipose tissue has been shown to enhance dramatically with occurrence of disseminating cancer cells in the peritoneal cavity. Increased appearance of milky spots was also correlated with enhanced metastatic spread in the peritoneum and they are seen as target of disseminating tumor cells [36, 38]. In addition, they are thought to play a major role in proliferation and invasion of cancer cells [36]. On the contrary, adipocyte tissue cells of omentum seem to promote tumor cell migration and growth by providing cells with fatty acids [36, 39].

Ascites formation in EOC

HGSOC is highly associated with production of ascites in the peritoneal cavity. Tumor cells are mostly observed to float either as single cells or as spheroids in the ascites through the peritoneal cavity. Ascites is assumed to promote the metastasizing process on the mesothelium [5, 14].

Lymphatic tissues in the peritoneum are responsible for fluid circulation between the peritoneal surface, the submesothelial lymphatics and the vasculare [5]. Under physiological conditions, small fluid production and reabsorption allow a low osmotic pressure across the peritoneal membrane, exerted by proteins and macromolecules, since it is a semipermeable membrane [35]. In EOC patients with malignancies however, this balance is disrupted due to increased generation of micro vessels in the omentum that line the peritoneal cavity. This structure is thought to allow ascites formation via increasing fluid infiltration through the membrane [40]. Additionally, increased protein concentration assists in altering the peritoneal membrane permeability [35]. Overexpression of vascular endothelial growth factor (VEGF) from ovarian carcinoma cells was found to be accumulated selectively in malignant ascites and was involved in altering the permeability of the peritoneal membrane to induce ascites formation [35, 41, 42]. However, in mouse models ascites accumulation could be triggered in the absence of a tumor. Furthermore, massive lymphatic blockage preventing fluid outflow into the peritoneal cavity and resulting ascites fluid accumulation is supposed to passively facilitate migration of disseminating tumor cells through the peritoneal cavity [35, 40]. The combination of changed vascular permeability with lymphatic obstruction and activated mesothelial cells are the main contributing factors for ascites accumulation [43]. Ascites provides a source of many different cell populations and a wide variety of immunomodulatory factors secreted by tumor and immune cells. Not only high numbers of tumor and immune cells, but also other cell populations e.g. activated mesothelial cells, endothelial cells and cancer-associated fibroblasts (CAFs) are present in ascites. Thus, ascites creates a microenvironment facilitating interaction of various cell types and therefore actively involved in cancer development and progression.

Immune system in cancer

Cancer related inflammation

Tumor is surrounded by a microenvironment such as stroma, which creates a complex network of diverse cell components and molecular factors. This network enables communication between different cells and immune modulators to provide a dynamic environment determining tumor progression [41].

Predominant cell populations in the tumor microenvironment are epithelial, endothelial, mesothelial cells and fibroblasts, but the most abundant populations in

the tumor microenvironment are cells of hematopoietic origin (Fig. 2) [41, 44]. A main feature of cancer related inflammation is a high number of leukocyte infiltration into the tumor microenvironment, which reflects inflammatory condition at the tumor site [44-46]. Tumor associated inflammation is referred to as “smoldering inflammation” or “non-resolving inflammation”, which adapts enduring chronic inflammation with retaining immune cells and inflammatory mediators [47]. Tumor associated inflammation is thought to be caused either by extrinsic conditions, such as stimulated inflammatory responses or by intrinsic factors, such as genetic instability driven by mutated oncogenes or tumor suppressor genes [47, 48].

Under physiological conditions immune cells are recruited in response to locally synthesized inflammatory mediators. They are involved in wound healing, inflammation and pathogen elimination [46]. In a malignant tumor, similar inflammatory factors seem to be involved in accumulation of a high number of tumor infiltrating lymphocytes (TILs) [46]. This in turn, is associated with inflammation triggered by inflammatory mediators, such as cytokines, chemokines and growth factors, produced by tumor infiltrating lymphocytes [45].

In the past, the predominating immunosurveillance hypothesis implied that highly infiltrating leukocyte populations represented a strong evidence of an antitumor immune response. However, tumors seem to process and modulate their microenvironment and the resulting tumor and immune cells maintain a tumor supporting milieu [44]. Immune cells are able to recognize and eliminate tumor cells at the early stage of tumor development. However, with tumor progression, the balance between immunosurveillance and tumor growth can shift toward immune cell escape of tumor cell [44, 49]. According to the hypothesis of immunoediting, tumor cells undergo a clonal selection favoring less immunogenic cells and those able to edit its environment and to avoid anti-tumorigenic immune responses. The immunoediting is observed in almost all tumors [50]. Therefore, the tumor promoting inflammation and avoiding immune destruction were added to the next generation of seventh hallmarks of cancer [51, 52].

Immune cell components of innate and adaptive immunity in cancer

The tumor microenvironment contains both innate and adaptive immune cells, which are shown to play both positive and negative roles in tumor initiation and progression [41, 53]. The dynamic crosstalk between tumor cells and immune cells contributes to every stage of tumor development and progression including proliferation, survival of

malignant cancer cells, angiogenesis and metastasis [47, 48, 54]. One of the most vigorous leukocytes in the tumor microenvironment is **T lymphocytes** [46, 55]. T lymphocytes participate both in tumor control and tumor promotion determined by their effector functions [55].

In general, tumor cells express antigens, which can be recognized by $CD8^+$ cytotoxic T lymphocytes (CTL) and can be killed by them. CTLs are therefore considered as primary mediators of anti-tumor responses [55, 56]. However, high levels of **$CD8^+$ CTL** accumulation have been shown to be involved in promoting immunologic tolerance via recruiting naïve T cells, under chronic inflammatory condition. Attraction of inactivated naïve T cells without antigen presentation, in combination with immature dendritic cells (DCs) was commonly observed in the tumor microenvironment and associated with immunosuppressive responses [55].

$CD4^+$ T cell are capable of killing tumor cells either by activating $CD8^+$ CTL or other immune cells via production of stimulatory cytokines, such as tumor necrosis factor α (TNF-α), interleukin (IL-2), interferon γ (IFN-γ) or macrophage-derived chemokines [44, 55]. After activation by antigen presenting cells (APC), mature $CD4^+$T lymphocytes differentiate into several subtypes of effector T cells, including Th1, Th2, Th17, follicular helper T cells and regulatory T cells (Treg), as well as natural killer T (NKT) cells [44]. A high number of $CD4^+$ T cells at the tumor site was described to induce accumulation of leukocytes, specifically neutrophils and macrophages into premalignant tumor site and to contribute to the formation of a chronic inflammatory microenvironment [41, 46]. However, different phenotypes of $CD4^+$ T cells exert distinct effects on both tumor promotion and tumor suppression. Upon Th1 activation, major cytokines and chemokines are released from $CD4^+$ cells to induce immune responses, such as antigen presentation, cytotoxicity, phagocytosis, and naïve T cell activation, mediated by macrophages and DCs [57]. Natural killer cells (**NK**) cells are main components of the proinflammatory Th1 signature involved in tumor immunosurveillance. Although, NK cells are reported to infiltrate relatively infrequently in tumors, their presence is mostly correlated with good prognosis in different tumor types [58].

Another important $CD4^+$ T cell population in tumor microenvironment is **Tregs**. The natural role of Treg cells is to protect cells against autoimmune reactions by suppressing effector T cell action [49]. In tumors, Tregs participate mainly in immune escape [44, 50, 56].

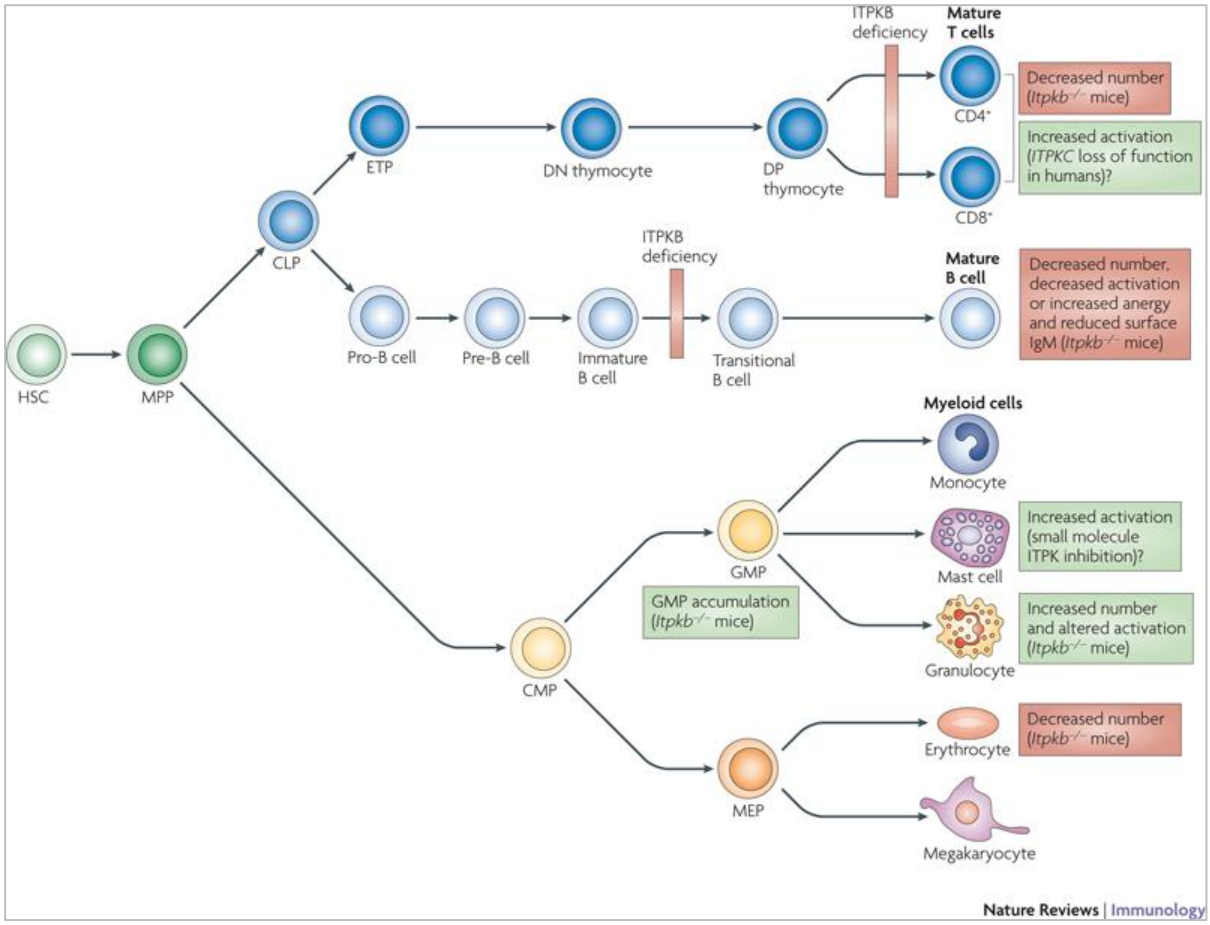

Figure 2: Hematopoietic stem cells and progenitor cells. Multipotent hematopoietic stem cells (HSCs) can give rise to multipotent progenitors (MPPs), which further initiates either common lymphoid progenitors (CLPs) or common myeloid progenitors (CMP), followed by development of granulocyte-macrophage progenitors (GMPs) and megakaryocyte/erythrocyte progenitors (MEPs). GMPs are specified progenitors of the myeloid cell lineage, including monocytes, mast cells and granulocytes. (Image adapted from [59]).

A main component of the adaptive immune system is **B cells**. One of the important role of B cells under physiological condition is to present processed antigens efficiently to antigen-specific $CD4^+$ T cells [60], [61]. B lymphocytes and mast cells seem to be rather important contributors of immune-mediated tumor growth [44, 53]. B cells are reported to promote $CD8^+$ T cell mediated antitumor immunity and therefore associated mostly with good patient prognosis [62].

Although granulocytes also called **polymorphonuclear leukocytes** (PMN) are the first cells that arrive at the site of inflammation– attracted by cytokines, such as growth regulated peptide (GRO) – they are generally not considered as a major player of cancer related inflammation [58]. In fact, their infiltration seems to be associated with tumor growth, enhanced angiogenesis and invasion [46].

Dendritic cells (DC) are able to detect and present antigens. Thus, they are responsible for activating naïve T cells upon antigen presentation in lymph nodes. Therefore, they provide a link between innate and adaptive immunity [56, 63]. Both plasmacytoid DCs (pDC) and myeloid DCs (mDC) cell lineages are reported to be present in the tumor microenvironment [55]. Mainly, activated through granulocyte-macrophage colony-stimulating factor (GM-CSF) stimulation, DCs are thought to induce antitumor responses due to their ability to activate CTL and T helper cells. At the tumor site, $CD4^+$ T cells recruit DCs and monocytes and activate them through CD40-CD40L interactions [49]. Their role in inducing immune tolerance is also discussed [46] and their behavior in the tumor can be dependent on the tumor microenvironment [64]. However, the exact role of DC population in tumor development is still unknown.

Macrophages are the most abundant immune cell subset of the myeloid lineage in the tumor microenvironment. Conventional macrophages are important APC. They can also act as immunoregulatory cells with their broad chemokine profile. In the tumor microenvironment, subtypes of macrophages perform immunoregulatory functions associated with tumor progression due to their active participation in inducing cancer related inflammation [44, 46]. Macrophages and their development are in the focus of this project and therefore addressed specifically in the next section.

In general, the composition and differentiation of different leukocyte populations in the tumor the microenvironment determines conditions for tumor development.

Immune system in ascites of HGSOC patients

Peritoneal ascites represents a very heterogeneous inflammatory environment comprising various immune cells and immune-modulatory factors [43, 65]. The chronic inflammation should therefore, be one of the most important factors in tumor spread in the peritoneal cavity, which can trigger sustained immune cell recruitment into the surrounding epithelium and increases the risk of malignant transformation [66]. Gene expression profiling of malignant ascites revealed that most abundantly detected myeloid derived cell populations in malignant ascites are monocytes, tumor-associated macrophages (TAMs), T lymphocytes, such as Tregs or Th17 cells, B cells and DCs, but not NK cells [58]. From these, $CD8^+$ CTL and macrophages were the most predominant cell population in ascites [31, 65, 67].

Incessant ovulation is believed to create continuous damage due to rupturing of the ovulating follicle and this causes chronic inflammation due to activation of wound repair mechanisms with increased epithelial cell proliferation in the peritoneal cavity [68]. This seems to be the underlying cause for DNA damage, release of reactive oxygens (RO), production of various cytokines and therefore, one of the driving forces in ovarian cancer progression [56]. Various immune cell accumulations in ascites were reported to efficiently support escape of tumor cells from immunosurveillance effectively [31]. The omentum with milky spots, that basically facilitates intact homeostasis are revealed to be involved particularly in the proliferation and growth of tumor cells by attracting high number of immune cells [31, 36, 69]. Therefore, progression of EOC is highly associated with changes in the peritoneal cavity including the immune system profile.

Malignant ascites was shown to contain immunoregulatory factors, such as IL-10, impairing the innate immunity of NK or antigen presentation of DCs and macrophages [70]. In addition, DCs were shown to differentiate to a $CD14^+$ macrophage-like phenotype in ascites. However, their antigen presenting function was inhibited so that they were kept in an immature condition [31, 64]. Moreover, DCs of myeloid origin were reported to produce high concentrations of IFN-γ, which probably is involved in suppressing tumor angiogenesis [31, 56]. Macrophages were found to be the most abundant immune cells in ascites, which secrete immunoregulatory mediators, involved in chronic inflammation in ovarian cancers [71].

Lymphocytes in ovarian carcinomas showed predominantly late activation markers, such as human leukocyte antigens–DR (HLA-DR) [56]. Among T lymphocytes, specifically mature CTL and Treg cells were detected at high levels at primary tumor sites [31, 54, 56]. Interestingly, infiltration of T cells occurred dependent on ICAM-1 and VCAM-1 binding and therefore, the majority of T cells were reported to be accumulated on epithelia [72]. In general, accumulation of high numbers of T cells, including $CD8^+$, $CD4^+$ and Th17 activated cells were correlated with tumor eradication and improved clinical outcome [31, 73], whereas presence of increased number of Treg cells showed controversial results [74, 75]. Although, B cell infiltration mostly correlated with good patient prognosis, in ovarian carcinomas a worse clinical outcome was observed associated with significant high number of $CD19^+$ B lymphocytes and NK cells [76, 77].

Monocytes and macrophages in a tumor

TAMs in tumor

Macrophages are the most frequently found leukocyte population in the tumor microenvironment. Their presence has been shown to be highly associated with tumor progression, angiogenesis, migration, invasion and immune system suppression [54].

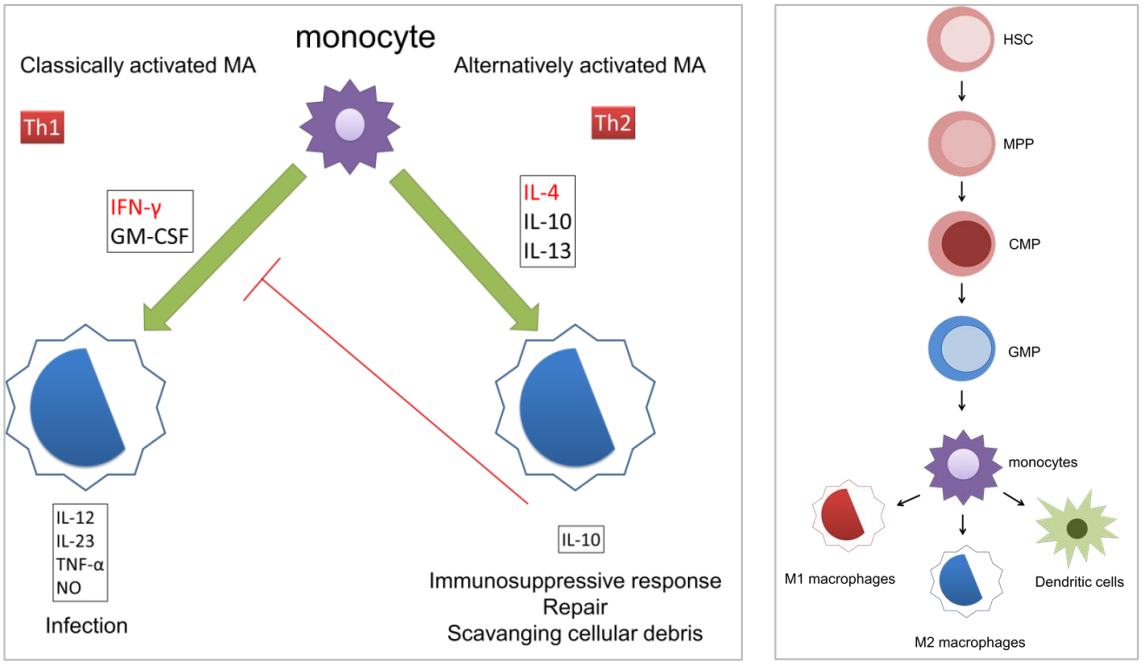

Figure 3: Differentiating subclasses of macrophages. Model of classically and alternatively polarized macrophages illustrates the mechanisms of macrophage differentiation with contributing cytokines and with resulted outcome of the reaction. The red blunt arrow indicates negative inhibition. Because Th1 and Th2 helper cell activations are also involved in regulating macrophage differentiation. The predominant roles of differentially maturated macrophages are presented. The M1 differentiated macrophage causes elevated expression of proinflammatory cytokines, such as IL-1, IL-6, IL12, IL23, TNF-α and nitric oxide to prime antitumor immune reactions [54]. M2 differentiated macrophages express typical anti-inflammatory cytokines, such as IL-10 and scavenger receptor A [44]. Development of monocyte derived cell lineage (right box).

Macrophages carry out a wide range of physiological functions in tissue repair and in immunity [46, 78]. Upon infection, they penetrate into tissue to exhibit their role as APC. Macrophages are able to differentiate into different phagocytic phenotypes [56, 79], dependent on local immune response (Fig. 3) [71].

Classically activated M1 polarized macrophages are typically activated by IFN-γ, GM-CSF and toll-like receptor (TLR) agonists mediated by Th1 helper cell responses. They acquire immune-stimulatory functions and therefore have notable tumor cell

eliminating capacity [55]. On the contrary, alternatively activated M2 polarized macrophages differentiate in response to IL4, IL-10, and IL-13, released mostly by Th2 helper cells. M2 macrophages infiltrate tissue in response to Th2 cell activation and are involved in IL-10 mediated immunosuppression targeting Th1 cell mediated adaptive immunity. They also have poor APC capacity [44, 71, 78].

According to their functional heterogeneity, distinct macrophage subtypes play different roles in tumor progression [80]. Under the condition of cancer related inflammation, monocytes differentiate mostly into TAMs showing both differentiation types, however with more alternatively M2 related phenotype [48]. Gene profiling of TAMs supported the shift of the macrophage phenotype from inflammatory to one which resembles macrophages of developmental origin [81, 82]. Therefore tumor specific TAMs are also referred as tropic M2 activated macrophages. Moreover, monocyte and macrophage lineages in the tumor environment exhibit considerable high plasticity and diversity. One of these heterogeneous TAM populations is characterized by their TIE-2 expression. TIE-2 is an angiopoietin receptor that actively participates in the formation of a pro-tumor inflammatory microenvironment and angiogenesis [47, 78].

Monocyte and macrophage recruitment to the tumor site is regulated via different mechanisms (Fig 4). TAMs have been shown to accumulate excessively in necrotic regions of tumor, where hypoxia dominates. Colony-stimulating factor (CSF-1) and macrophage colony-stimulating factor (M-CSF) are the common macrophage chemoattractants and growth factors, which then induce differentiation of TAMs with tropic M2 polarization. The mechanism of hypoxia mediated TAM accumulation at the tumor site is shown to be markedly dependent on CSF-1 secretion of tumor cells and macrophage feedback with epithelial growth factor (EGF) expression, first observed in *in vivo* tumor models [54, 78, 83]. This interaction between tumor cell and macrophage leads to high macrophage accumulation and is also involved in tumor migration during metastasis (Fig 5) [78].

Functions of monocytes and macrophages in tumor

Consistent with its heterogeneous phenotype, TAMs take over various specific functions in tumor development. They are involved in growth, invasion, metastasis, angiogenesis and immunosuppression in microenvironment [54]. Although there is evidence of a positive association between improved patient outcome and infiltrating macrophage population, high TAM content mostly correlated with poor prognosis in

most of the tumors [54, 84]. At the early stage of tumor initiation, macrophages seem to be actively involved in forming a mutagenic inflammatory environment [47].

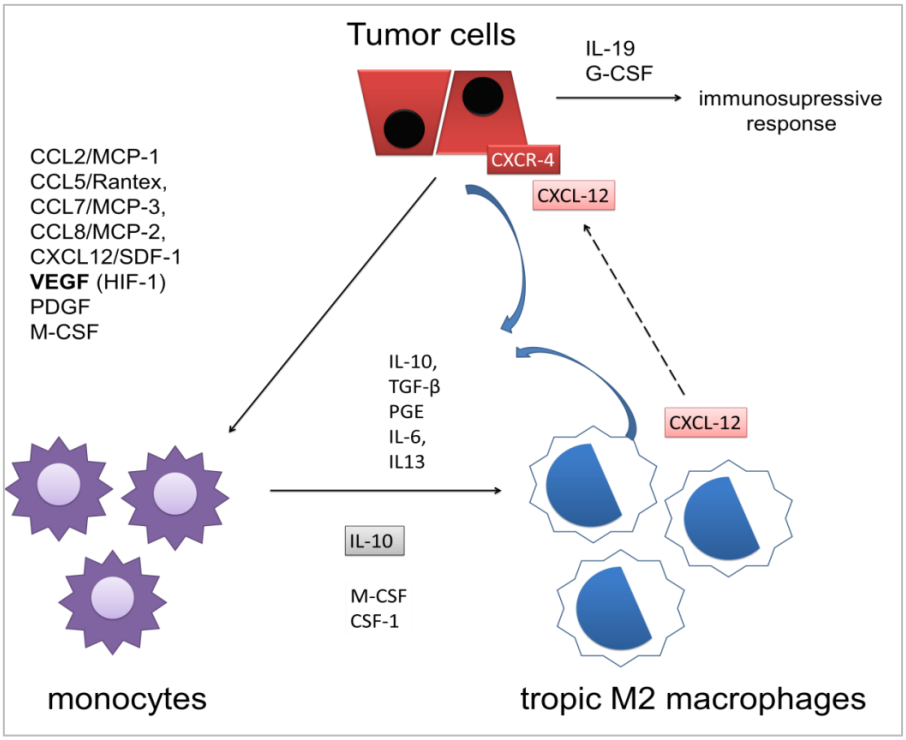

Figure 4: Cytokines and chemokines involved in macrophage recruitment and differentiation regarding to activation of immunosuppressive response. Schematic representation of blood monocyte recruitment to the tumor site mediated by tumor signaling and their differentiation into tropic M2 activated macrophages is shown here. Some prominent monocyte attracting cytokines and chemokines are displayed. Arrows are showing direct regulation pathways, whereas dashed arrow indicates signaling, which results in cell movement. Looping arrows show positive feedback.

Mediated by hypoxia-inducible factor 1 (HIF-1), TAMs are able to induce immunosuppressive response mediated by tumor cells. The function of TAMs as immunosuppressive component in the tumor is demonstrated in different tumor models [55, 71] and shown to be dependent on CXCL12 secretion of TAMs to recruit Treg cells at the tumor site (Fig 5) [85]. TAMs are also able to secrete immunosuppressive cytokines and growth factors e.g. IL-10 and IL-4 [54, 78]. Additional immunosuppression can be promoted by inactivated naïve T cells, which are recruited at high levels in response to IL-10 production by macrophages. Because infiltrating naïve T cells mostly remain without any cytotoxic function, this often results in T cell anergy in the tumor microenvironment [55]. Through the action of IL-10, DC differentiation was reported to be blocked, so that a very efficient immunosuppression in the tumor microenvironment can be reached (Fig 5) [44, 78].

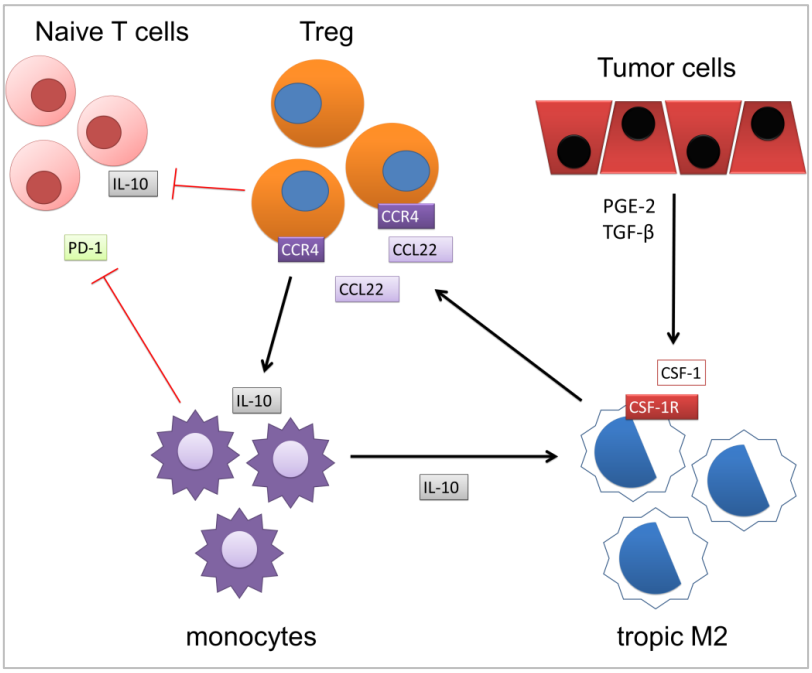

Figure 5: A simplified illustration of immunosuppressive effect of TAMs in tumor microenvironment. Illustrated mechanisms of tumor cell mediated immunosuppression of TAMs are also observed in EOC. Receptors are depicted in dark colored boxes and their interacting chemokines or cytokines in bright colored boxes. Tumor cells are able to secrete CSF-1 to recruit monocytes, which express their receptors CSFR-1. In turn, macrophages produced high level of EGF to interact with tumor cells. In addition, TAMs produce high amount of chemokine CXCL12 in the tumor microenvironment, which binds to its receptor CXCR4, expressed on Treg cells. As a result of this ligand receptor interaction, high amount of Tregs are accumulated in the tumor microenvironment and inhibit cytotoxic T cell response in an IL-10 dependent manner.

TAMs also promote tumor growth and progression through other mechanisms [54, 71, 86]. Large numbers of macrophage accumulation were observed in benign tumor, when tumors start to develop malignant features, suggesting that TAMs are important in early events of tumor progression and metastasis [87]. Recruitment of macrophages based on CSF-1 and EGF signaling has been shown to be crucial for collective migration of tumor cells and macrophages upon metastasizing [54, 88]. Macrophage migration inhibitory factor (MIF) secreted by tumor cells is important to promote TAM associated migration, invasion and angiogenesis by stimulating TAM specific chemokine production, e.g. CCL2 and CCL12 [89]. In advanced tumor stages, TAMs are reported to contribute to vascular remodeling mediated by platelet derived growth factor (PDGF), TNF-α, basic fibroblast growth factor (FGF-basic) and IL-8 (CXCL8) [78, 90, 91].

TAMs in ovarian cancer

The relationship of tumor cells with TAMs was demonstrated to be very interactive, since it was shown that tumor cells were actively involved in macrophage differentiation. In EOC, macrophages were the most dominant population in malignant ascites and were greatly associated with poor patient outcomes [31, 56]. Several studies characterized monocyte and macrophage populations in primary tumors and in malignant ascites, as well as in patient blood samples [92-94]. A variety of monocyte subtypes was identified in ascites and blood, indicating that TAMs represent a most heterogeneous population in ovarian carcinoma. Fluorescence-activated cell sorting (FACS) based quantification analysis of malignant ascites using common monocyte and macrophage markers (CD14, CD16 and CD54) exhibited five phenotypically distinct subpopulations. From these two major subpopulations were prevalent, i.e. $CD14^{++}CD16^{-}$ and $CD14^{++}CD16^{+}$ [92]. These monocyte subtypes were reported to show a high immunosuppressive IL-10 expression signature, less or no cytotoxic activity and were able to suppress proliferation of T cells [94].

Furthermore, ovarian tumor cells were reported to be able to recruit a high number of circulating monocytes from blood into ascites [71]. The majority of circulating monocytes were attracted classically through the action of locally produced chemotactic factors such as CSF-1 or CCL2 [71, 95]. Transported through ascites, monocytes differentiate into TAMs with an immunosuppressive phenotype [71, 89]. TAMs, isolated from tissue and ascites of EOC patients, showed inhibiting effect on T lymphocyte toxicity and stimulation of inhibitory Treg cells *in vitro* [31, 49]. It was also reported that Tregs were attracted to the tumor site via CXCL12– CXCR4, ligand and chemokines receptor, interplay [31, 54, 71, 78].

Another interesting mechanism of immunosuppression has been observed in ovarian carcinoma. A mannose receptor CD206 expressed on surface of TAMs, which normally binds to tumor mucins such as MUC16 or CD125, correlated with high IL-10 expression level. Also a decreased concentration of T cell chemoattractant CCL3 was detected, which apparently caused augmented escape of ovarian tumor cells from NK cell recognition [96].

TAMs were also shown to promote invasiveness and metastasis in ovarian cancer effectively through multiple mechanisms [47, 97]. Macrophages cocultured with human OC cell lines resulted in reinforced migration and invasiveness of tumor cells

in a TNF-α dependent manner [98, 99]. Also, downregulation of MIF led to significantly attenuated macrophage infiltration in ascites. This in turn, led to reduced release of TAM promoting cytokines such as IL-6, TNF-α and increased level of IL-12, which stimulates M1-differentiation [89]. These data about TAMs demonstrated their supporting role in tumor cell invasion and migration [71].

Furthermore, density of macrophages was highly associated with increased angiogenesis [91, 100]. Specifically, high accumulation of macrophages in ascites was shown to promote angiogenesis [101]. Further cell culture experiments suggested that expression of proangiogenic factor, such as VEGF and CXCL8 (IL-8) corresponds to high ascites accumulation [90, 91].

Cytokines and chemokines in a tumor

Cytokines and chemokines and their role in inflammation

Cytokines and chemokines are a group of small molecules, produced by various cells in response to different environmental stimuli. Cells communicate with each other either directly or by production of these chemical mediators. Bound to their receptors on target cells, they can act either in an autocrine manner, affecting the cell that synthesizes the cytokine or in a paracrine manners, directing towards adjacent cells or in an endocrine manner, targeted to distant cells [44, 102].

Cytokines are about 25kDa and mainly secreted by immune cells to regulate the immune system in inflammation and infections [103]. Different types of cytokines are grouped by their structure into the IL-1 family, TNF family cytokines and hematopoietins, as well as type-I-interferons [63, 102].

Chemokines, also termed as chemoattractants or chemoattractant cytokines, are 8-10 kDa small proteins and represents a subgroup of cytokines. According to their role, ‘‘homeostatic’’ and ‘‘inflammatory’’ chemokines can be distinguished. Homeostatic chemokines are involved in controlling leukocyte homing and lymphocyte recirculation in normal conditions, whereas inflammatory chemokines are released mainly in response to inflammatory stimuli [58, 104]. Synthesized by distinct cells in response to pathogenic or inflammatory stimuli, they create a chemical gradient of a ligand and cause directed migration of leukocytes along this gradient. The migration of the leukocytes is based also on chemokine and ligand receptor interactions, which mediates directed movements of cells [41]. Today, about 50 human chemokines are known and they are classified into four highly conserved

groups of chemokines - CXC, CC, C and CX3C chemokines– based on the position of the first two cysteines that are located adjacent to the amino terminus (Fig 6) [105]. The receptors of chemokines are mainly G-protein coupled receptors. Expression profiling of chemokine receptors can be used to determine their corresponding ligands by its lineage and differentiation stage. This can provide information concerning presence of inflammation or hypoxia (Fig 6) [41].

In inflammation, most common cytokines IL-6, IL-1β, IL-12 and TNF-α are produced initially by antigen presenting DCs and macrophages to mediate naïve T cell activation and to recruit monocytes and neutrophils into the tissue. This movement of monocytes and neutrophils is mainly induced by the action of monocyte – and neutrophil attractants, such as CCL2 or CXCL8, released by macrophages ([63, 107]. Dependent on the signals they receive, monocytes differentiate into various macrophage subtypes or into DCs mediated by cytokines such as CSF-1, M-CSF or GM-CSF and IL-4 [63, 108]. An important cytokine at the inflammation site is TNF-α, which stimulates endothelial cells to secrete adhesion molecules to support migration and penetration of immune cells into the tissue [63].

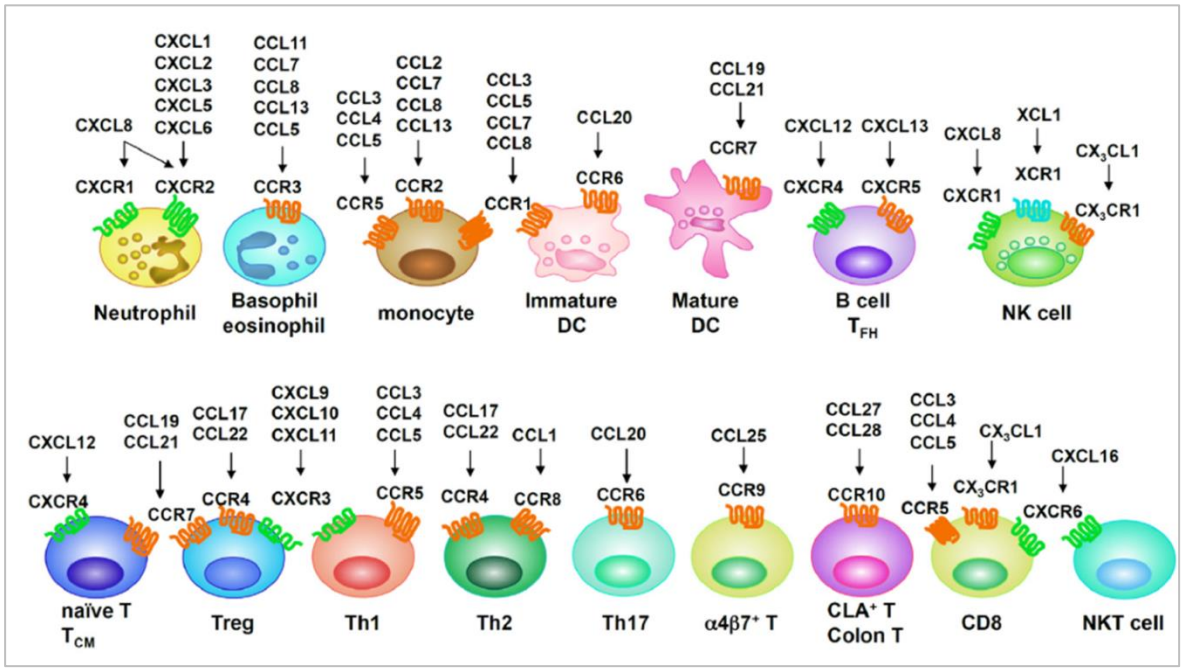

Figure 6: Major CC-, CXCL- and CX3CL chemokines and their corresponding receptors on leukocyte populations. Chemokines are released to attract variety of leukocytes and other cells expressing their respective receptors. (Illustration adapted from [106]).

Diversity of cytokines, chemokines and growth factors in tumor

The balance between positive and negative immune response is largely regulated by communication of immune cells through cytokines and chemokine. Not only the presence of inflammatory cells, but also modulation of inflammatory mediators showed a link to cancer related inflammation [47]. Chronic inflammation emergence in the tumor microenvironment is affected by cytokines first, released from immune cells, which in turn induces production of chemokines from malignant and stromal cells to attract further immune cells to the tumor site. This circulation of cytokines mostly reinforces the maintenance of cancer related inflammation to promote tumor growth, metastasis and angiogenesis [109].

Under persistent inflammatory conditions, such as smoldering inflammation in tumor, the regulation of chemokine effector function is disturbed in response to diverse signals. In cancer, epithelial cells were found to have lost their positional identity due to mutational alterations and to secrete chemokines continuously that recruits leukocytes for supporting tumor progression [110]. Therefore, in the tumor microenvironment, these factors are major drivers of tumor progression produced by tumor, stromal and immune cells [41, 44].

The complex chemokine network can be characteristic for a cancer type, because it determines the extent and phenotype of infiltrating cells in the tumor microenvironment. Thus, the cytokine and chemokine network together can affect spread of cancer and the state of malignancy [41, 111].

Tumor cells, stromal cells and macrophages are considered as main source of chemokines, which stimulates accumulation of leukocytes in the tumor microenvironemnt. CAFs and mast cells were also demonstrated to be essential chemokine providing populations [44]. Increased infiltration of these cells mostly contributes to antitumor responses. The majority of the determinants of macrophage and monocyte migration are CC chemokines, which were shown to be continuously produced by both tumor and stromal cells and predominantly involved in Th2 mediated responses [41, 58]. However, most of the cytokines and chemokine were reported to affect immune cell response negatively, resulting in a favorable condition for tumor growth and progression.

Growth factors or fate-determining factors are mostly polypeptides, which act on their single-pass transmembrane receptors to stimulate intracellular tyrosine kinase activity of different signaling pathways. As a consequence of this signal cascade

extracellular signaling pathways are activated which are responsible for tissue homeostasis [112]. However, many growth factors are secreted in tumors for activating sustained proliferation and growth. Therefore, they are seen as regulators of all subsequent steps of tumor progression including clonal expansion, invasion, migration and angiogenesis [112, 113].

Role of cytokines and chemokines in tumor progression

Cytokine and chemokine profiles vary between different cancer types markedly and this complexity corresponds tumor development and malignancy [58, 109, 114]. Predominantly chemokines expressed by malignant cells, bound to their receptors CCR1, CCR7, CCR9, CCR10, CXCR1, CXCR2, CXCR3, CXCR5, CXCR7 and CX3CR1, were demonstrated to be implicated in organ-specific metastasis [47]. One prominent example is the interplay between chemokine CXCL12 and its receptor CXCR4, as described above.

Several chemokines, cytokines and their receptors are involved in regulating angiogenesis either directly by acting on receptors, expressed on endothelial cells, or indirectly by recruiting leukocytes, which provide angiogenic factors [48, 99]. Co-regulation of abundant cytokine and chemokines and growth factors, such as TNF-α and IL6, CCL2, CXCL12 and VEGF specifically have been shown to accelerate angiogenesis through paracrine action [47, 98]. Myeloid derived cells, such as monocytes, TAMs and DCs or the so called TIE-2 positive monocytes are considered as the most effective angiogenesis promoting counterparts in the tumor microenvironment, by producing various angiogenic factors, such as VEGF, PDGF and CXCL8 (IL-8) [58, 115].

Understanding of complex network of cytokines, chemokines and growth factors can be helpful to predict or to evaluate different stages of tumor process and the extent of cancer related inflammation.

Ovarian cancer specific cytokine, chemokine and growth factors

Ascites contains a variety of cytokines, chemokines and tumor markers, which were shown to be involved mainly in immunosuppressive responses [56].

By chemokine, cytokine profiling in ovarian cancer cell lines, a network of TNF-α related molecules comprising CXCL12, IL-6 and TNF-α were identified in highly elevated levels and correlated with high tumor grade [48, 98, 99]. RNA interference based mRNAs knockdown of these cytokines resulted in significantly reduced levels

of main components of the network, specifically that of CXCL12 [98]. Further analysis of the TNF-α network in malignant ascites showed that main components were released mainly by TAMs and associated with colonization of tumor cells in the peritoneum and affected angiogenesis [48, 98]. A gene set enrichment analysis (GSEA) revealed strong interaction between the TNF-α network and leukocyte infiltration [98]. Interestingly, a strong association between high TNF-α network and CD68 positive macrophages was found in human ovarian cancer microenvironment, but not in tumor or in stromal areas [48]. The immune suppressing effect of CXCL12, based on recruiting Treg cells, was demonstrated to be augmented in EOC due to additional recruitment of premature DCs, which also express CXCR4 on their surface [41, 58, 78]. These studies have indicated that cell composition and immune-modulatory mediators in ascites mainly establish a pro-tumor environment rather than tumor repressing milieu [56].

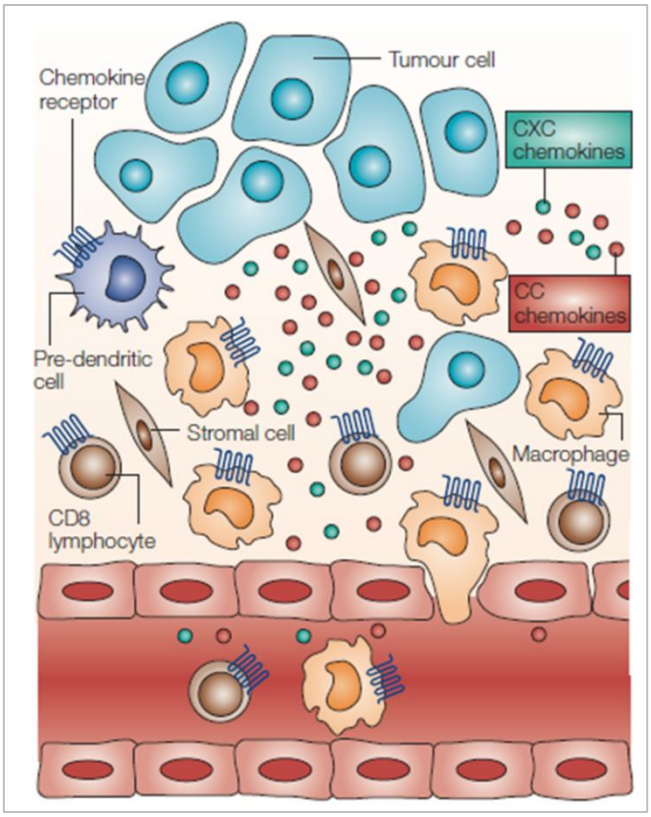

Figure 7: Summarized illustration of different chemokines and cytokines, tumor and immune cells in EOC. Through the action of different cytokines and chemokines released from tumor cells and other components of tumor microenvironment, variety of immune cells is recruited to the tumor site. First of all, TAMs and T lymphocytes, as well as DCs are accumulated (Figure is adapted from [41]).

Several studies have performed wide range profiling experiments of cytokines and chemokines in ascites. These studies demonstrated that malignant ascites is a rich

source of immune-regulatory factors. Profiling of 120 cytokines and chemokines showed that peritoneal mesothelial cells were also actively involved in cytokines production [43, 116]. The complex interplay between different cell populations and cytokines, chemokines in EOC is summarized in figure 7.

The studies describing expression of various growth factors in ascites mostly demonstrated the presence of high concentrated growth factors. Besides ascites, patient sera represent a possible source of biomarkers, which can be used as indicator of disease progression in some cases. For example several growth factors were described as consistently increased in plasma of Type II ovarian cancer patients [117]. These included e.g. prolactin, osteopontin and VEGF, whereas some growth factors such as leptin and Insulin-like growth factor 2 (IGF-2) were shown to be decreased [112, 118, 119].

Hypothesis and aim of the project

Tumor growth and progression have often been shown to be associated with an inflammatory condition in the tumor microenvironment, which is also described as “smoldering inflammation” [47, 48, 109]. High levels of tumor infiltrating immune cells contribute to tumor growth by creating an immunosuppressive and pro-tumor condition, enabling tumor cells to escape anti-tumor immune responses [44, 49]. In addition, a complex network of molecular factors including cytokines, chemokines and tumor growth factors are the main modulators of tumor inflammation [99, 109].

In advanced stages of ovarian cancer, tumors spread predominantly occurs in the peritoneal cavity [5, 14]. Ascites is considered as inflammatory source, which participates in tumor spread in the peritoneal cavity. Two different patterns of tumor spread have been observed by our clinical collaborators: miliary, which is uniquely defined as a wide spread of numerous small implants throughout the peritoneum and non-miliary, which is characterized by the presence of few big implants. In addition, preliminary FACS and RNA sequencing data analysis of EpCAM positive single tumor cells and aggregated spheroids in ascites, delivered results indicating clear differentiation between the two described groups (Auer K, manuscript in preparation).

We hypothesize that dependent on inflammatory conditions in the peritoneal cavity, tumor spread is mediated differentially, which may result in development of two different spread patterns. Immune cells, specifically monocyte derived cell populations including macrophages and DCs in ascites, contribute to formation of various metastatic patterns in the peritoneum, since they are reported to be highly involved in tumor migration, invasion and metastasizing [47, 54, 71, 86].

Firstly, by means of multicolor IF analysis with different markers specific for tumor cells, monocytes, macrophages or DCs, I wanted to determine the association of immune cell populations with the different tumor spread types. Additionally, the proliferation index of all cell populations can be determined with nuclear proliferation marker Ki67. Characterization of tumor and immune cell phenotypes with IF can provide useful indication of distinctive features of these cells and their role in metastasis.

Ascites does not only contain high amounts of leukocytes, which are responsible for inflammation in the peritoneal cavity [43, 65], but accordingly also high levels of immune-mediators, such as cytokines, chemokines and tumor growth factors [56].

Therefore, the second part of the project focuses on assessing these immune-modulators. For this purpose, an extensively multiplexed immunoassay measurement of cell free ascites and serum was performed.

Via characterizing immune cells in ascites combined with cytokine and tumor growth factor measurements, I expected to gain information about the inflammatory condition in ascites, which could be associated with the two different metastatic spread types, observed in the peritoneal cavity of HGSOC patients. Furthermore, by detailed examination of CD14 and CD16 expressing immune cells, such as monocytes, macrophages, DCs and NK cells using multicolor IF staining, the involvement of these cell populations in the development of different types of metastatic spread could be elucidated.

Methods

Patient samples

Ascites samples were obtained from chemotherapy naïve patients, diagnosed with serious ovarian carcinoma. Predominantly, high grade advanced stage (grade 2/3 and FIGO III/IV) epithelial ovarian cancers patients with serous histological subtypes were included. Only patients with known metastatic pattern were included. Four to eight patients characterized with miliary spread of peritoneal metastases and twelve to fourteen patients characterized with non-miliary spread type were included for IF staining and Luminex assays (see Table 2). Metastatic spread types were determined during surgery by experienced clinicians. Complete patient information, including classifications and spread types, from all analysis are summarized in table2.

Sample names	Ascites			Serum
Methods	IF panel 1	IF panel 2	Luminex	Luminex
Patients	N=20	N=17	N=25	N=29
Age at diagnosis	53.3	53.3	53.6	53.7
FIGO				
II	1	1	1	3
III	16	12	18	24
IV	3	4	6	2
Grade				
1	1	1	1	2
2	4	3	6	5
3	15	13	17*	22
M.code				
miliary	4	4	5	8
non-miliary	14	12	13	14
n.a.	2	1	7	7

Table 2: Patient data from IF and Luminex assays: data includes median age, FIGO staging, grade and metastatic patterns, classified into metastatic miliary and non-miliary spread types (M.code). * Grade of a patient was not clearly defined (Grade 2/3).

For IF analysis, only patients with ascitic fluid were included. For cytokine, chemokine and tumor growth factor measurements ascites samples and their matched serum (if available) were used.

Preparation of FFPE tissue slides for IF

Formalin-fixed paraffin-embedded (FFPE) tissue blocks from patient materials were prepared according to standard procedure. Prepared tissue sections of 4 µm were first deparaffinized at 58°C, for 60 min with subsequent incubation in Xylol, 2x for 5 min. For rehydrating the tissue sections were treated in descending alcohol concentration as follows: 2x 100% each 3 min, 1x 96% for 1 min, 1x 80% for 1min and 1x 70% for 1min.

IF of FFPE tissue sections

Multi-color IF staining of FFPE tissue sections from patient materials were first deparaffinized and rehydrated as described above. Heat-induced epitope retrieval (HIER) was performed by heating up the slides in EDTA pH 8.0 (1:50 EDTA in distilled water) using microwave (850 W for 2.5 min, followed by 160W for 13 min). After cooling down the buffer slowly to room temperature (RT), slides were washed 2 times in PBS for 3 min each. The slides were blocked with Ultra V Block (Thermo Fisher Scientific, MA, USA) for 7 min. After rinsing, the slides were treated with primary antibodies directly (diluted in DAKO antibody diluent with background reducing components) in appropriate concentrations for 45-60 min at RT in a humidity chamber.

IF staining of immune cell populations was performed with the following primary antibodies: anti-CD45 (dilution 1:1000, source rat, isotype IgG2b, clone orb96558, Biorbyt, Cambridge, UK), anti-EpCAM (dilution 1:300, source mouse, isotype IgG1, clone VU1D9, Cell Signaling, Cambridge, UK), anti-CD16 (dilution 1:50, source mouse, isotype IgG2a, clone 2H7, Thermo Scientific, MA, USA) and anti-CD14 (dilution 1:250, source rabbit, isotype IgG, clone EPR3653, Novus Biologicals, CO, USA). The second IF panel was performed on FFPE tissue sections with following primary antibodies: anti-CD45 (dilution 1:1000, source rat, isotype IgG2b, clone orb96558, Biorbyt, Cambridge, UK), anti-EpCAM (dilution 1:300, source mouse, isotype IgG1a, clone VU1D9, Cell Signaling, Cambridge, UK), anti-CD44 (dilution 1:1000, source mouse, isotype IgG2a, clone 156-3C11, Cell Signaling, Cambridge, UK) and anti-Ki67 (dilution 1:400, source rabbit, isotype IgG1, clone MIB-1, Dako, Glostrup, Denmark). As negative controls antibodies omitted and primary isotypes were used as positive controls.

After 3x washing in PBS with 0.1% Tween® (PBS-T) 20 for 3 min, the slides were incubated with secondary antibodies for 30-60 min, prepared in 6% bovine serum albumin (BSA) in PBS. For detection of both panels, the following fluorescence labeled secondary antibodies were used: goat anti-rat Alexa Fluor® 555, goat anti-mouse IgG1 Alexa Fluor® 647, goat anti-mouse IgG2a Alexa Fluor® 488 and goat anti-rabbit Alexa Fluor® 750 secondary antibodies, all diluted 1:1000. For negative controls, FLEX Ready-to-Use Mouse Negative Control containing cocktail of mouse IgG_1, IgG_{2a}, IgG_{2b}, IgG_3 and IgM (DAKO Autostainer/ Autostainer Plus, Glostrup, Denmark) was used. The slides were washed again properly in PBS three times and the nuclei were counterstained with DAPI for 5 min. The tissue sections were mounted with Fluoromount-G™ (Southern Biothech, AL, USA). The stained slides were imaged with TissueFAXS fluorescence microscopy (TissueGnostics) and laser scanning microscopy (Zeiss, LSM-700). Pictures were *in silico* enhanced to see weak signals.

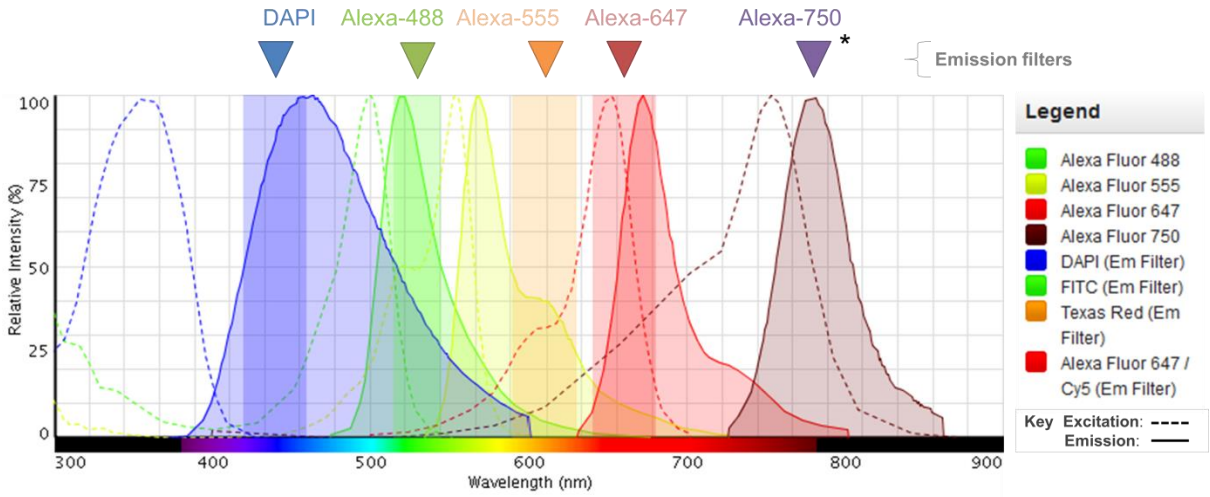

Figure 8: The excitation, emission spectra for used secondary Alexa antibody series are shown by using tool "Fluorescence SpectraViewer" of LifeTechnologies. Emission filters are depicted as colored boxes on the graph and as triangles on the top. *Only emission filter information for Alexa750 is missing.

By means of 'Fluorescence SpectraViewer' of LifeTechnologies, applied Alexa secondary antibody series are analyzed for their cross reaction and spectral overlapping (Fig 8). Additionally, filters used in fluorescence microscopy are presented. Although in some cases emission spectrum of dyes showed overlaps (e.g. Alexa-488 and Alexa-555) with appropriate emission filters the separation of individual channel was possible. Quantification of cells was performed using automated cell analyzing software CellProfiler v.2.1.1 [120]. For choosing the cutoffs

for positive stained signals, negative control fluorescence intensities (of each sample) were first determined and the cutoff was selected based on their measurement.

Preparation of serum samples

Serum samples were processed according to standard protocols.

Quantification of cytokines, chemokines and growth factors

The measurement of cytokine, chemokine and tumor growth factor concentrations in ascites and in blood serum of HGSOC patients were conducted using Bio-Plex Pro™ Human Chemokine Assays (Bio-Rad) and Bio-Plex Pro™ Human Cancer Biomarker Assays (Panel 1, 16-plex) (Bio-Rad). The measurements were done according to manufacturer's instruction and the evaluation was performed using Luminex® 200 Assay technology (Bio-Rad, CA, USA). Bio-Plex Pro™ Human Chemokine Assays consists of following forty analyts: 6Ckine/ CCL21 (secondary lymphoid chemokine), BCA-1/ CXCL13 (B cell attracting chemokine 1), CTACK/ CCL27 (Cutaneous T-cell-attracting chemokine), ENA-78/ CXCL5 (epithelial-derived neutrophil-activating peptide 78), Eotaxin/ CCL11, Eotaxin-2/ CCL24, Eotaxin-3/ CCL26, Fractalkine/ CX3CL1, GCP-2/ CXCL6 (granulocyte chemotactic protein 2), GM-CSF, Gro-α/ CXCL1 (growth regulated peptide α), Gro-β/ CXCL2, I-309/ CCL1 (T lymphocyte-secreted protein I-309), IFN-γ, IL-1β, IL-2, IL-4, IL-6, IL-8/ CXCL8, IL-10, IL-16, IP-10/ CXCL10 (Interferon gamma-induced protein 10), I-TAC/ CXCL11 (Interferon-inducible T-cell alpha chemoattractant), MCP-1/ CCL2 (monocyte chemoattractant protein 1), MCP-2/ CCL8, MCP-3/ CCL7, MCP-4/ CCL13, MDC/ CCL22 (macrophage-derived chemokine), MIF, MIG/ CXCL9 (monocyte/macrophage-activating IFN-γ-inducible protein), MIP-1α/ CCL3 (macrophage inflammatory protein), MIP-1β/ CCL15, MIP-3α/ CCL20, MIP-3β/ CCL19, MPIF-1/CCL23 (myeloid progenitor inhibitory factor 1), SCYB16/CXCL16 (small inducible cytokine subfamily B member 16), SDF-1α+β/CXCL12 (stromal cell-derived factor 1), TARC/ CCL17 (thymus and activation regulated chemokine), TECK/CCL25 (thymus-expressed chemokine), TNF-α.

Bio-Plex Pro™ Human Cancer Biomarker Assays comprises following growth factors and chemotactic analyts: sEGFR (epidermal growth factor receptor), FGF-basic, Follistatin, G-CSF (granulocyte-colony stimulating factor), sHER-2/neu (human epidermal growth factor receptor 2), HGF (hepatocyte growth factor), sIL-6Rα (soluble interleukin-6 receptor α), Leptin, Osteopontin, PDGF-AB/BB (platelet-derived

growth factor), PECAM-1 (platelet endothelial cell adhesion molecule 1), Prolactin, SCF (stem cell factor), sTIE-2 (soluble TEK tyrosine kinase endothelial receptor 2 or angiopoietin receptor 2), sVEGFR-1 (soluble vascular endothelial growth factor 1 receptor), sVEGFR-2.

Data analysis and statistics

Comparative statistical analysis between the two metastatic spread groups was performed applying non-parametric Mann-Whitney Wilcoxon test with 'R' (RStudio 0.97.551). For determination of cytokine, chemokine and tumor growth factor concentrations, a p-value ≤ 0.05 was considered as statistically significant. For analysis of IF staining, raw p-value were corrected for multiple testing using the false discovery rate (FDR). A FDR of ≤ 0.1 was considered as statistically significant.

For cluster analysis of immune and tumor cell populations in ascites, dimensionally reduction method principal component analysis (PCA) was used. PCA bases on determination of 'eigenvalues' of all variables to extract principle components with greatest variances [121]. With further dimension reduction, a cluster analysis can be executed. Statistical analyses of principle components were performed using 'R' and 'Statgraphics centurion XVI' [122]. In addition, a further cluster analysis was carried out with a new method called Quantitative Set Analysis of Gene Expression (QuSAGE), which was originally developed for gene set enrichment analysis [123]. A complete probability density function for comparison of cytokine/chemokine sets (originally gene sets) was employed to extract P-values and confidence intervals and post hoc analysis can be carried out while maintaining statistical traceability. Data with estimated differentiating activity between compared groups are then visualized with 95% confidence intervals [123]. For this analysis, cytokines and chemokines were classified based on knowledge about their target cell populations and their expression was compared between two different metastatic spread groups.

Results

Characterization of tumor and immune cell populations in ascites of HGSOC patients

For characterization of immune cell and tumor cell populations, sections of FFPE embedded ascites cells from HGSOC patients (N=20) were stained with EpCAM, which is a frequently used tumor marker in epithelial ovarian cancer [124] and the pan-leukocyte marker CD45 to stain the total immune cell population. The images were visualized by fluorescence (Tissue FAXS) and confocal laser scanning microscope (LSM-700). IF analysis of tumor cells with EpCAM showed presence of two different tumor cell types: i) single tumor cells, and ii) aggregated tumor cells, also referred to as spheroids (Fig. 9A). Stained with DAPI, tumor cells usually have larger nuclei, compared to $CD45^+$ immune cells with smaller nuclei. Immune cells were also shown to form an aggregated structure in some patients (Fig. 9B).

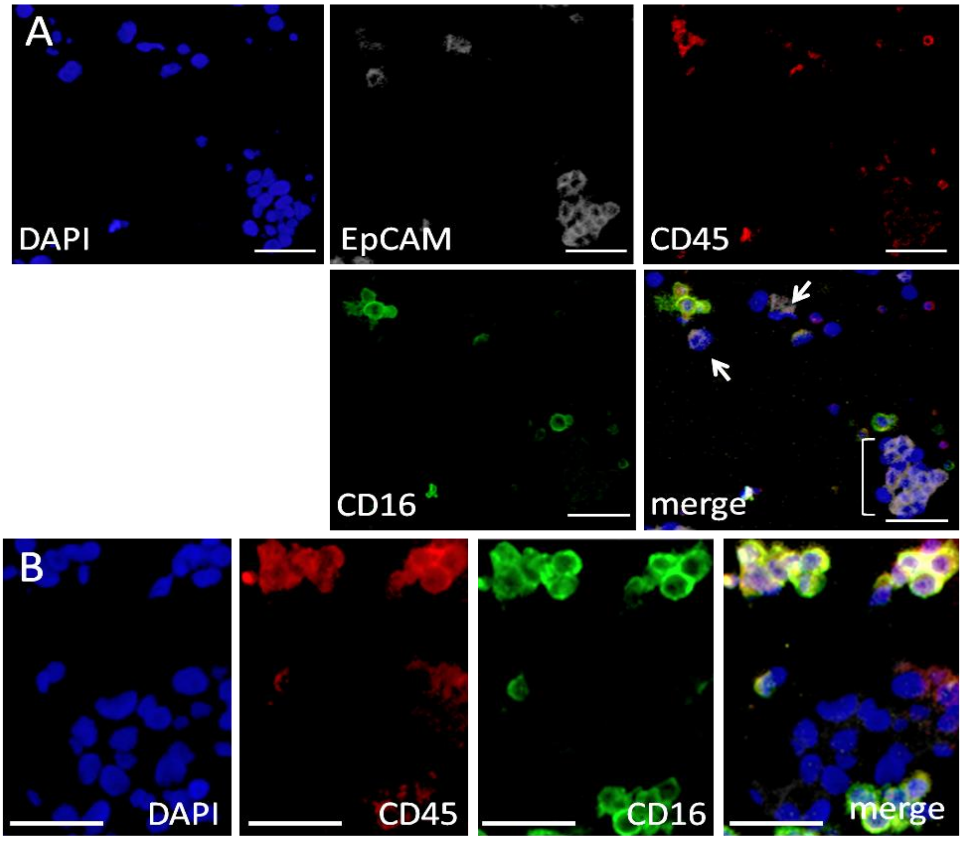

Figure 9: $EpCAM^+$ single tumor cells and spheroids could be recognized in ascites of HGSOC patients. Cells were processed for IF analysis with EpCAM, CD45, CD16 and counterstained with DAPI (A). $EpCAM^+$ single tumor cells and aggregated spheroids are indicated with arrows and bracket on the merged image (A). In some patients aggregated immune cell populations were identified (B). Images were visualized using fluorescence microscopy at 200x magnification (scale bar 50 µm).

Results

According to quantitative assessment of tumor and immune cell marker expression, the amount of immune cells varied notably among patients (9-96%), as well as the amount of $EpCAM^+$ cells (0-62%), (Fig. 10). In only one patient sample, the sum of total immune cells and tumor cells reached the total cell population of 100% in ascites. However, in most of the patient samples, these two cell types together encompassed 18-98%, which reveals that ascites contain other types of cells in varying levels. $CD45^+$ immune cells were further characterized by expression of monocyte related markers: CD14 and CD16 (Fig. 11). The quantification of expression levels of $CD14^+$ (0-24%) and $CD16^+$ (0-20%), as well as $CD14^+/CD16^+$ double positive cells (0-6%) showed that their content vary considerably between patients (Fig 10).

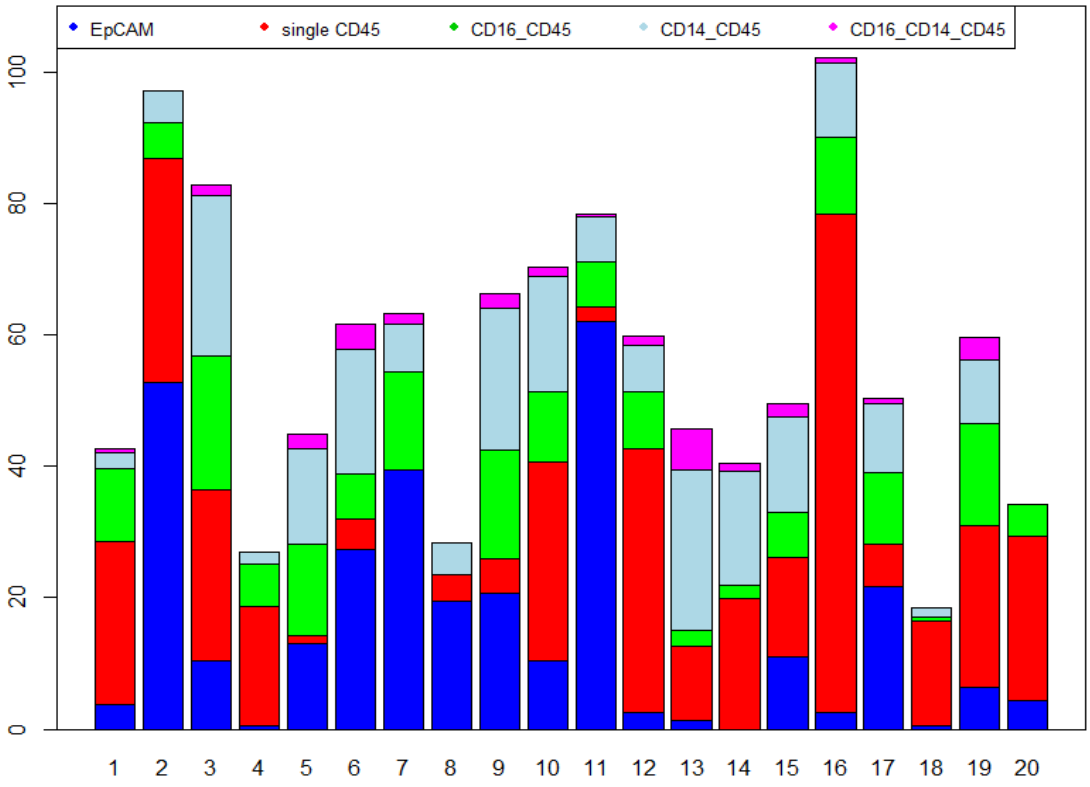

Figure 10: Quantification of tumor cells and immune cells in HGSOC ascites (N=20). Stacked barplots represent calculated cell contents (in %) in each analyzed patient samples: comprising $EpCAM^+$ tumor cells (blue bars), single $CD45^+$ immune cell populations (red bars), as well as monocyte derived cell populations, including double $CD14^+/CD16^-/CD45^+$ cells (light blue bars), $CD14^-/CD16^+/CD45^+$ cells (green bars) and $CD14^+/CD16^+/CD45^+$ triple positive cells (magenta).

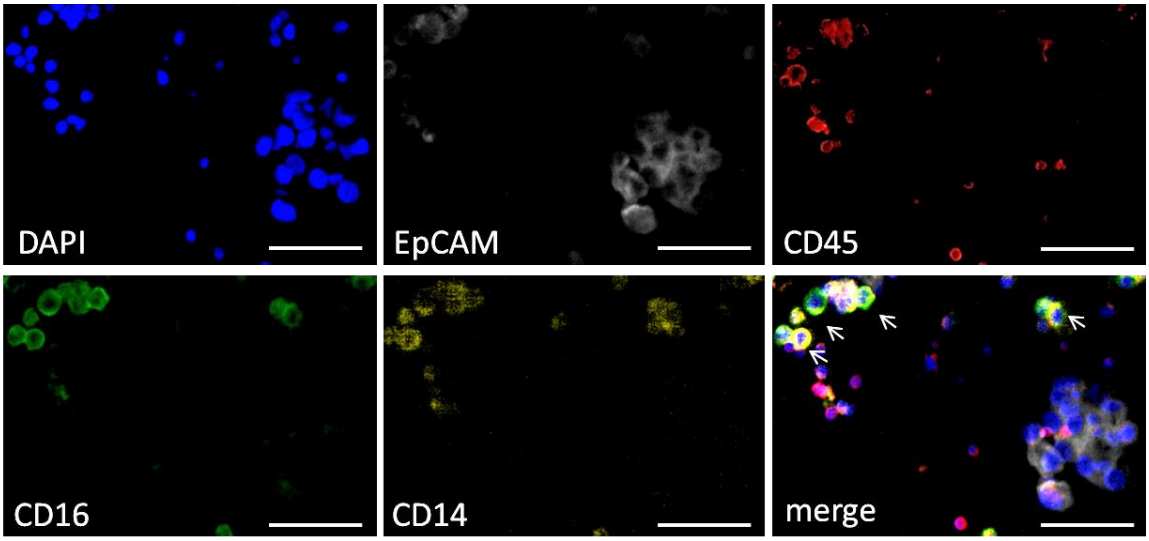

Figure 11: IF staining analysis of tumor and immune cells in ascites. The cell nuclei were counterstained with DAPI and tumor cells were stained with EpCAM. Immune cells were visualized with CD45, CD16 and CD14. Merged image shows mostly $CD14^{+}/CD16^{+}/CD45^{+}$ triple positive monocytes (arrows). Images were visualized using fluorescence microscopy at 200x magnification (scale bar 50 µm).

Additionally, proliferation indices of individual cell populations were determined with nuclear proliferation marker Ki67 (N=17). Both tumor cells and immune cells were positive for Ki67 expression at equivalent level (Fig. 12).

The expression level of CD44 is indicative of stem cell feature of cells, but also involved in cell adhesion, cell migration and T cell homing [33, 34]. IF staining revealed presence of abundant CD44 expressing immune cells (Fig. 12). Very few tumor cells were positive for $CD44^{+}$.

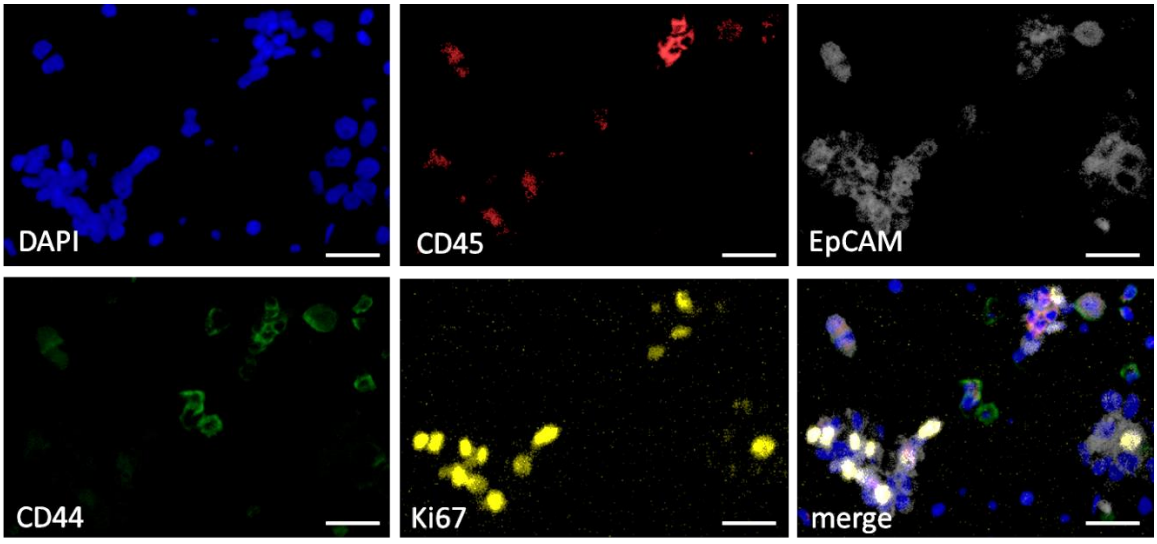

Figure 12: **IF staining of immune cells in ascites indicate CD45, EpCAM, CD44, and Ki67 expression.** The cell nuclei were counterstained with DAPI. Images were visualized using fluorescence microscopy at 200x magnification (scale bar 50 µm).

These results indicated heterogeneity of cell populations in ascites. To ascertain whether tumor and immune cells in ascites are associated with two different metastatic spread groups, patient samples were divided into two groups on the basis of metastatic mode determined by clinicians and the cell composition was analyzed quantitatively (N=17, 5 miliary and 12 non-miliary), (Fig 13 A-F). For all comparative statistical analysis between two groups (miliary *vs* non-miliary) Mann-Whitney Wilcoxon -Test was used.

In general, more $EpCAM^+$ tumor cells were detected in ascites of patients with miliary metastasized peritoneal cavity, compared to non-miliary (17% *vs* 4%, FDR=0.12) accordingly more proliferating tumor cells were detected in miliary related ascites (7.4% *vs* 0.7%, FDR=0.09, Fig 13A and B). Non-miliary associated ascites on the contrary, indicated a trend of more infiltrating immune cells ($CD45^+$ cells: 28% *vs* 13%, FDR=0.19, Fig 13D). The proliferation indices of immune cells did not differ between the two metastatic groups (Fig 13E).

Further quantification of tumor and immune cell population confirmed that the majority of $CD45^+$ immune cells in ascites were $CD44^+$. Concerning expression of $CD44^+/CD45^+$ immune cells solely, there was no big difference between miliary and non-miliary (40% *vs* 35%, FDR=0.9, Fig. 13F). It was reported that primary ovarian tumor cells show high CD44 expression on their surface. However, their expression was reduced on free circulating tumor cells in ascites [125, 126]. In this analysis, very few $CD44^+$ tumor cells were detected and their expression level did not vary between the two groups of metastatic spreads (1% *vs* 1.7%, FDR=0.4, Fig. 13C).

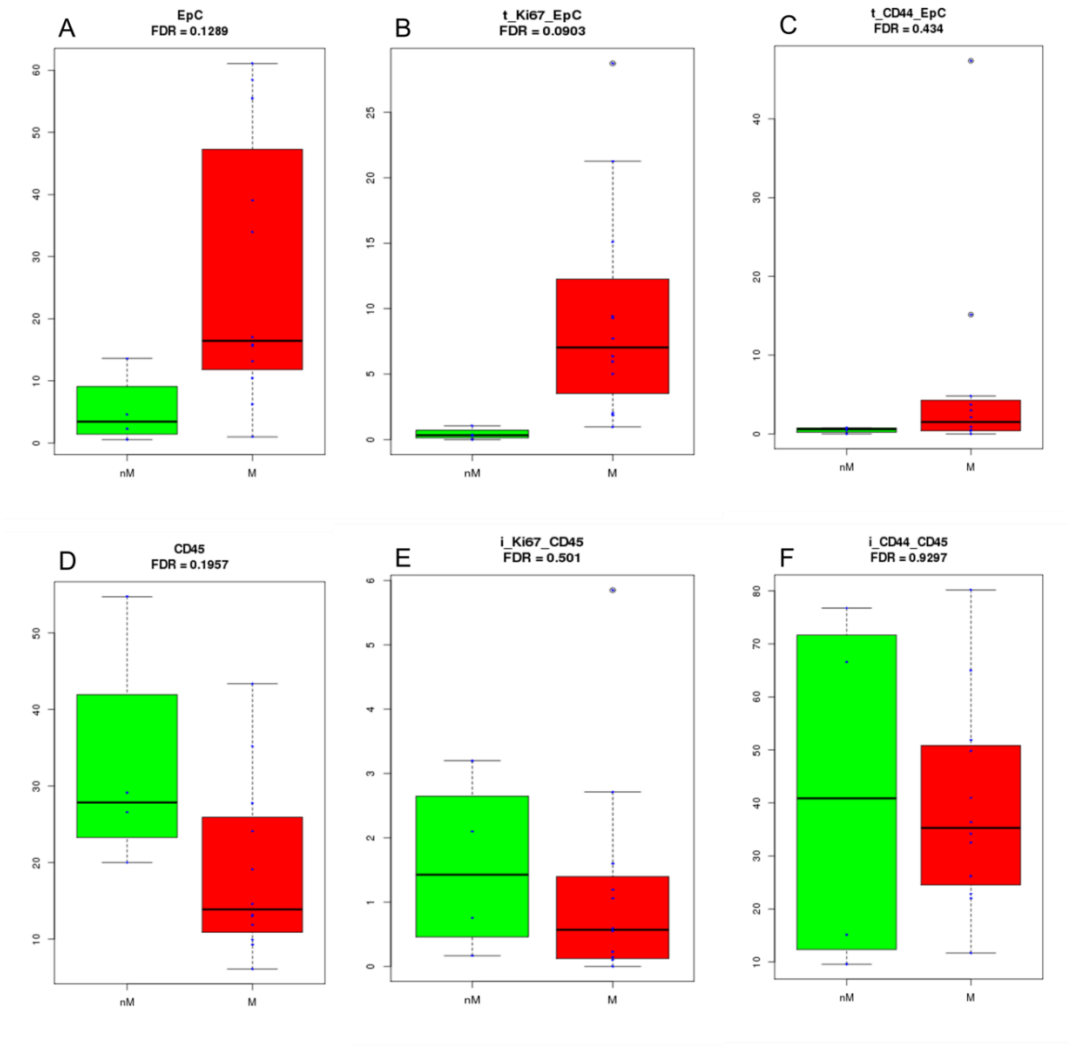

Figure 13: **Quantification of tumor and immune cells in ascites of two different metastatic types**. EpCAM$^+$ (A) and CD45$^+$ (D) cell population in ascites were analyzed with IF and quantified using CellProfiler to show cell content difference in percentage between two metastatic patterns. Moreover, the proliferation status of tumor cells (B) and immune cells (E) was characterized with nuclear Ki67 staining. CD44 expression of tumor (C) and immune cells (F) were evaluated, as well. Note: the initial 't', before title, stands for total tumor cell and 'i' for total immune cell quantification, which were counted as total for determining proliferating and CD44 positive cell populations.

Two different metastatic spread types vary in their CD14$^+$ and CD16$^+$ cell content in ascites

Series of IF analysis was performed in order to determine the possible role of CD14$^+$ and CD16$^+$ cells in metastasizing patterns. These include very heterogeneous cell populations such as monocytes, DCs macrophages and also NK cells. Of these different CD14$^+$ and CD16$^+$ monocyte and macrophage subtypes were reported to be highly correlated with tumor growth and metastasis [54].

To investigate total $CD45^+$ immune cells in ascites in more detail, IF analysis with $CD14^+$ and $CD16^+$ markers was performed. As described above, ascites in non-miliary spread type harbored more immune cells. Corresponding to this result, increased number of $CD14^+/CD45^+$ (3.8% *vs* 0.5%, FDR=0.027) and $CD16^+/CD45^+$ (3.2% *vs* 1.1%, FDR=0.31), as well as higher number of $CD14^+/CD16^+/CD45^+$ triple positive cells (4% *vs* 1%, FDR=0.07) were detected in ascites of patients with non-miliary metastatic type compared to miliary (Fig 14 A-C).

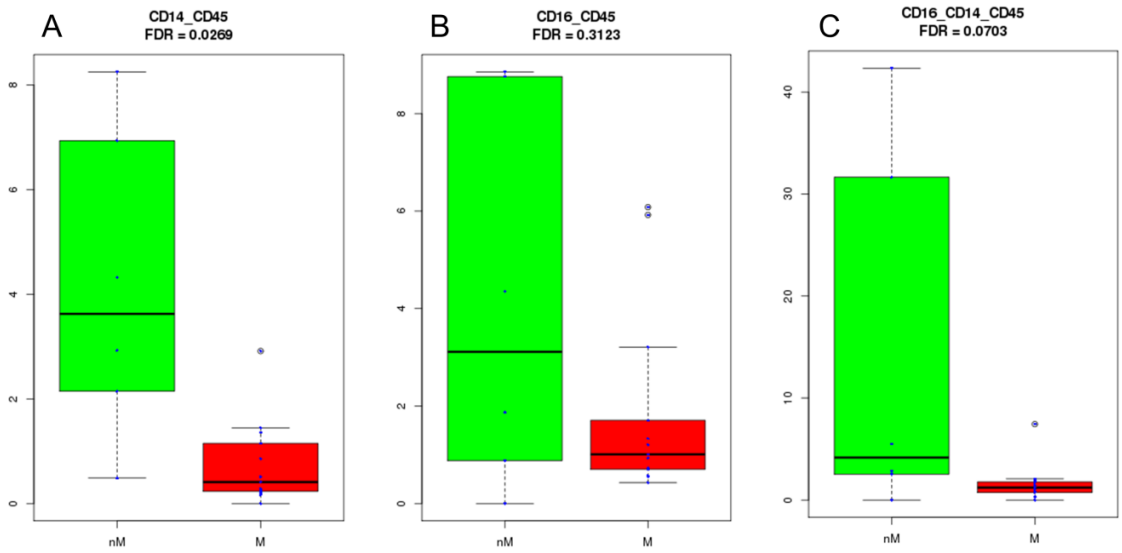

Figure 14: Quantification of double $CD14^+/CD16^-/CD45^+$ and $CD14^-/CD16^+/CD45^+$ immune cells, as well as $CD14^+/CD16^+/CD45^+$ triple positive cells in two different conditions of ascites. IF analysis of single $CD14^+$ (A), single $CD16^+$ (B) and $CD14^+/CD16^+$ (C) immune cells was quantified in ascites and plotted in percentage. The results showed differences between two metastatic patterns. Note: percentage of CD14 and/or CD16 positive immune cells were calculated based on quantification of total $CD45^+$ immune cells.

We next performed PCA analysis, to find out whether differences in various cell populations in ascites can lead to clear clustering of the two groups based on dimensionality reduction. The PCA revealed that ascites of patients with miliary and non-miliary metastatic spread types were clearly clustered together in two distinct groups (Fig 15). Analysis of principle components PC1 and PC2 indicates the most weighted variables (Fig 16).

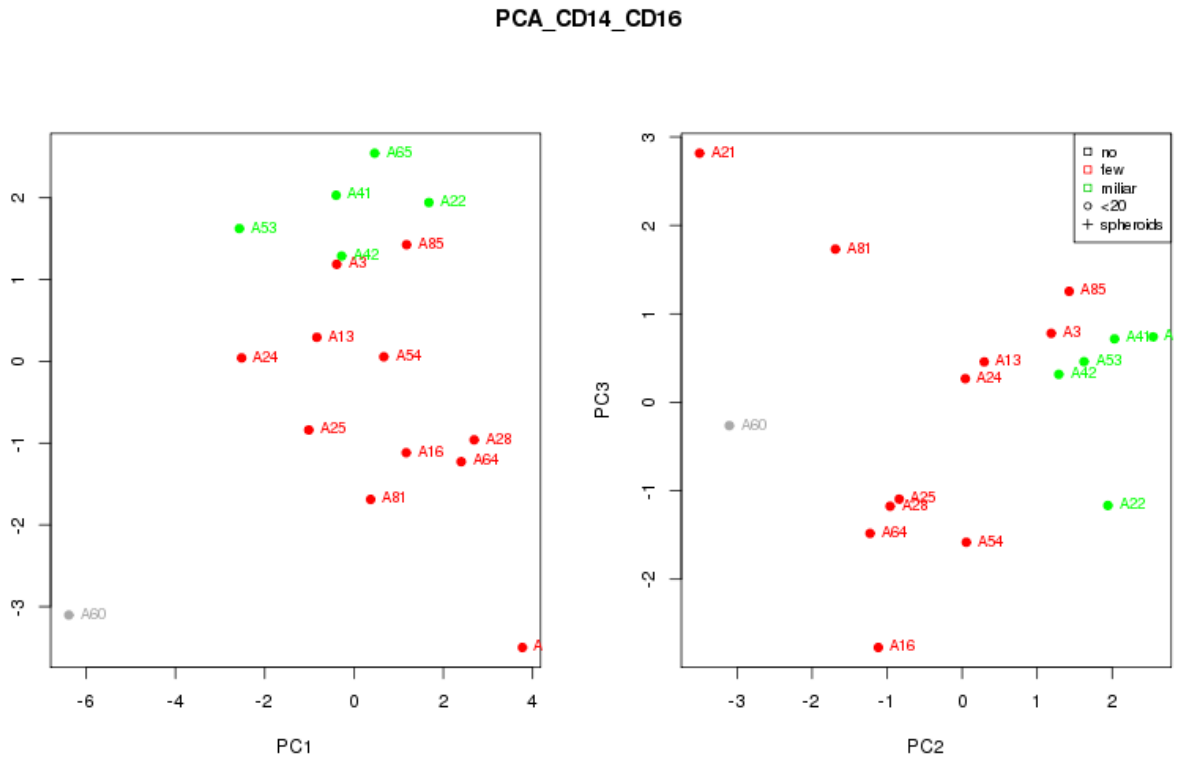

Figure 15: PCA analysis includes quantification of all cell populations in ascites (N=17). Patient materials, designated with A for ascites plus the assigned patient number were subdivided into two groups of metastatic modes, of which 5 patients represented with miliary spread (red) and 11 patients with non-miliary spread (green). The results indicated obvious difference between miliary and non-miliary metastatic groups (red *vs* green). PCA results consisting of three main components (PC1-PC3) were displayed in two plots. Together they accounted for 83.42% of the variability in the original data.

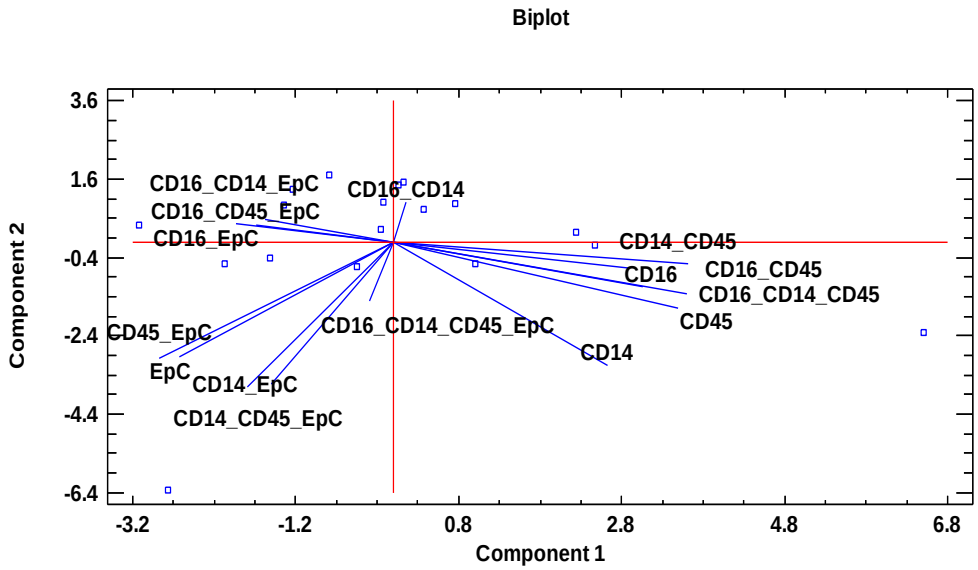

Figure 16: Biplot of principle components. PC1 and PC2 are plotted. Variances of CD16 and CD14 cells were shown to be main weighted components.

These results suggest that tumor and immune cell content variations in ascites are associated with two different metastatic patterns.

Cytokines in ascites affect local inflammation associated with metastatic spread types

Ascites provides an environment containing various immune cell populations and immune-modulatory factors, which determines inflammatory conditions. Therefore, the amount of different cytokine, chemokine and tumor growth factors were measured, since we postulated that inflammatory condition in the peritoneal cavity contributes to metastatic patterns.

High numbers of immune cells were detected in non-miliary conditions. However, it did not necessarily reflect, whether these immune cells contribute to an activated inflammatory condition, or to a more cancer associated immunosuppressive state, which was found to be common in ascites of HGSOC patients [56, 98, 99]

In order to determine inflammatory mediators in ascites possibly related to the two different metastatic groups, two multiplex Bio-Plex Pro^{TM} human chemokine and cancer biomarker systems (Bio-Rad) were used: one consists of 40 different magnetic bead bound antibodies directed against different cytokines and chemokines, whereas the other panel allows detection of 16 common tumor growth markers. Subsequently, their concentrations were determined using a Luminex 200^{TM} system. First, the cytokine and chemokine assay facilitated detection of both important pro-inflammatory cytokines, such as IL-1β, IL-2, IL-6, IFN-γ, GM-CSF and TNF-α and common immune-regulatory cytokines, including IL-10 and IL-4 in ascites of 25 and in sera of 29 HGSOC patients [43].

Of these inflammatory cytokines, GM-CSF was significantly increased in ascites of patients with non-miliary spread type (2.1 fold increase in non-miliary compared to miliary, p=0.004, Fig. 17F). Except for TNF-α and IL-6, the majority of pro-inflammatory cytokine concentrations were slightly elevated in ascites of non-miliary type, which coincided with increased presence of immune cells in this metastatic mode (Fig. 17 A-F). However, TNF-α, IL-6 and CXCL12 together, known as TNF- α network, were also reported to be highly associated with malignancy and metastasis in SOC [48, 98, 99, 127].

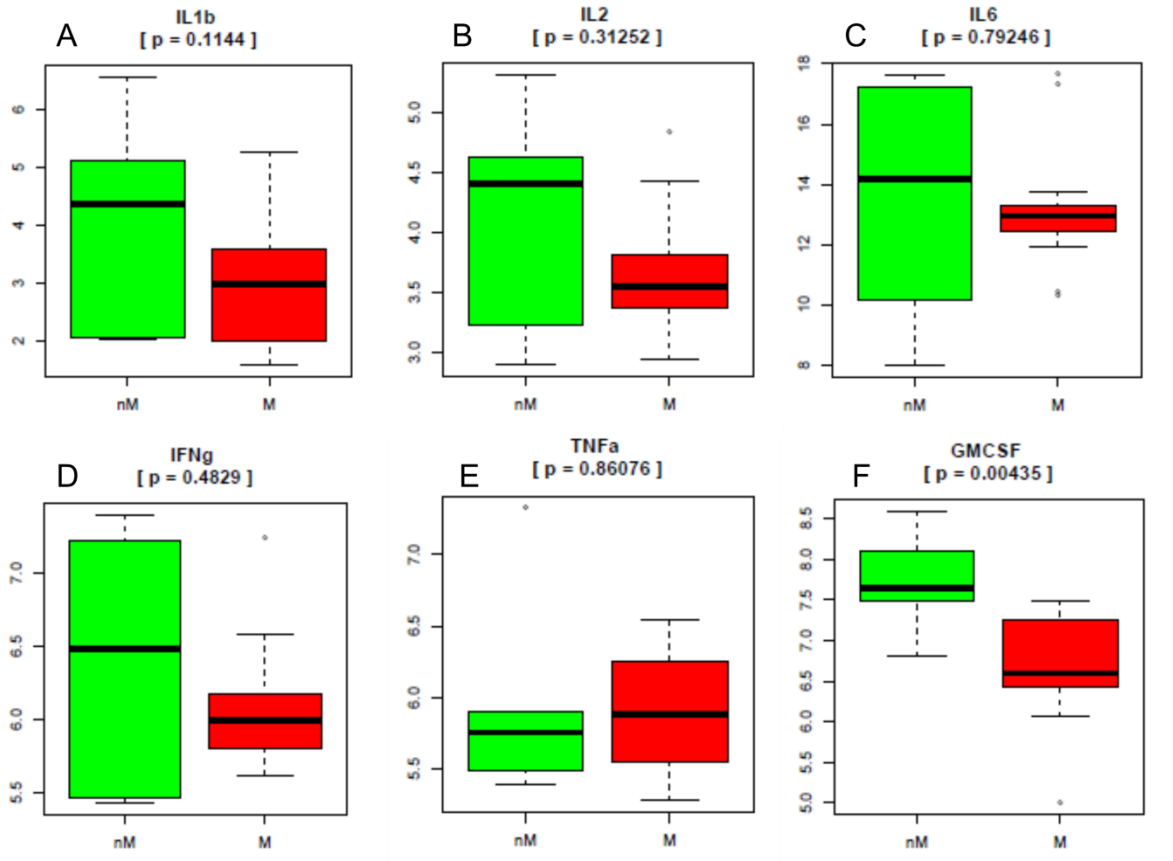

Figure 17: Detection of well-known pro-inflammatory cytokines in HGSOC patients. Measured concentrations are represented in log2 [pg/ml]. Concentrations of IL-1β (designated as IL1b) (A), IL-2 (B), IL-6 (C), IFN-γ (designated as IFNg) (D), TNF-α (designated as TNFa) (E) and GM-CSF (F) were then compared in ascites of patients with the two spread types.

On the contrary, release of immune response inhibitory cytokine IL-10 (2.5 fold decrease in non-miliary compared to miliary, p=0.07) was reduced markedly in non-miliary associated ascites (Fig. 18A). IL-4, which operates immune inhibitory by stimulating Th2 cell activation, did not show a significant difference (Fig. 18B).

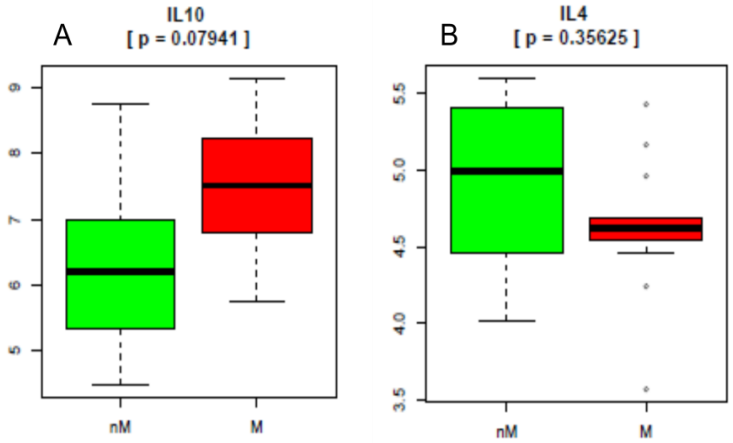

Figure 18: Comparison of immunosuppressive cytokine concentrations in ascites from HGSOC patients compared between miliary and non-miliary**.** Log2 concentrations [pg/ml] of IL-10 (A) and IL-4 (B) are plotted and were compared based on Mann-Whitney Wilcox tests.

These data indicated that non-miliary related ascites recruits high number of immune cells and stimulates more inflammatory active responses in ascites, whereas in miliary spread associated ascites local inflammation seemed to be mainly suppressed by action of high IL-10 expression and a lower number of immune cells.

Chemokine regulation in ascites determines differences between two metastatic groups

Chemokines are other important participants of inflammation, which mostly attract different types of immune cells to the tumor site and are primarily regulated by cytokine action. Different chemokine groups were assessed to examine to which extent the various chemokines were associated with the two different metastatic spread types. By analyzing chemokine composition in ascites, inflammatory activation in ascites can be determined.

Several chemokine levels were found to be significantly changed in ascites of miliary and non-miliary spread groups (Fig. 19). These included the B cell chemoattractant CXCL13 (3.25 fold increase in miliary compared to non-miliary, p=0.005, Fig 19I), the neutrophil attractant CXCL6 (1.8 fold increase in miliary compared to non-miliary, p=0.065, Fig. 19H), the monocyte attractant CCL13 (4.1 fold increase in miliary compared to non-miliary, p=0.014, Fig. 19C) and CCL25, which is responsible for T cell homing, specifically in mucosa (2.4 fold decrease in miliary compared to non-miliary, p=0.002, Fig. 19F). Additionally, CCL25 was reported to be an important player of tumor migration during metastasis [128, 129]. Of these CXCL13, CXCL6 and CCL13 were shown to be increased in ascites of patients with miliary spread type, whereas CCL25 was higher in non-miliary (Fig. 19 boxplots in red boxes (C, F, H, I)).

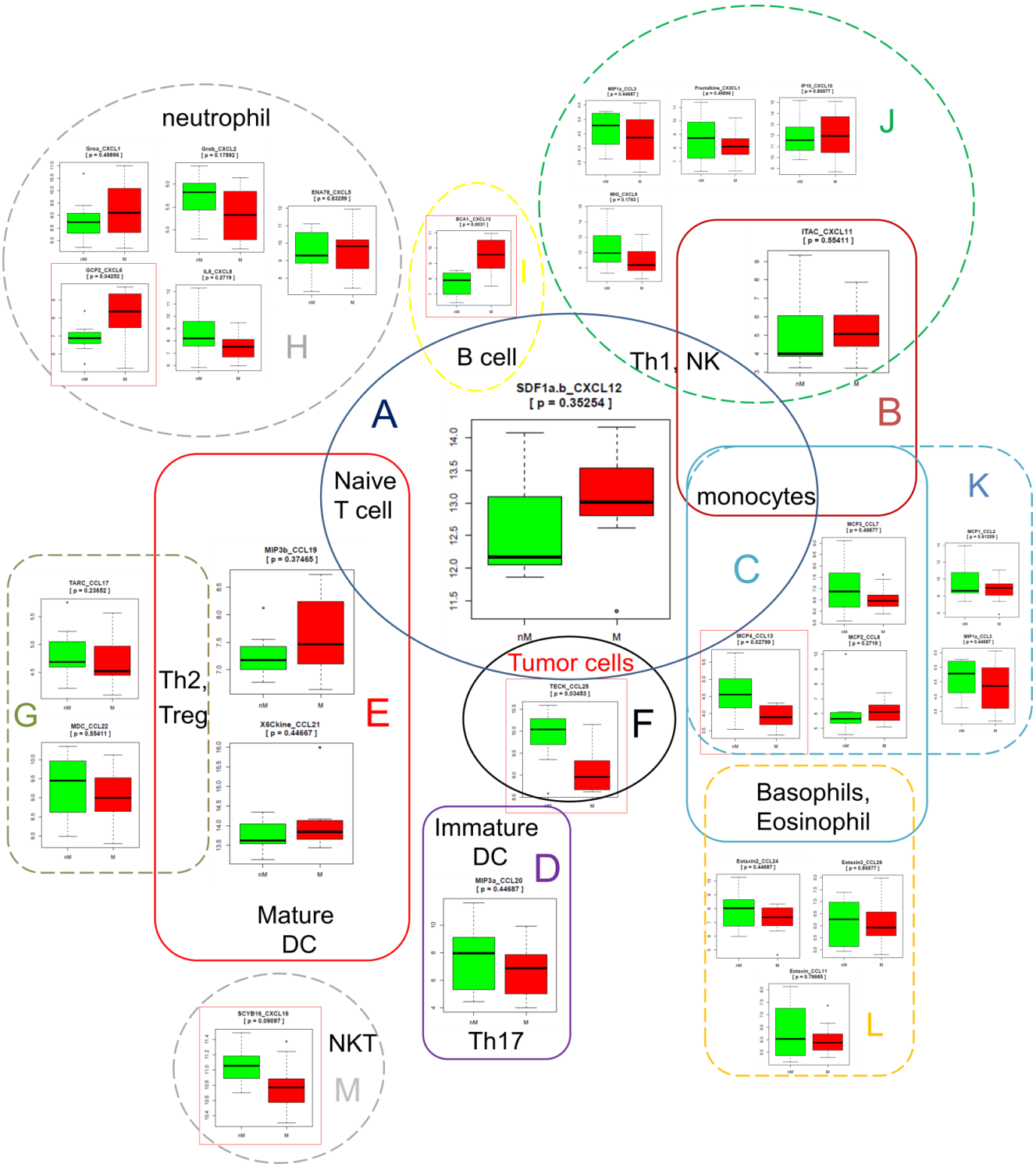

Figure 19: Classification of measured chemokines based on their action on various immune cell populations. This illustration is constructed based on knowledge of interaction between chemokines and their receptors, expressed on various cell populations. The results from comparative analysis of chemokines between two different metastatic groups are also grouped according to corresponding chemokines classifications (A-K). Chemokines, which are known to act on several cell types simultaneously, are arranged together in solid-framed boxes and circles with different color-codes with corresponding cell names (A-F). Immune cell specific chemokines, which are known to be expressed only on one type of immune cells, are framed in dashed boxes or circles with respective immune cell names (G-M). Chemokines, which showed significant difference between two groups, are red-framed.

Since numerous chemokines exhibited not significant but noticeable differences between miliary and non-miliary metastatic patterns, we performed a more sensitive cytokine/chemokine set analysis using QuSAGE, to find out more about the interplay of complex chemokine networks and their activation [123].

The clustering quantification identified cytokines associated with M1 characteristic macrophages and B cells as highly significantly changed in ascites of miliary and non-miliary spread types (red labeled p-values and FDR on table 3). On the contrary, in serum none of the cytokine and chemokine groups showed significant differences between the two metastatic spread groups.

Ascites				**Serum**		
pathway.name	log.fold.change	p.Value	FDR	log.fold.change	p.Value	FDR
macrophage M1	-1.5518	0.0002	0.0024	-0.2400	0.6100	0.9500
mucosal T cell	-1.0788	0.0004	0.0032	0.0300	0.8700	0.9500
B cell	1.1875	0.0030	0.0161	-0.1800	0.4600	0.9500
naive T cell	0.4460	0.1142	0.4240	-0.1400	0.4200	0.9500
T activated	-0.2365	0.1346	0.4240	0.2300	0.5100	0.9500
DC activated	0.4111	0.1590	0.4240	0.2300	0.6400	0.9500
skin T cell	0.5312	0.2260	0.4520	0.1800	0.3900	0.9500
DC naive	-0.7047	0.2111	0.4520	-0.0100	0.9600	0.9600
NK	-0.9646	0.2847	0.4555	-0.1400	0.7800	0.9500
Eosino/basophils	-0.3029	0.2597	0.4555	0.0400	0.8900	0.9500
Th1	-0.5219	0.3861	0.5148	-0.1500	0.6400	0.9500
monocyte	-0.3787	0.3626	0.5148	-0.1400	0.5600	0.9500
Th2	0.1664	0.5626	0.6430	0.0600	0.7800	0.9500
Treg	-0.1777	0.5265	0.6430	0.2500	0.5000	0.9500
macrophage M2	-0.1094	0.8579	0.9151	-0.3000	0.5800	0.9500
neutrophils	-0.0164	0.9917	0.9917	0.0500	0.8600	0.9500

Table 3: Results from QuSAGE cluster analysis. Cytokines and chemokines are classified based on their target cells. The table contains fold changes of cytokine expression (log2) in ascites and sera from HGSOC patients.

The visualization of the four individual cytokines of the M1 characteristic macrophage pathway and the three individual cytokines of the B cell pathway revealed that fold changes of all components in a group (black lines beneath the plots) contributed to clustering to similar extents. Furthermore, cytokines in the M1 characteristic macrophage pathway and the B cell pathway show opposite directed fold changes, which indicate that, the amount of these two cell populations differ markedly between miliary and non-miliary metastatic phenotypes (Fig. 20).

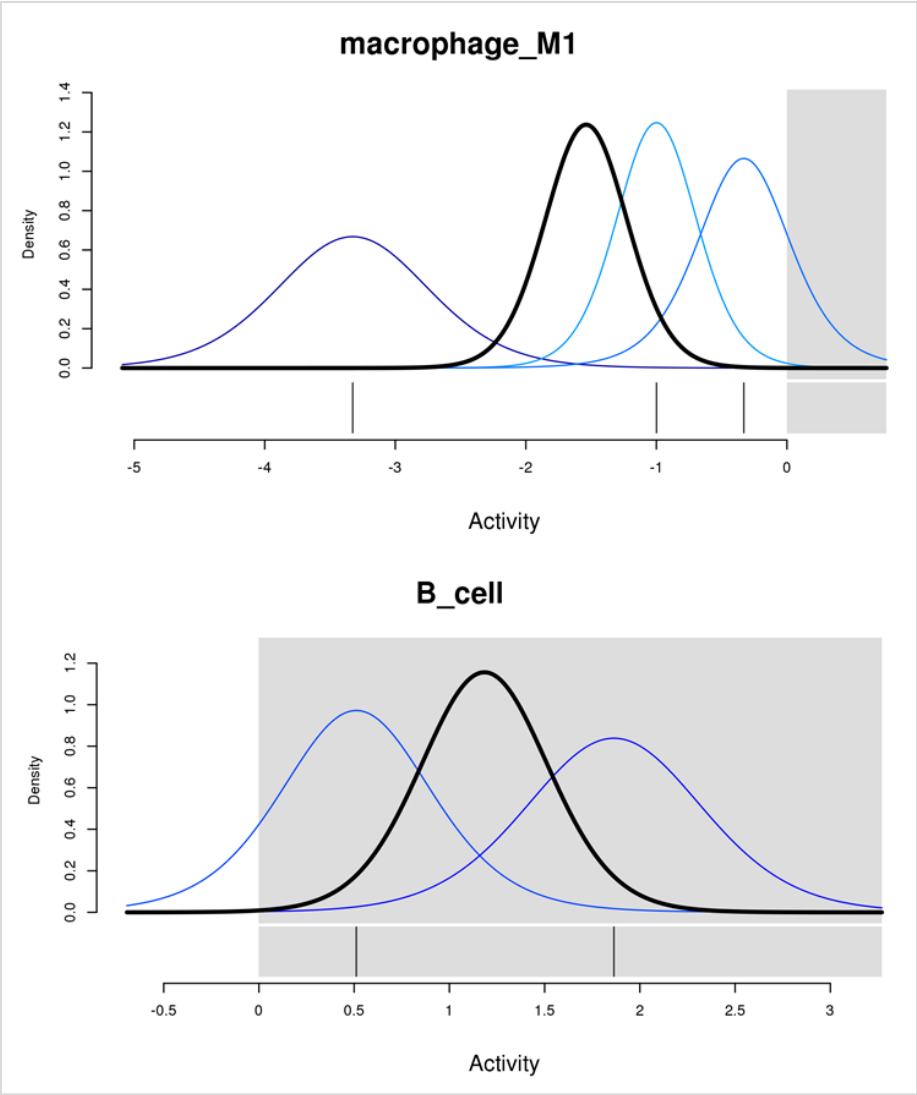

Figure 20: QuSAGE analysis of cytokines and chemokines. This cluster analysis detected chemokines and cytokines responsible for accumulation and activation of macrophages (consists of three components) and B cells (consists of two components) as significantly different between the two metastatic spread types. The mean expression of the cytokine/chemokine set is shown bold. The mean differential expressions for individual cytokines in the sets are indicated as lines below the plots. Density corresponds to standard deviations.

A comparison of chemokine concentrations between ascites and serum indicated that generally the majority of chemoattractants were more abundant in ascites compared to serum (whole plots of serum and ascites data are shown in the supplement). The following cytokines showed major differences between serum and ascites: IL-1β, IL-6, IL-8, IL-16, MIF, the DC attractant CCL20 and the mucosal T cell attractant CCL25 (all more than twofold increased). The B cell chemoattractant CXCL13 revealed very high increase in ascites compared to serum (5 fold increase in non-miliary and 17 fold increase in miliary). Only the neutrophil attractant CXCL2 and the Treg

chemokine CCL17 showed decreased levels in ascites compared to serum (CXCL2: 10 fold decrease and CCL17: 5.5 fold decrease). Higher levels of cytokines and chemokines (with an exception of CXCL2 and CCL17) in ascites than in sera suggested that ascites creates an inflammatory activated milieu compared to the situation in peripheral blood.

Our data indicated that ascites contain higher levels of cytokines and chemokines and is more inflammation prone compared to serum. Furthermore, the results from chemokine measurement suggested that ascites in miliary type seemed to attract B cells (3.25 fold increase of CXCL13 in miliary). On the contrary, ascites in non-miliary showed higher levels of cytokines associated with mucosal T cell presence (2.4 fold increase of CCL25 in non-miliary).

Summarizing, in respect to different metastatic patterns, I observed that ascites in patients of the miliary spread type was characterized by lower immune cell and higher tumor cell content and by a predominantly tumor promoting immunosuppressive milieu with an abundant B cell attractant. In contrast, in ascites of non-miliary spread type, higher abundance of immune cells and more inflammatory milieu with more mucosal T cell homing and monocyte recruiting cytokines were observed.

Macrophage differentiation varies between the two metastatic spread groups

Based on monocyte directed cytokine and chemokine measurements in ascites, we tried to assess the effect of monocytes, macrophages and DCs, on the metastasizing pattern. First, chemokines attracting monocytes were analyzed; since we found that there was a noticeable variation of monocyte abundance between the two metastatic groups according to IF evaluating. In addition, important cytokines and chemokines involved in differentiation of monocytes into macrophages and DCs were analyzed.

The majority of measured monocyte attracting chemokines, such as G-CSF, CCL2, CCL8 and CXCL11 (Fig. 21 A, B, D and F), did not show any significant change. In non-miliary ascites, concentrations of CCL3 (1.7 fold increase in non-miliary compared to miliary, p=0.25) and CCL7 (1.6 fold increase in non-miliary compared to miliary, p=0.25) were increased, but not significant (Fig. 21C and E). CCL3 is a common monocyte recruiting chemokine, whose concentration was also increased in ascites compared to serum, however not significantly (2 fold increase).

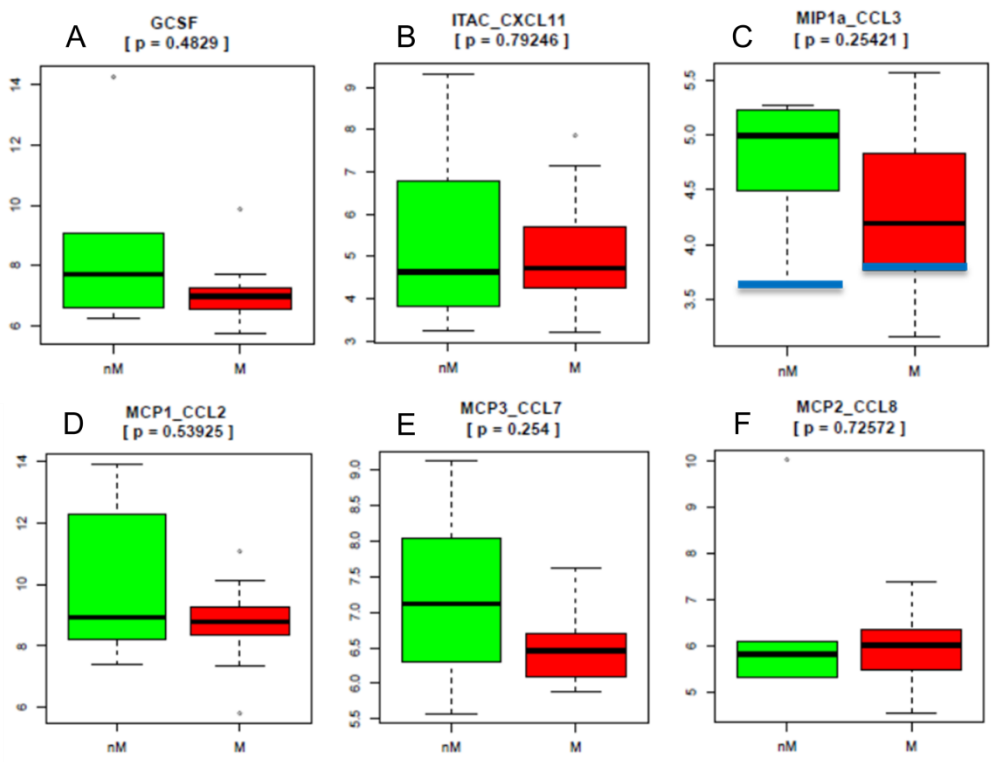

Figure 21: Comparison of concentrations of known monocyte attracting chemokines between two different metastatic groups. Log2 concentrations [pg/ml] of G-CSF (A), CXCL11 (B), CCL3 with its corresponding serum concentration (medians of serum concentration are added to the ascites bar plot and indicated with blue lines) (C), CCL2 (D), CCL7 (E) and CCL8 (F) in two different ascites conditions were compared.

Triggered by the inflammatory condition in the tissue, differentiation of monocyte can vary [130]. M1 type macrophages have been shown to be simulated mainly by G-CSF, GM-CSF and IFN-γ, whereas M2 differentiation is mediated mostly by IL-10, but also by IL-6 [44, 55, 71, 78]. Therefore, assessing attraction and differentiation of monocytes can give an indication for the metastatic patterns, since macrophages play crucial roles in metastasizing [54, 71, 78, 86]. The monocyte specific chemokine and cytokine measurements revealed that concentrations of M2 differentiation stimulating factors were significantly increased in ascites compared to serum concentration; specifically concentration of IL-6 showed a very strong increase in ascites compared to serum (>600 fold increase in ascites compared to serum). Analysis of inflammatory cytokines in ascites of the two metastatic spread groups revealed that M1 differentiation mediator GM-CSF was highly elevated in non-miliary (2.1 fold increase in non-miliary compared to miliary, p=0.004, Fig. 22A). Similarly, IFN-γ showed a slight elevation in non-miliary (Fig. 22B). In general, according to the cytokine and chemokine measurements in ascites, in miliary, M2 differentiation of

monocytes was favored, whereas in non-miliary enhanced differentiation of M1 characteristic macrophages seemed to be promoted.

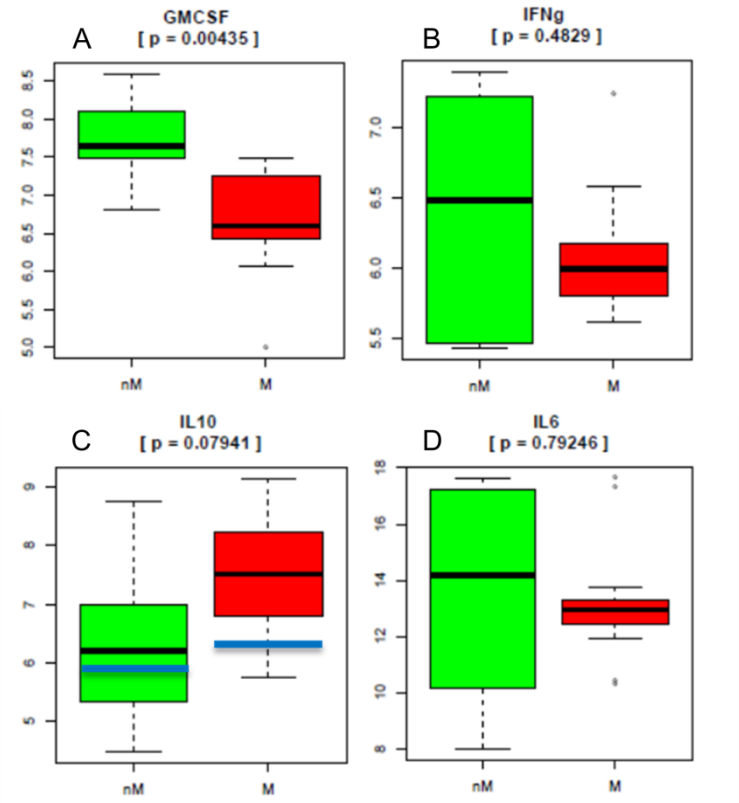

Figure 22: Comparison of cytokine and chemokine concentrations, which are known to be involved in M1 and M2 differentiation of macrophages. Concentrations of cytokines [pg/ml] (plotted in log2), which stimulate M1 differentiation of monocytes, including GM-CSF (A), IFN-γ (B), as well as cytokines responsible for M2 differentiation of monocytes, such as IL-10 (C) and IL-6 (D) were selected and analyzed. Medians of serum concentration are indicated with blue lines on the ascites bar plots of IL-10 (C).

IL-10 is one of the main inhibitory cytokines, which suppresses Th1 mediated immune activation by stimulating inhibitory Th2 response and Tregs [78, 131]. In ascites of patients with miliary spread type IL-10 concentrations were measured in significantly higher levels compared to non-miliary (2.5 fold increase in miliary compared to non-miliary, p=0.07, Fig. 22C), as well as lower levels inflammatory cytokines such as GM-CSF and IFN-γ (Fig. 17 and 22). This implies that in ascites of miliary type a highly immunosuppressive milieu prevails, whereas in non-miliary an inflammatory activated condition predominates.

One of the chemokine, which was demonstrated to induce monocyte differentiation into TAMs with an immunosuppressive phenotype, is CXCL12 [98]. Also, a higher level of CXCL12 was measured in ascites, particularly in miliary, compared to serum

(2.8 fold increase in miliary compared to non-miliary, Fig. 23B). Moreover, a slight increase of CXCL12 was detected in ascites in miliary associated immunosuppressive condition compared to non-miliary.

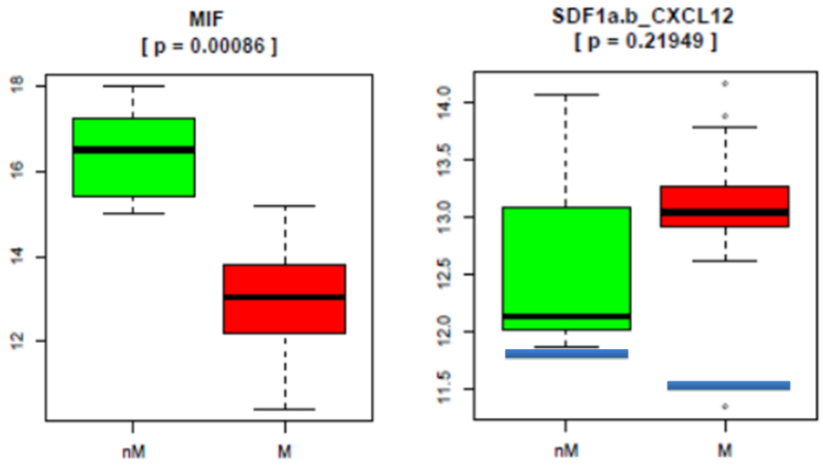

Figure 23: The expression levels of two specific cytokines were considered, which were shown to be involved in immunosuppressive TAM associated metastasizing in SOCs. CXCL-12 (A) and MIF (B) concentrations were compared in ascites between two metastatic groups [pg/ml] and concentrations were plotted in log2 scale. Medians of CXCL-12 serum concentrations are indicated with blue lines on the ascites bar plots (A).

MIF was reported to be an important regulatory cytokine of TAM differentiation in SOC [98]. It was found that MIF mediates M1 polarization of macrophage by reducing release of cytokines, such as IL-6, TNF-α and increasing IL-12 levels [98, 99]. One of the immune-modulating factors, which was increased significantly in ascites in non-miliary spread type was MIF (11.3 fold increase in non-miliary compared to miliary, p=0.00086, Fig. 23A).

These data from analysis of monocyte recruitment and differentiation suggest that the two distinct metastatic patterns are also associated with heterogeneous macrophage differentiation phenotypes.

Growth factors involved in angiogenesis affect tumor spread

To examine whether factors in ascites, other than cytokines and chemokines, also contribute to progression of the two different metastatic spread phenotypes, the abundance of 16 different growth factors in ascites and serum of HGSOC patients were analyzed (ascites: N=25, serum: N=29).

Results

Investigation of different growth factor concentrations by means of Luminex 200 system (Bio-Rad) in ascites indicated that mostly tumor growth promoting factors such as sEGFR (2 fold increase in non-miliary compared to miliary, p=0.022), sIL-6Rα (1.3 fold increase in non-miliary compared to miliary, p=0.05) and SCF (1.6 fold increase in non-miliary compared to miliary, p=0.09) showed increasing trend in non-miliary (Fig. 24 A-C). Additionally, these factors have been revealed to promote not only tumor growth, but also migration, invasion of tumor cells during metastasizing [98, 99]. Also other growth factors, such as osteopontin, follistatin, sHER2neu, HGF and leptin were moderately elevated in ascites in non-miliary spread type (data shown in the supplement). Another important observation was that several growth factors, which stimulate angiogenesis, were measured in significantly higher levels in ascites of non-miliary type compared to miliary. These include FGF-basic (2.5 fold increase in non-miliary compared to miliary, p=0.0028), PDGF-αβ_ββ (1.5 fold increase in non-miliary compared to miliary, p=0.03) and sVEGFR1 (3.2 fold increase in non-miliary compared to miliary, p=0.01, Fig. 24 D-F). Also, sVEGFR2 was raised in ascites of the non-miliary spread type, albeit not sifnificant (1.4 fold increase in non-miliary compared to miliary, p=0.21, data shown in the supplement). The Bio-Plex Pro^{TM} Human Cancer Biomarker Assay (Bio-Rad, CA, USA) allowed only detection of VEGF receptor expression and not of VEGF. Studies reported about highly increased VEGF productions, associated with elevated VEGFRs in ovarian cancers [132-134]. In addition, both VEGF overexpression and VEGFR mediated signaling are revealed to be major angiogenesis driving factors [135]. Therefore, it is assumed that higher levels of receptors, what we have measured, associate with VEGF elevation in ascites.

Prolactin is a growth factor, which was reported to be overexpressed in ovarian cancers and correlated with tumor development [118]. Specifically its role in modulating the immune function in case of ovarian tumor related inflammation was discussed [118]. This growth factor was increased significantly in ascites of the non-miliary spread type compared to miliary (5 fold increase in non-miliary compared to miliary, p=0.005), indicating again a pro-inflammatory condition in non-miliary associated ascites (Fig 24G).

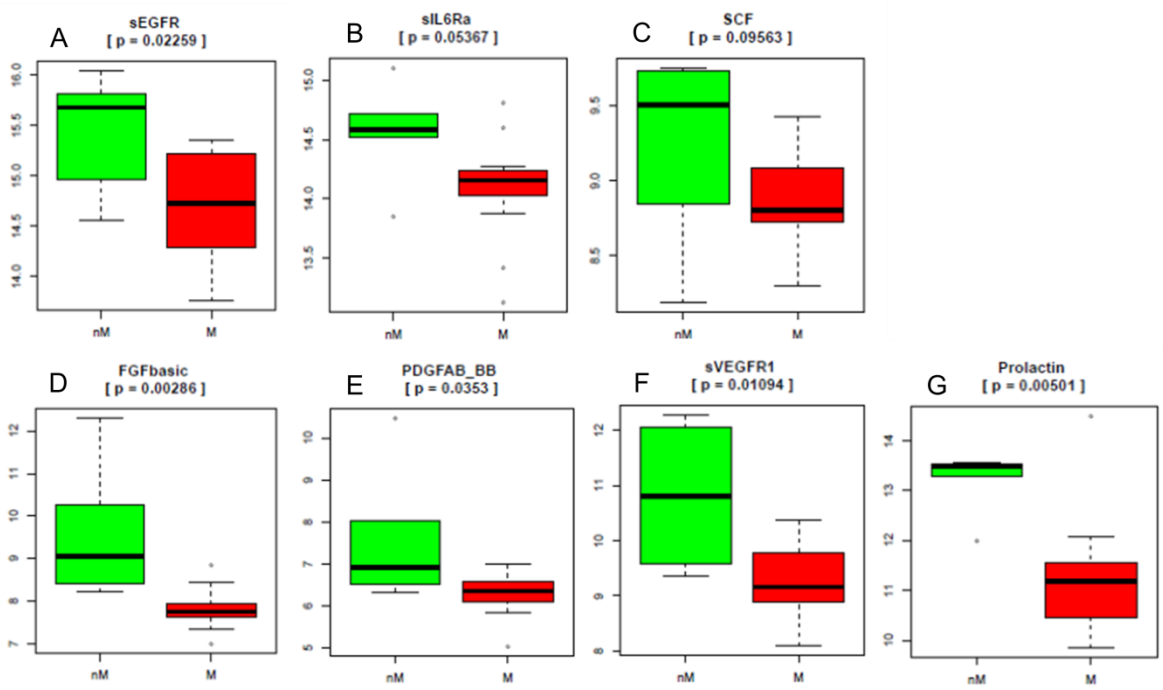

Figure 24: Measurements of growth factors in ascites. The concentrations of 20 different growth factors were measured in ascites of two distinct metastatic spread types using Luminex 200 system. Growth factors such as sEGFR (A), sIL6Rα (B) and SCF (C) can be assigned to increased tumor growth and metastasis, whereas FGF-basic (D), PDGFαβ_ββ (E) and sVEGFR1 (F) are well-known angiogenesis promoting factors. Prolactin, as an immune modulating factor (G).

Discussion

Recently, two different patterns of metastatic spread were proposed in the peritoneal cavity of HGSOC patients: the miliary type is characterized by spread of small implants widely distributed in the peritoneum, whereas the occurrence of few large implants is described as non-miliary spread. We postulated that inflammatory conditions in ascites of HGSOC patients contribute to the development of these two different metastatic types, because inflammatory alteration in the peritoneal cavity is known to affect tumor development, markedly [32]. Specifically, varieties of leukocytes determine different inflammatory conditions in ascites and monocyte derived populations, including TAMs are shown to play a major role in metastasizing [47, 97]. In addition, ascites provides a large source of soluble immune-modulatory factors, which trigger inflammation and support metastasis [35, 98].

Therefore, this project aimed at characterization of immune cell populations and their control through immune-modulating cytokines and growth factors in ascites, with particular focus on monocytes and macrophages, in order to determine their role in the development of two distinct metastasizing modes.

Tumor and immune cell content in ascites varies between two different metastatic spread types

Cancer related inflammation is characterized by a high number of leukocyte infiltration in the tumor microenvironment [44-46]. In the peritoneal cavity, sustained accumulation of a high number of TILs due to chronic inflammation is described [46, 56]. In accordance with that, monocytes, TAMs, T lymphocytes, specifically Treg cells, B cells and DCs were described as the most abundant immune cell populations in malignant ascites, but not NK cells [58, 136]. The analysis of the cell composition in ascites showed that tumor cells and immune cells together account for 18-90% of the total cell population. This result suggested the manifoldness of cells in ascites. Accumulation of different cell populations in ascites facilitates a dynamic interplay between different cell types, specifically between tumor cells and immune cells. These cell-cell interactions further determine the feature of tumor growth or metastasis and thereby, the balance between immunosurveillance and immunoediting at tumor site [44, 49, 50]. Therefore, investigation of immune cell composition in ascites can provide a coherent view over the inflammatory condition and the metastatic pattern in ascites. Quantification of cells by multicolor IF analysis

in ascites revealed that miliary and non-miliary metastatic spreads differ considerably in their cell content. Ascites of non-miliary spread type was characterized by high $CD45^+$ immune cell numbers. On the contrary, ascites in miliary type tend to contain a high number of $EpCAM^+$ tumor cells compared to non-miliary.

Main regulators of the immune system are various chemoattractive and immune-modulatory factors, such as chemokines and cytokines. They also play a crucial role in inflammation. As major determinants of cancer related inflammation, they are suggested to be an important factor in spread of malignant metastasis in the peritoneal cavity [65, 66]. With the analysis of cytokines and chemokines in ascites, pro- and anti-inflammatory immune modulations can be estimated, which may indicate variations between the two different metastatic patterns. An important observation from cytokine and chemokine measurement was that ascites contained higher levels of the majority of the total 56 determined cytokines, chemokines and growth factors compared to serum. Many studies have confirmed the maintenance of high concentrations of cytokines in malignant ascites, which were mostly associated with an immunosuppressive effect [43, 65]. Our cytokine and chemokine measurements indicated also a highly increased release of these immune modulators in ascites compared to serum. Only, concentrations of two chemoattractants, including neutrophil chemoattractants CXCL2 and Treg attracting chemokine CCL17 were decreased more than twofold in ascites compared to corresponding serum chemokine concentrations. These results indicate that ascites may facilitate attraction and polarization of high numbers immune cells, which associates with pro-inflammatory role of ascites.

Furthermore, the comparison of important chemokines in ascites between the two metastatic groups revealed that particularly chemokines were differently represented. These include primarily, the B cell specific chemokine CXCL13 and the neutrophil chemoattractant CXCL6, which were found to be significantly increased in ascites of the miliary spread type. Because, CXCL13 is a strong attractant for B cells besides CXCL12, which also showed a trend of increased levels in miliary spread type, B cells seem to be more attracted into ascites of patients with the miliary tumor spread type. Although neutrophil chemoattractant CXCL6 was significantly increased in ascites of miliary spread type, other neutrophil specific chemokines in ascites did not show any association with different metastatic phenotypes. In addition, NKT cell chemoattractants CXCL12 and CX3CL1 were elevated in ascites of the non-miliary

type. So ascites of non-miliary type could be interrelated with attraction of high numbers of NKT cells.

In addition, a cytokine/chemokine set analysis was performed using QuSAGE, where immune-modulatory mediators belonging to the same pathway were analyzed with regard to differences in the tumor spread types. B cells and M1 characteristic macrophage targeting cytokine and chemokine groups were identified as main contributors, which were most significantly varied between the two metastatic spread types. In sera of the patients, no cytokine or chemokine groups were detected, which associated with differences between the two metastatic spread types. From these analyses, I conclude that ascites in general contains high numbers of a variety of immune cells sustaining tumor related inflammation, which differ between the two spread types.

Two different metastatic patterns are associated with distinct inflammatory conditions in ascites

It was reported that initially high numbers of $CD4^+$ T cells infiltrate into ascites, which determine the formation of a chronic inflammatory environment by supporting the accumulation of various other components of the immune system into the premalignant tumor site [41, 111]. Specifically, neutrophils and macrophages then contribute to persisting inflammation and malignancy [58]. The analysis of the cell content in ascites demonstrated that ascites represents a complex milieu, comprising varying cell populations, including different types of immune cells. With further analysis of chemokines and immune-modulatory cytokines, we wanted to define the inflammatory condition in ascites. As to the question, whether an inflammatory condition affecting the composition of various immune cells in ascites is correlated with different metastatic patterns, concentrations of common cytokines of pro-inflammatory and anti-inflammatory origins were determined in two patient groups. Upon analysis of typical pro-inflammatory cytokines, including GM-CSF, IL-1β, IL-2, IL-6, IFN-γ and TNF-α, high concentrations of GM-CSF were measured in ascites in the non-miliary spread type. In addition, other pro-inflammatory cytokines showed a tendency of elevation in ascites of the non-miliary type, except for TNF-α. However, TNF-α was also reported to show both pro- and antitumor responses dependent on local concentrations and on its expression site in the tumor, e.g. whether they are acting on epithelial cells or on the inflammatory cells in the surrounding stroma [49, 137]. On the contrary, significant lower levels of an important immune suppressive

cytokine IL-10 were measured in non-miliary ascites. IL-10 acts as immunosuppressive cytokine by inhibiting functions of DCs and macrophages, by virtue of Th2 response activation. In tumors, a high amount of IL-10 was revealed to allow tumor cells to evade immune surveillance by activating TAM mediated immunosuppressive response [41, 78]. Therefore, an elevated IL-10 value in ascites in the miliary spread type may indicate an anti-inflammatory milieu associated with presence of more tumor cells. Thus, I suggest that the two different metastatic modes probably developed in accordance with differentiating inflammatory responses in ascites, facilitated by attracting various cell populations and by producing of particular soluble chemokines and cytokines. In fact, in ascites of patients with the non-miliary spread type, which was characteristic of high numbers of immune cells, displayed a more inflammatory active tumor microenvironment as seen in increased concentrations of some pro-inflammatory cytokines. In contrast, miliary associated ascites was characterized by an immunosuppressive milieu mediated by inhibitory IL-10, which seemed to promote circulation of elevated number of tumor cells.

To validate results for pro- and anti-inflammatory cytokines in ascites, additionally, levels of common immune cell recruiting chemokines were analyzed.

An inflammatory condition in tumors is mostly reported to be associated with accumulation of activated T cells, whereas an immunosuppressive tumor microenvironment is linked to a high amount of inactivated naïve T cells, immature DCs without antigen presentation and TAMs [55, 56]. In tumors, Tregs are also reported to act immunosuppressively or pro-tumorigenic by suppressing T cell mediated antitumor immune response [44, 50, 56]. Chemokines, which are responsible for T cell and DC recruitment in response to inflammation and inhibitory Treg specific chemokines, did not provide evidence of metastatic spread specific alteration. Chemokine analysis indicated significantly elevated NKT cell chemoattractants in ascites in the non-miliary spread type.

Interestingly, growth factor measurements delivered additional confirmation of a pro-inflammatory milieu in non-miliary ascites. One of strong inflammatory reaction modulating factors in advanced ovarian cancers is prolactin [117, 118], which was revealed to be produced in very high level in non-miliary associated ascites.

In conclusion, these data indicate that ascites of non-miliary spread type is associated with more inflammatory responses by recruiting high number of immune cells with specific NKT cell attraction. On the other hand, miliary specific ascites is characterized by high tumor cell presence and IL-10 mediated immunosuppressive

response. I also demonstrated that ascites in the miliary spread type is characterized by a high amount of B cell attractants in ascites. B cells can also play a pro-tumor role, since B cells were shown to infiltrate in high numbers into the peritoneal microenvironment and correlated with worse patient outcome [76, 77].

It was shown that ascites in the two different metastatic modes vary in their tumor and immune cell compositions. Since monocyte derived populations, specifically TAMs were shown to not only play a crucial role in sustaining immunosuppressive condition [55, 78, 85], but also contribute to metastatic development actively, their distribution and regulation were investigated in more detail.

Macrophages in ascites reveal two distinct differentiation phenotypes related to the two metastatic spread types

Monocyte derived cells are the most abundant cell population in ascites [44, 71] and play important roles in almost every step of the tumor development, primarily with tumor promoting effects [54, 71]. Induced by hypoxia, monocytes and macrophages accumulate in the tumor microenvironment in high abundance and macrophages are shown to be involved in metastasis by promoting collective migration with tumor cells [54, 88]. Monocytes and macrophages are very heterogeneous due to various differentiating phenotypes including DCs, macrophages and their subtypes [54].

To investigate the role of monocytes and macrophages in the two different modes of tumor spread, I first carried out IF analysis with the markers CD14 and CD16 and determined their distribution in ascites. Some studies based on FACS analysis with these antibody combinations identified up to five different monocyte and macrophage populations [70, 92], which indicates heterogeneity of this cell population. According to the IF analysis carried out in this project, high amounts of $CD14^+$ and $CD16^+$, as well as $CD14^+/CD16^+$ double positive cells were present in non-miliary ascites compared to miliary ascites. In addition, PCA analysis was performed to ascertain phenotype specific clustering of the two different metastatic spreads. The results showed clear differentiation in ascites of the two distinct groups of miliary and non-miliary types.

Macrophages derive from circulating monocyte precursors and produce two main differentiated subclasses M1 and M2 [138, 139]. Under condition of cancer induced inflammation, monocytes differentiate mostly to TAMs showing a more alternatively activated tropic M2 related phenotype in the tumor microenvironment [139]. The differentiation of M1 and M2 is highly regulated by different pro-inflammatory or anti-

inflammatory cytokines, thus dependent on inflammatory responses in the tumor microenvironment [138].

Next, cytokines and chemokines involved in monocyte recruitment and macrophage differentiation were examined to demonstrate their role in the two different metastatic spread types. The majority of the circulating monocytes are known to be attracted classically through the action of locally produced chemotactic factors such as CSF-1 or CCL2, CCL3, CCL8, CCL13, CXCL12 and CXCL11. Of these chemokines, only the concentration of CCL3 was significantly increased in ascites compared to serum. In addition, in combination with CCL7, CCL3 was revealed to be elevated in ascites in non-miliary ascites. As majority of these chemokines did not show a clear indication of significant alteration in ascites of the two malignant metastatic types, macrophage differentiating signals were considered.

Classically M1 polarized macrophages are typically activated by IFN-γ and GM-CSF mediated by Th1 helper cell responses [55]. Analysis of M1 specific cytokines revealed that the M1 differentiation mediator GM-CSF was highly increased and IFN-γ showed an elevation as trend in ascites of the non-miliary spread type. These cytokines indicated a slight raise in ascites of the non-miliary spread type.

On the contrary, alternatively activated M2 polarized macrophages differentiate in response to IL4, IL-10, and IL-13, released mostly by $CD4^+$ Th2 cells [138]. First, the cytokine measurements in both ascites and serum showed significantly increased concentrations of M2 differentiation stimulating factors in ascites; specifically, the concentration of IL-6 was increased more than threefold. Second, in ascites of miliary spread type, significantly higher IL-10 concentrations were measured compared to ascites in non-miliary spread type. Therefore, it appears that in ascites of the miliary spread type is representative of high concentrations of M2 macrophage characteristic cytokines, which may in turn be involved in mediating an IL-10 dependent immunosuppressive response. In comparison to this, ascites of the non-miliary spread type may allow differentiation of M1 macrophages in a more inflammatory milieu.

MIFs are considered as major regulators of inflammation in ascites [89]. Studies revealed that MIF is mostly downregulated in ovarian cancers in order to attenuate macrophage infiltration in ascites [71, 89]. Activation of MIF leads to release of cytokines, which have supporting role in M1 macrophage differentiation e.g. IL-12 [89]. It was also reported to inhibit the release of TAM promoting cytokines, such as IL-6, TNF-α [98, 99]. According to our cytokine measurement, the MIF concentration

was higher in ascites, more extensively in the non-miliary type. This result supports our assumption that ascites of the non-miliary spread type maintain inflammatory active milieu with more M1 differentiated macrophages.

Additionally, CCL12 and CXCL12 in combination with TNF-α and IL-6 secretion were reported to promote TAM associated migration and angiogenesis in SOC [48, 71, 127]. Several studies approved reinforcement of TAM dependent metastasis and invasion, correlated with a high dispersed tumor grade due to increased secretion of so called 'TNF network', which includes CXCL12, IL-6 and TNF- α [48, 71, 98]. As expected, higher levels of CXCL12 were determined in ascites compared to serum. Moreover, a slight increase of CXCL12 and TNF-α was observed in immunosuppressive ascites of the miliary spread type. Taken together, it appears that differentially modulated inflammatory conditions in ascites of HGSOC patients associate with distinct macrophage differentiation features. Because metastatic progression in advanced ovarian cancers has been shown to be associated largely with immunosuppressive TAMs [54, 78, 85], I suppose that distinct inflammatory conditions in ascites are the driving force behind the two different metastatic spread types with varying macrophage differentiation phenotypes.

Various angiogenesis promoting growth factors contribute to different tumor spread types

To examine whether factors in ascites, other than cytokines and chemokines, also contributed to the progression of the two different metastatic phenotypes, we determined concentration of 16 different growth factors in ascites and serum of HGSOC patients.

Many growth factors in the tumor microenvironment as well as in angiogenesis, supporting cytokines and chemokines were overexpressed in malignant ascites and provide for maintenance of tumor growth and progression [5, 140]. Among these CCL2, CCL12, MIF, TNF-α and CXCL12, mainly produced by TAMs, were reported to stimulate production of angiogenic factors such as VEGF, PDGF, CXCL8 (IL-8) and PDGF [46, 47, 58, 71, 141]. Furthermore, VEGF released from ovarian carcinoma cells was found to be involved not only in angiogenesis stimulation but also in production and accumulation of ascites due to its ability to change the permeability of the peritoneal membrane [35, 41]. Determination of growth factor concentrations in ascites revealed that 17 of 20 measured growth factors were higher in ascites of non-miliary spread type. Of these, sEGFR, sIL-6Rα, and SCF

concentrations were significantly higher. These results demonstrate that ascites provides a tumor promoting milieu and supports migration, invasion of tumor cells by activating the majority of tumor growth factors.

Interestingly, detailed growth factor analysis indicated that several angiogenesis promoting factors were synthesized in significant high levels in ascites of the non-miliary type. These included FGF-basic, PDGF-αβ_ββ and sVEGFRs, particularly sVEGFR1. Because ascites in the non-miliary spread type was characterized by growth of few large implants at the peritoneum, I suggest that angiogenesis promoting growth factors together with other in ascites highly elevated tumor growth factors may determine the development of metastasis in the peritoneal cavity and allow tumors to gain in size.

It was also reported that ovarian cancer metastasis cannot grow greater than 1mm without blood vessel formation [6]. Therefore, I postulate that few, large implants developed in the non-miliary spread type are highly promoted by angiogenesis promoting growth factors in ascites, whereas in ascites of the miliary spread type, these growth factors are present in rather low level, which affect tumor growth less strongly. Encouraged by the immunosuppressive milieu in ascites in the miliary spread type, high numbers of tumor cells seem to colonize throughout the peritoneal cavity to develop many small, widely distributed implants. However, their growth is not strongly supported as in ascites in the non-miliary spread type due to less availability of growth factors and angiogenesis stimulating factors. Therefore, ascites probably constitutes the main source of immune-modulators, which is involved in determining metastatic patterns in the peritoneal cavity.

Conclusion

In this project, two distinct metastatic spread phenotypes of HGSOC patients were characterized, performing the following analysis: i) ascitic immune cell populations were characterized using IF, specifically by considering $CD14^+$ and $CD16^+$ cells, such as monocytes, macrophages and DCs, as well as $CD16^+$ NK cells and neutrophils and ii) soluble content of ascites, including immune-modulating cytokines, chemokines and tumor growth factors were analyzed using highly multiplexed immunoassays.

Ascites from patients exhibiting the miliary metastatic spread type, which is characterized by many small implants, revealed high numbers of tumor cells and a lower percentage of immune cell populations, compared to ascites in the non-miliary

spread type. In addition, analysis of cytokines and chemokines revealed a predominant immunosuppressive milieu. Although ascites in the miliary spread type was shown to promote tumor cell homing, metastasis of tumor cells on the peritoneum does not seem to depend on angiogenesis and common tumor growth factors because of the low concentration of angiogenesis promoting factors and other growth factors in ascites (e.g. FGF-basic, PDGF-αβ_ββ and sVEGFR). This may explain, why in miliary spread type, the metastasizing implants remain small, but spread aggressively in the peritoneal cavity. The metastasizing behavior of these tumor cells could also be supported by the immunosuppressive environment and probably further by differentiated TAM accumulation.

On the contrary, HGSOC patients with non-miliary spread of metastasis revealed a more inflammatory ascites, characterized by accumulation of high inflammatory cytokines such as IFN-γ, GM-CSF and MIF. Furthermore, high immune cell frequencies, including $CD14^+$, $CD16^+$ and $CD14^+/CD16^+$ and NKT cells were present in ascites. Moreover, macrophages with more M1 differentiated phenotypes seemed to be favored in ascites in the non-miliary metastatic spread type. However, which role M1 differentiated macrophages are playing in ascites of non-miliary spread type, could not be elucidated. In addition, ascites in the non-miliary spread type was indicated to have more tumor growth and angiogenesis promoting effects.

The final conclusion is that non-miliary and miliary metastatic spreads differ markedly due to varying inflammatory conditions in ascites. Ascites creates an environment, which determines composition of cell populations at the tumor site and regulates cancer related inflammation by manipulating immune-modulatory factors. Furthermore, prevailing conditions in ascites was shown to be associated with two described metastatic spread modes in HGSOC patients.

Outlook

This project revealed inflammatory differences in ascites of miliary and non-miliary spread types. The results from IF analysis and cytokine and growth factor measurements showed that two different metastatic spread types vary markedly in their tumor and immune cell content and cytokine, chemokine as well as growth factor expressions. A further validating analysis with more patients is necessary for more accuracy. For IF analysis $CD14^+$ and $CD16^+$ surface markers were used to detect monocytes and macrophages. However, other immune cells such as NKs, DCs and neutrophils were also reported to express them on their surface. Thus,

further IF staining or FACS analysis with more specific markers should be performed for more detailed distinction. Furthermore, I observed several important trends (CXCL3, CXCL7, CXCL12 and sVEGFR2), which could be assessed. Particularly, the B cell attractant CXCL13 showed clear differentiation in ascites between two different metastatic spread types. B cell markers were not included in the IF panels, but should be considered for further analysis. Finally, VEGFR1 and VEGFR2 detection indicated that ascites may create a milieu, which supports angiogenesis differentially in the two metastatic spread types. Unfortunately, only the detection of VEGF receptor expression was possible in the test. Therefore, the determination of VEGF concentration in ascites could deliver further, interesting results.

Part II

Characterization of Proliferating CD45 and EpCAM Double Positive Cells in Ascites of an Ovarian Cancer Patient with Two Different TP53 Mutations

Introduction

During IF staining analysis, an unusual cell population in ascites of a HGSOC patient was observed, which was shown to co-express the pan-leucocyte cell marker CD45 and the epithelial cell surface marker EpCAM in higher amounts compared to the other patients (10% vs 0-5%). The existence of these double positive cells ($CD45^+/EpCAM^+$) was reported before. Interestingly, they discussed the involvement of macrophages, that double positive cells could result from fusion of a macrophage with a tumor cell in the presence of inflammatory cells [142]. For further determination of the cell phenotype and to characterize their origin in the patient, we performed TP53 mutation analysis by ddPCR, a new and accurate method [143].
The analysis led to the interesting observation that the patient carried two different TP53 mutations distributed independently: one in ovarian tumor and the other in the peritoneal tumor mass, exclusively. This case was investigated further and a case report was prepared.

TP53 gene mutation

The mutation of the tumor suppressor gene, TP53 is regarded as an important driver in cancer onset and progression. Hence, structure and function of common mutations have been studied extensively since its discovery [144-146].
The gene is mutated at almost every codon of the DNA binding core domain, shown in many different tumor types. However, mutations mostly occur in clusters and in varying frequency at certain hot spot regions and different tumor types show specific mutational spectrums [147, 148]. Among all reported TP53 mutations, missense mutations are more common [149, 150]. The structure of the wild type and most frequent mutants of the p53 protein were well characterized by NMR [151-153] and in complex with its cognate DNA by X-ray [154-158]. The TP53 gene consists of eleven exons and encodes for four functional domains including a hydrophobic central core region with specific DNA binding sequences spanning exons 5-8, flanked by an acidic N-terminal transactivation domain and a basic C-terminal oligomerisation and regulatory domains.

Part II

The central core domain is of special interest (Fig 25). It contains several structural features as described in figure 25. The main core domain binds specifically to double stranded target DNA at the 10 base-pair motif 5'-PuPuPu-C(A/T)(T/A)GPyPyPy-3' [159]. The residues from the loop-sheet-helix motif contact the major groove of bound target DNA, whereas the L3 loop is anchored to the minor groove via Arg-248.

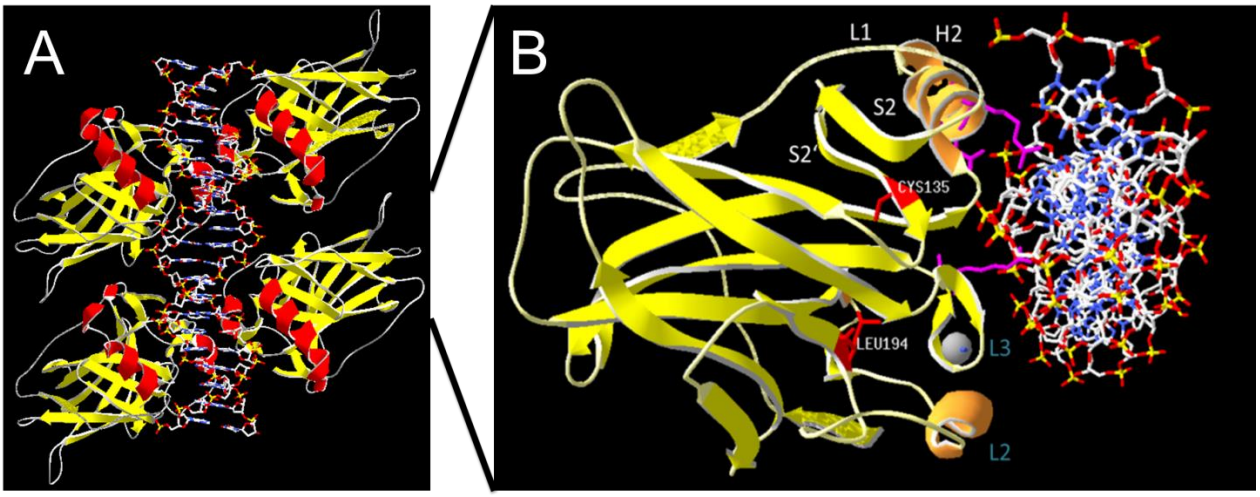

Figure 25: The structure of human wildtype p53 with its consensus DNA sequence (A) and specific features (B). (A) Four functional domains including a hydrophobic central core region with specific DNA binding sequences are depicted. **(B)** The specific surface is formed by two large loops L2 (164-194), which are interrupted by a short H1 helix and L3 loop (237-250). The surface is stabilized by an immunoglobulin-like central β-sandwich of two antiparallel β-sheets, which provides a basic scaffold for the DNA binding surface and a loop-sheet-helix motif including L1 loop, β-strands S2 and S2'. The end of the extended β-strands S10, and the C terminal helix H2 are involved in DNA binding. The zinc ion is also involved in structure stabilization and coordinated by a histidine and three cysteine side chains (Cys-176, His-179, Cys-238 and Cys-242). PDB ID: 4HJE [160].Structures were created using Swiss-PdbViewer v4.1[161].

Structurally, mutants are differentiated into DNA contact mutants, located at DNA-binding contact sites and structural hotspot mutations, located at crucial structure stabilizing sites [162]. The mutations can result in loss of the p53 wild type allele, resulting in sole expression of mutant proteins [163]. However, particular mutants can either retain the physiological conformation but interferes with protein-protein interactions and with other regulatory elements or exhibit temperature sensitivity [6, 162]. Moreover, many mutants show increased activity including altered transactivation, gain of novel transforming function, or a dominant negative effect over the wild type gene [149]. The consequence of these versatile mutant conformations is that most p53 mutant proteins accumulate in the nucleus of affected tumor cells [154, 164]. Interestingly, various TP53 somatic mutations are associated

with different penetrance and tumor phenotypes, which do not always give rise to accumulated proteins in the nucleus [165]. Due to dynamic instability of TP53 gene mutations, advantageous mutants are clonally selected for tumor cells under tumor promoting conditions, e.g. hypoxia [150, 166, 167]. Although mutational structures and frequencies in various cancer types have been extensively studied, the main link between the mutation spectrum and its functional role in disease progression is still missing.

TP53 gene mutation in ovarian cancer

One of the best known tumor types - reported to be high frequently mutated in the TP53 gene - is serous ovarian carcinoma (SOC) [168]. Specifically at advanced stages, i.e. FIGO III-IV stages, the (over)expression of mutant proteins was found to be higher than in low grade ovarian tumors. According to the International Agency for Research on Cancer (IARC) TP53 database [169], 78% (552) out of 706 analyzed SOCs have been shown to be mutated. Among all SOC cases 70% were missense mutations (657/970). According to the cosmic database, 66% of all detected SOCs were TP53 mutated (804/1217), from this 57% were missense mutations (874/1135) [170]. In addition, it was shown that the mutation frequency can reach up to 96% in HGSOC [22]. Furthermore, loss of wild type p53 is shown to confer an aggressive phenotype associated with more rapid metastatic dissemination in the peritoneal cavity [171]. Participation of TP53 mutations in the pathogenesis of HGSOC was demonstrated in mouse models [6, 172]. Most protein inactivating mutations were reported to be associated with a more aggressive histological types [6, 173], whereas gain of function mutations within TP53 hotspots [174, 175] were shown to be involved in increased distant metastasis [172].

Part II

Aim of the project

Based on identified $CD45^+/EpCAM^+$ double positive cells in ascites from a HGSOC patient, we aimed to characterize the tumor phenotype with further tumor- and immune cell markers. Although, the existence of atypical cells expressing EpCAM and CD45 simultaneously was reported before–mainly in the field of circulating tumor cells in blood–we characterized their phenotype in ascites of a HGSOC patient by IF combined with confocal and fluorescence microscopy.

In order to investigate if double positive cells ($CD45^+/EpCAM^+$) are of cancerous origin, we performed TP53 mutation analysis by ddPCR and compared their status to that of the ovarian cancer mass, peritoneal implants and cancer cell aggregates isolated from ascites of this patient.

Methods

Overview of patient information and sample summary

A 50 years old patient was diagnosed with HGSOC (grade 3, FIGO stage of IIIc and serum CA125 concentration 191.9 kU/L). Before chemotherapy the patient underwent primary cytoreductive surgery, during which tumor masses from both ovaries and several peritoneal masses (in the omentum majus, appendix vermiformis, ligamentum falciforme, Douglas pouch biopsy, diaphragm and lymph node implant in mesocolon), as well as ascites were obtained.

Collection and preparation of ovarian and peritoneal tumor masses

Ovarian and peritoneal tissues, obtained during surgery, were immediately transferred to buffered growth medium (DMEM + 10 mM HEPES, pH 7.2). Tissues were cut into small pieces. Centrifuged at 120 x g for 2 min, the collected tissue pieces were digested in a mix of Liberase DH (0.26 U/ml, 400 mg) in DMEM (10 mM HEPES, pH 7.2) for 60 min at 37°C. The reaction was stopped by adding 10 µl fetal calf serums (FCS). The cell suspension was filtered through a 40 µm cell strainer followed by 2-3x rinsing with DMEM supplemented with 4 mM EDTA. The cells were centrifuged at 120 x g for 10 min and the pellet was washed twice in PBS. At last cells were re-suspended in 1ml DMEM and either cryostored at -80°C (addition of 5% DMSO to growth medium) or prepared immediately for cell enrichment as described below.

Part II

Collection and preparation of cells and tissue slides from tumor implants and ascites of the patient

All patients' materials were procured directly from the surgery. Sample overview:

sample names	origin	preparations and methods
ovarian mass I	ovar	total EpCAM enriched cells
ovarian mass II	ovar, random region 1	microdissected from FFPE
ovarian mass III	ovar, random region 2	microdissected from FFPE
ovarian mass IV	ovar	WGA EpCAM positive cells
ascites tumor cells I	peritoneal cavity	total tissue
ascites tumor cells II	peritoneal cavity	EpCAM enriched cells from ascites
spheroids	peritoneal cavity	spheroids selectively cut from FFPE
double positive cells I	peritoneal cavity	picked $EpCAM^{+}/CD45^{+}$ cells
double positive cells II	peritoneal cavity	picked $EpCAM^{+}/CD45^{+}$ cells
ascites tumor cells III	peritoneal cavity	random picked cells
peritoneal mass I	random tissue implant	total EpCAM enriched cells
peritoneal mass II	omentum majus	microdissected from FFPE
peritoneal mass III	appendix vermiformis	microdissected from FFPE
peritoneal mass IV	diaphragma	microdissected from FFPE
peritoneal mass V	random tissue	microdissected from FFPE
peritoneal mass VI	lymph node implant in mesocolon	IF staining
peritoneal mass VII	ligamentum falciforme	IF staining
peritoneal mass VIII	Douglas pouch biopsy	IF staining
peritoneal mass IX	diaphragm	IF staining
peritoneal mass X	random tissue	total EpCAM enriched cells
plasma	blood	free circulating nucleic acid
serum	blood	free circulating nucleic acid

Table 4: Overview of sample preparations and analysis: Different processed ovarian tumor masses, peritoneal tumor masses and ascites preparations are indicated in roman numerals (I-VI). Preparation methods reveal various strategies used in quantification of cells or validation of mutational analysis.

Collection and preparation of ascites cells

Cell aggregates, also referred to as spheroids and single cells from the ascites were separated using 30 µm (retentate contained spheroids) and 20 µm filters (flow through contained single cells) (BD, NJ, USA). The filters (cell strainer) were washed once with 1x phosphate-buffered saline (PBS). The spheroids were collected from

the 30 µm cell strainer by inverting the cell strainer and washing the membrane with 5 ml pre-warmed DMEM. Single cells were collected in Dulbecco's modified eagle medium (DMEM) (Life Technologies, CA, USA) containing 0.5M Ethylenediaminetetraacetic acid (EDTA) (stock: 4mM, Sigma-Aldrich, MO, USA). After centrifugation at 120 x g for 10 min, both spheroids and single cell pellets were washed twice in PBS and re-suspended in ascites supernatant containing 5% dimethylsulfoxide (DMSO) (stock: 4mM, Sigma-Aldrich, MO, USA) for freeze alive.

Enrichment of $EpCAM^+$ tumor and $CD45^+$ immune cells from ovarian and peritoneal tissues and ascites preparations

For enrichment of CD45 and EpCAM positive cells from ascites and processed tumor tissues Macs multi and Vario Macs technology (Miltenyi biotec, Bergisch Gladbach Germany) was used. At least 5 x 10^6 cells were re-suspended in 7.5 ml DMEM and 2.5 ml 4x Miltenyi buffer was added. The well mixed CD45 or EpCAM beads were washed in 1ml Dynabeads wash buffer containing 1x PBS, 0.1% BSA, 0.6% sodium citrate on a magnetic stand. Beads were re-suspended in 50 µl PBS-T and added to the prepared sample. The mixture was incubated for 20 min while shaking at 4°C and bead bound cells were subsequently separated using Macs multi and Vario Macs columns according to the manufacturer's instructions.

Preparation of FFPE tissue slides

FFPE tissue sections were prepared as outlined before.

IHC and microdissection of FFPE tissue slides from ovarian and peritoneal tumor masses

Immunohistochemistry (IHC) staining was conducted according to standard protocol. Tissue slides were stained with haematoxylin for 2 min and the staining was stopped by rinsing the slides with water for about 10 min. Slides were counterstained with 0.5% Eosin-G solution for 45 sec. After stopping the reaction by rinsing with water, tissues were dehydrated with following ascending alcoholic treatment in 70%, 80%, 96% and 100% ethanol, respectively. FFPE tissue sections for microdissection were prepared on specific membrane slides to micro-dissect areas with predominantly tumor cells with mmi CellCut laser system (mmi, Glattbrugg, Switzerland).

Part II

Immunofluorescence and cell quantification of FFPE tissue sections

IF-staining of double positive cells was performed as described above. For double positive cell staining anti-CD45 (dilution 1:1000, source rat, isotype IgG2b, clone orb96558, Biorbyt, Cambridge, UK), anti-EpCAM (dilution 1:300, source mouse, isotype IgG1, clone VU1D9, Cell Signaling, Cambridge, UK) and anti-EpCAM (dilution 1:300, source rabbit, isotype IgG, clone E144, Abcam, Cambridge, UK) primary antibodies and for phenotype characterization anti-CD16 (dilution 1:50, source mouse, isotype IgG2a, clone 2H7, Thermo Scientific, MA, USA), anti-pan-cytokeratin (dilution 1:200, source mouse, isotype IgG1 CK8, 18, and 19, clone A45-B/B3, AS Diagnostics, Lancashire, UK), anti-CD44 (dilution 1:1000, source mouse, isotype IgG2a, clone 156-3C11, Cell Signaling, Cambridge, UK), anti-p53 (dilution 1:125, source mouse, isotype IgG2a, clone DO-1, Merck Millipore, MA, USA), anti-Ki67 (dilution 1:400, source rabbit, isotype IgG1, clone MIB-1, Dako, Glostrup, Denmark) and anti-CD14 (dilution 1:250, source rabbit, isotype IgG, clone EPR3653, Novus Biologicals, CO, USA) primary antibodies were used. For detection different goat Alexa Fluor® (Life Technologies, CA, USA) fluorescence labeled anti-rat, anti-mouse IgG1, anti-mouse IgG2a and anti-rabbit secondary antibodies were used. The nuclei were counterstained with DAPI. The positively stained cell components were imaged with TissueFAXC fluorescence microscopy (TissueGnostics) and laser scanning microscopy (Zeiss, LSM-700). Positively stained cells were quantified using automated cell analyzing software CellProfiler v.2.1.1 [120]. The analysis pipeline consists of image processing, illumination correction of images and cell identification based on fluorescence intensity measurements.

Picking of single cells, labeled with magnetic Dynabeads of different sizes

At least 10^6 ascites cells were prepared in 2 ml 1x PBS. Half of the cells suspension was first incubated with 1 µl/ml rabbit anti-CD45 antibody (clone E19-G, BD Biotech, NJ, US) (4°C, at least 20 min, rolling) followed by 20 µl/ml cell suspension Dynabeads® M280 sheep anti-rabbit IgG with a size of 2.8 µm to label $CD45^+$ antibody coupled cells (4°C, at least 20 min, rolling). 32.5 µl/ml 4.5 µm human EpCAM Dynabeads (Dynabeads® Epithelial Enrich magnetic beads, Ber-EP4, Invitrogen, CA, USA) were added to other half of the cells suspension to label $EpCAM^+$ cells (4°C, at leastc 20 min, rolling). Single $CD45^+$ or $EpCAM^+$ cells (labeled with 2.8 µm or 4.5 µm Dynabeads, respectively) were picked in 1x PBS using mmi

CellEctor Plus system using mmi CellTools v.4.3.2 software (MMI, Glattbrugg, Switzerland).

Isolation of DNA from whole tissue, FFPE tissue sections and EpCAM enriched tumor cells from ascites and total tissue pellet

Genomic DNA from the FFPE tissue sections (including ovarian tumor and four different peritoneal implants) and with magnetic beads enriched $EpCAM^+$ cells were isolated using QIAamp Qiagen FFPE DNA kit protocol from FFPE tissue sections (QIAGEN, Venlo, Niederlande) and 2x 12 µl DNA was eluted in ATE buffer at RT. DdPCR was performed with obtained DNA [143].

DNA extraction from picked single cells and the WGA

In order to extract DNA from single or few picked cells, cells were lysed with 5 µl lysis buffer containing 200 mM KOH and 50mM dithiothreitol (DTT), mixed 1:1 according to the previously described protocol [176].

The suspension was mixed gently, centrifuged briefly and incubated at 65°C for 10 min. The reaction was stopped in 10 µl stop solution with neutralization buffer (900 mM Tris-HCl pH 8.3, 300 mM KCl, 200 mM HCl) and washed with 3 µl 3 M NaOAc pH 5.3 and 1 µl Glycogen. Absolute EtOH was added and the whole mix was centrifuged at 16000 x g, 4°C for 1h. After two further washing steps using 70% EtOH, the resulting pellet was re-suspended in RNase free water. Whole genome amplification was carried out according to manufacturer's instructions using the Repli-g Single Cell Kit (QIAGEN, Venlo, Niederland). DNA was purified using the GenEluteTM PCR Clean-Up kit (Sigma-Aldrich, MO, USA). 16.8 µl purified DNA was digested with a mix of 1 µl restriction endonuclease MseI and 0.2 µl BSA in 2 µl 10x NE Buffer and incubated at 37°C for 2 h and at 65°C for 20 min. DNA was analyzed further with ddPCR as described below.

DNA extraction from plasma and serum

Plasma and serum were centrifuged at 4600 x g and 4°C for 15 min. DNA extraction from plasma and serum was performed according to QIAamp circulating nucleic acid protocol for 1 ml serum and 4 ml plasma. 40 ng/µl DNA was used for ddPCR (Bio-Rad, CA, USA) as described below.

Part II

Digital droplet PCR

DNA templates for ddPCR analysis were prepared from sample DNA extracts. With 20 µl mixture, containing; 20 ng DNA extract and 2x ddPCR Supermix (Bio-Rad, CA, USA) with duplexed p53/codon153 and p53/codon194 TaqMan system, PCR was performed with 10 min initial denaturation at 95°C followed by 40 cycles consisting of denaturation at 94°C for 30 sec annealing and extension at 60°C for 60 sec and a 10 min inactivation step at 98°C by means of thermal cycler (Eppendorf, Hamburg, Deutschland). PCR products were quantified with the QX100 droplet digital PCR system (Bio-Rad, CA, USA). Positive controls were used in order to evaluate reliability of mutation quantification using Quantasoft (Bio-Rad, CA, USA) [143].
The TP53 mutation analysis depends on two color fluorescence detection in FAM and VIC fluorescence channels. After a threshold was set between the average fluorescence amplitude of positive and negative droplet clusters on each of the two channels, the analysis was performed. For the analysis following 40x primer sets were used (Applied Biosystems, Life Technologies, CA, USA).

p53-cd194, CTT - CGT	**p53-cd135, TGC-TAC**
23bp fw: cactgattgctcttaggtctggc	27bp: fw: aactctgtctccttcctcttcctacag
22bp rv: gtcatccaaatactccacacgc	19bp: rv: ctgcacagggcaggtcttg
15bp FAM-ctcagcatcgtatcc-MGB	21bp: FAM-tcaacaagatgttttaccaac-MGB
15bp VIC-ctcagcatcttatcc-MGB	19bp: VIC-aacaagatgttttgccaac-MGB

Data analysis and statistics

The quantification of cell ratios (%) and mutational frequency were determined using Microsoft Excel 2010.

Results

Characterizing CD45+/EpCAM+ double positive cells

The IF staining revealed, that the CD45+/EpCAM+ double positive cells occur mostly either as single cells or in small aggregates consisting of two to five cells and can be distinguished from non-cancer cells by their larger nuclei. Fluorescence intensity of CD45 and EpCAM in double positive cells was weaker than that of single positive cell populations (Fig 26).

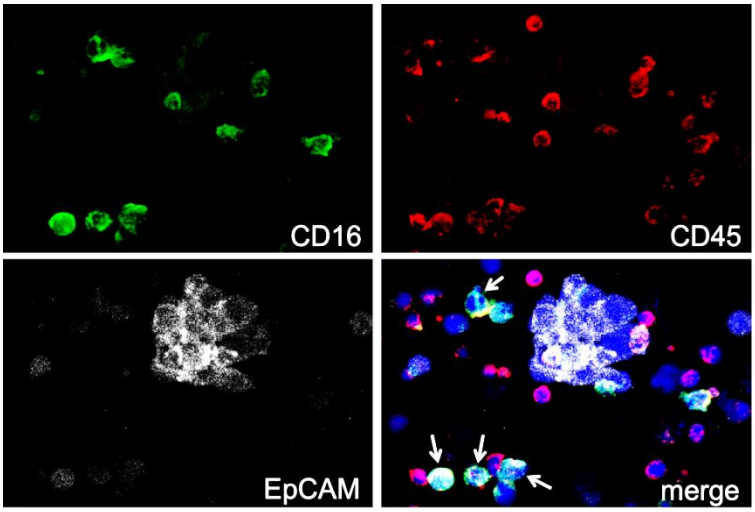

Figure 26: IF staining of ascites cell population. For staining CD16, CD45, and EpCAM antibodies are used and imaged on fluorescence microscopy at 200x magnification. The cell nuclei were counterstained with DAPI. $CD45^{+}/EpCAM^{+}$ double positive cells are indicated by white arrows on merged image.

In addition, staining of living cells with anti-EpCAM and anti-CD45 coupled magnetic micro-beads, differentiable by their sizes, confirmed the existence of these CD45+/EpCAM+ cells. Microbead staining of living ascites cells with small anti-CD45 coupled beads and larger anti-EpCAM coupled beads (both recognizing different epitopes compared to the antibodies used for IF staining allowed single cell isolation and subsequent whole genome amplification and mutation analysis (Fig 27).

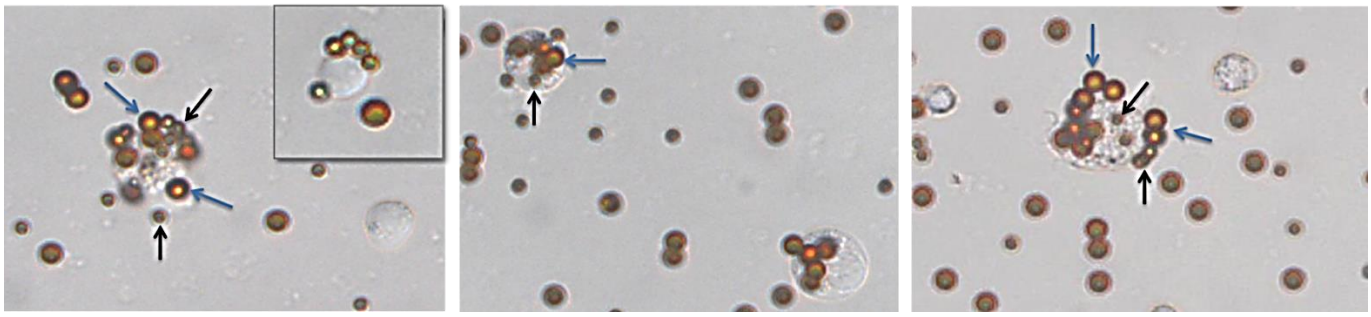

Figure 27: Staining double and single positive cells with microbeads of different sizes. Light microscopy imaging shows CD45 positive immune cells (left inset) covered with small beads and EpCAM positive tumor cells circled with larger beads (middle). $CD45^{+}/EpCAM^{+}$ double positive cells are tagged with black (small beads) and blue (large beads) arrows**.**

Interestingly, $CD45^+/EpCAM^+$ cells were more adhesive to the glass surface similar to CD45 cells, compared to the less adhesive EpCAM positive cells.

The further phenotypic characterization of this cell population according to the cell surface markers CD14, CD16, CD44, and pan-cytokeratin (CK8, 18, and 19) indicated high expression of these surface proteins, except for CKs (Figs. 26-29, CD14 not shown). Ki-67 staining (together with CD45 and EpCAM), a nuclear proliferation marker, revealed that some $CD45^+/EpCAM^+$ cells proliferate as well as tumor and immune cells (Fig. 30). Also the nuclear p53 staining of double positive cells (i.e. p53 signature) indicates a TP53 mutation (Fig. 30).

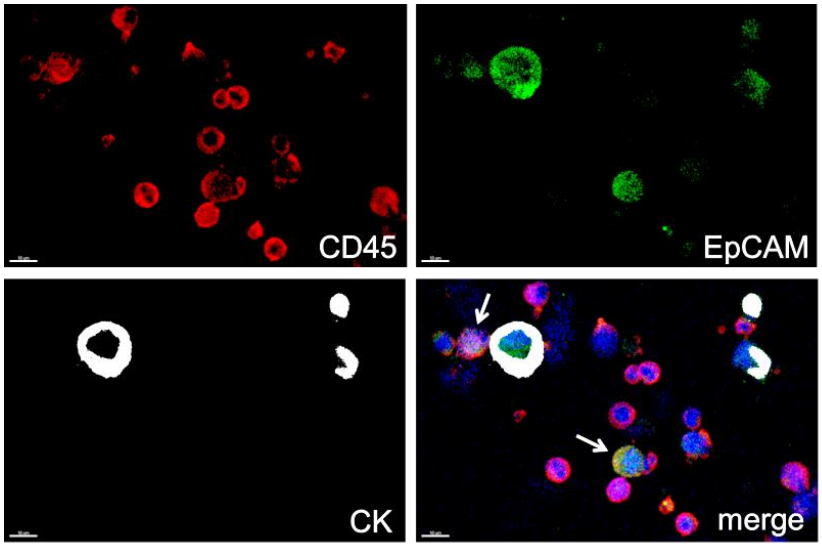

Figure 28: IF staining of double positive cells with further markers. Ascites cell populations were stained for CD45, EpCAM, and CK surface markers. The cell nuclei were counterstained with DAPI. Images were visualized with laser scanning microscopy. $CD45^+/EpCAM^+$ double positive cells are marked on the merged image by white arrows (scale bar 50 µm).

In general, the majority of cells in ascites of the patient were immune cells (7-50%). Among tumor cells the proliferation index was lower compared to the examined solid tissues (0.2-11%).

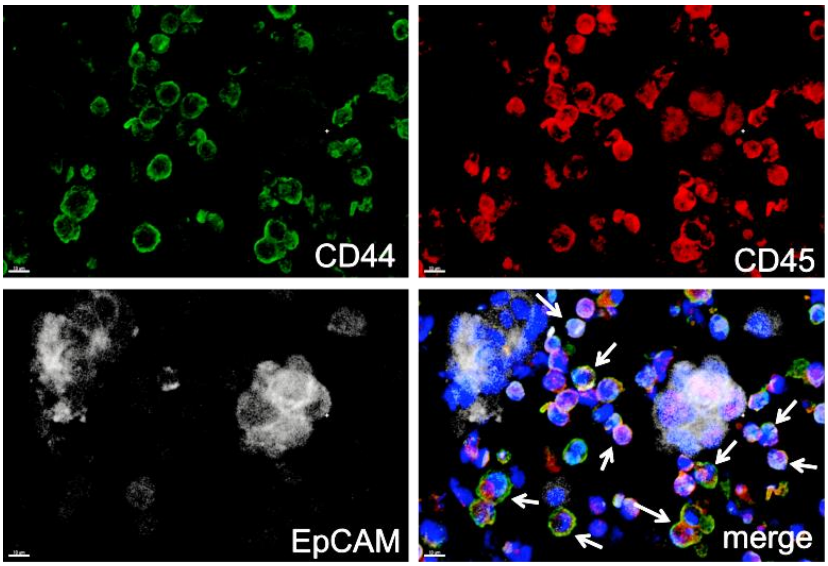

Figure 29: IF staining of double positive cells in ascites. Cell populations were stained for CD44, CD45, EpCAM, and CK surface markers. The cell nuclei were counterstained with DAPI. Images were visualized with laser scanning microscopy. $CD45^{+}/EpCAM^{+}$ double positive cells are marked on the merged image by white arrows (scale bar 50 µm).

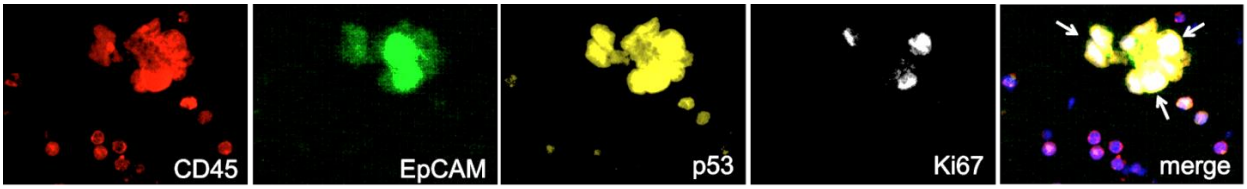

Figure 30: IF staining of tumor and immune cell populations in ascites: CD45, EpCAM, p53, and Ki67 expression were indicated. The cell nuclei were counterstained with DAPI. $CD45^{+}/EpCAM^{+}$ double positive cells are labeled on the merged image by white arrows. The images were visualized with fluorescence microscopy at 200x magnification.

TP53 mutational frequency in HGSOC

The sequencing analysis of the HGSOC patient showed two differentially distributed mutations: one identified as C135Y mutation in the ovarian tumor and the other L194R was detected only in the peritoneal tumor masses. According to the IARC both identified mutations were infrequent mutants with mutation rates of 0.114 and 0.043, respectively (Fig 31) (data from IARC) [169].

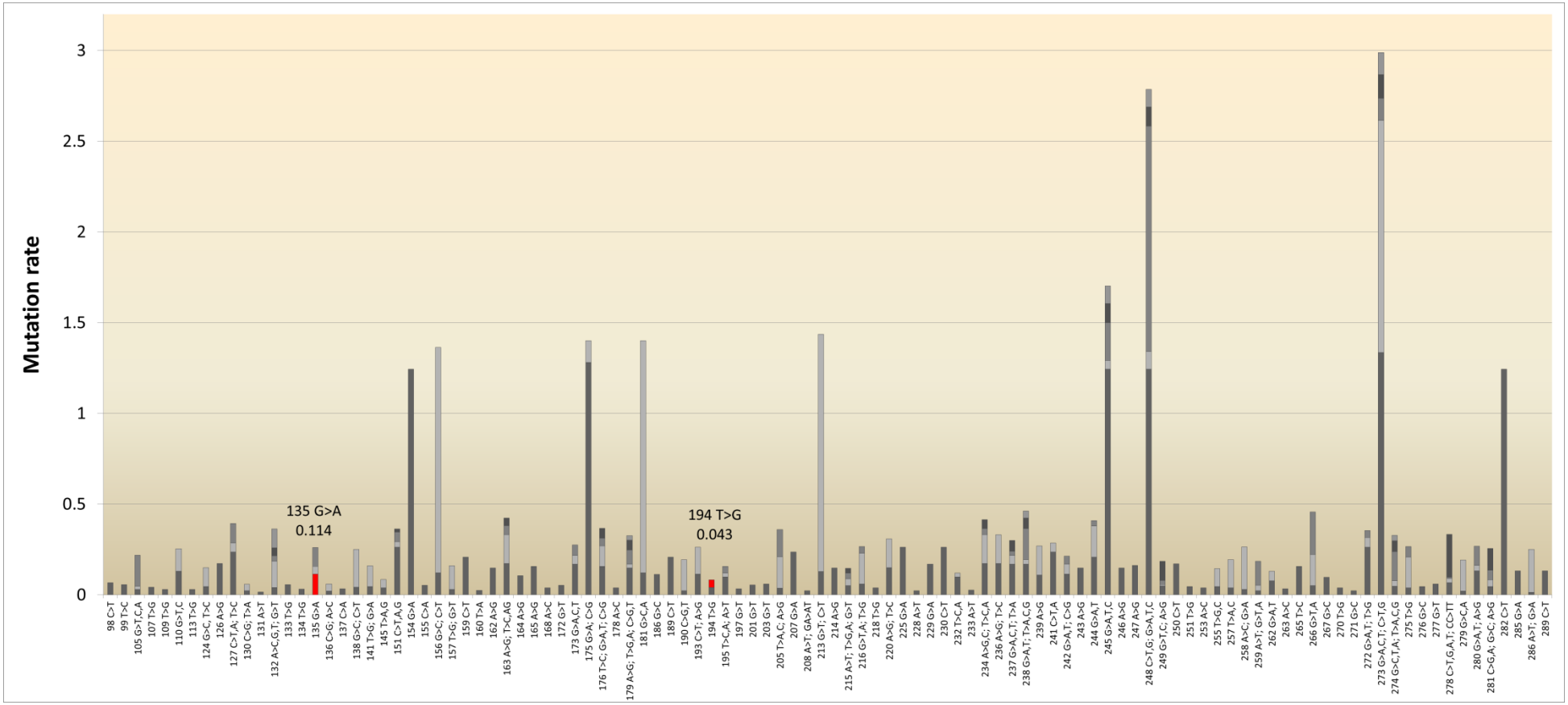

Figure 31: Mutational frequency in the DNA binding domain: Only missense mutations in the DNA binding domain were considered and analyzed, comprising 217 mutations from 658 in total. All indels, nonsense mutations, splice variants, FS and silent mutations were excluded. Six mutations outside of the DNA binding domain were removed. IARC TP53 database [169].

Distribution of two independent p53 mutations in HGSOC

Furthermore p53 mutational analysis was performed with whole genome amplification, and mutation analysis using ddPCR. We analyzed the ratio of the two different mutations in the ovarian and peritoneal tumor. The C135Y-p53 mutation was found exclusively in ovarian tumor masses, whereas the L194R-p53 mutation was solely detected in peritoneal tumor masses (Fig 32). ddPCR confirmed that both mutations were present at a high frequency; 51-76% of total alleles C135Y-TP53 in ovarian tumor and 11-91% of total alleles L194R-TP53 in peritoneal implants.

Interestingly, IF analysis of embedded cells from ascites revealed the presence of CD45 and EpCAM double positive cells at higher frequency (6.2-9.2%) compared to other patients (0-5%). Picked CD45 and EpCAM double positive single cells, identified with Dynabeads (Invitrogen, CA, USA), did not contain any of the two described mutations. Tumor cell spheroids (isolated from fresh ascites) mainly contained the “peritoneal mutation” L194R-p53, but also the “ovarian mutation” C135-p53, albeit in much less frequency (Fig 32) (93 % vs 5.5 %, respectively). In patient plasma, the “peritoneal” L194R-p53 mutation was detected (4%), but no “ovarian” C135-p53 mutation.

The structure of p53 protein in HGSOC patients

Both described mutations are located in highly conserved clusters of hotspot mutation regions among different cancers and affect so-called “buried amino acids”, known to be involved in destabilizing protein folding [154, 178].

3D structure of the DNA binding core domain of wild type p53 (Fig 33) shows that the two mutations are located at important secondary structures. The “ovarian” TP53 mutation (c.404 G>A mutation in exon 5) causes the alteration of a nucleophilic cysteine to an aromatic tyrosine at codon 135, which is located in the S2’ sheet region of the loop-sheet-helix motif. The C135Y-p53 mutation was described as protein destabilizing mutant [154]. This mutant was also reported to result in loss of function mutation and interferes with wild type p53, if present, but showed gain of function in the absence of wt p53 [179].

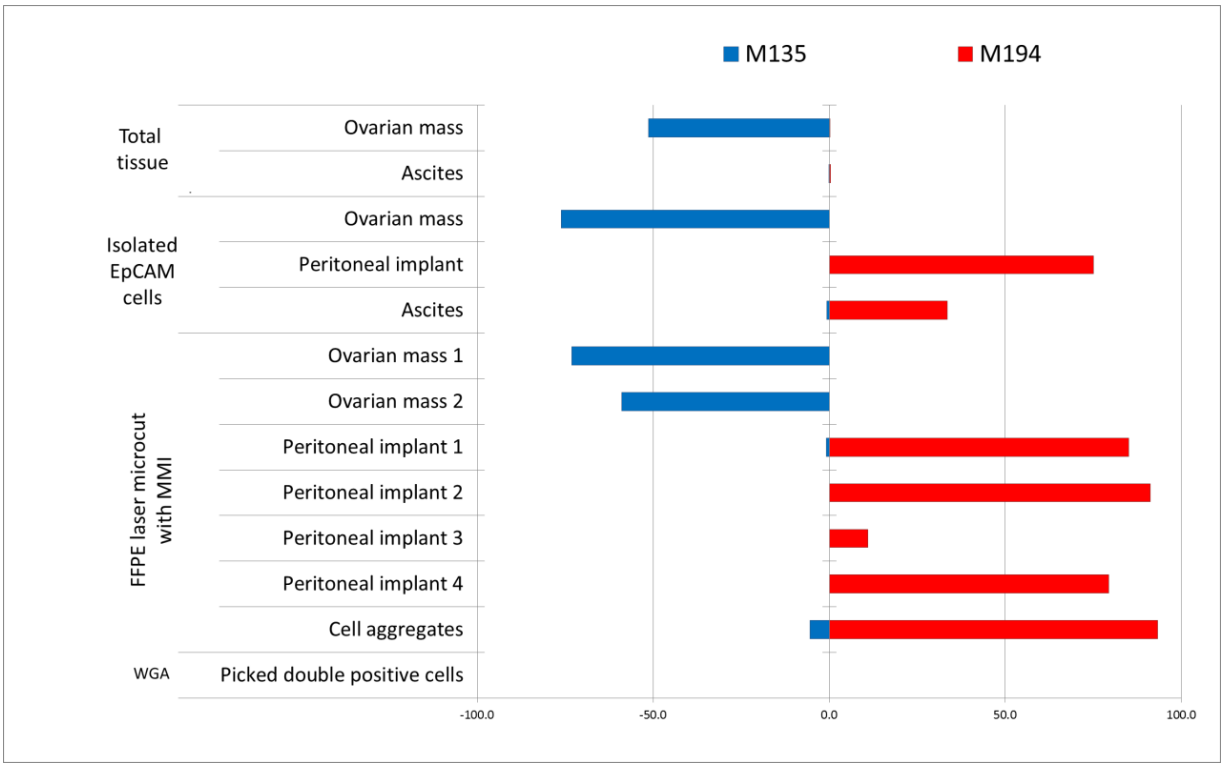

Figure 32: TP53 mutation analysis of ovarian tumor mass, isolated ascites cell aggregates, as well as isolated $CD45^{+}/EpCAM^{+}$ double positive cells and four different peritoneal implants from appendix vermiformis (1), omentum majus (2 and 4) and diaphragm (3).

The “peritoneal” TP53 mutation causes the replacement of a hydrophobic leucine by a basic arginine in the L2 loop of the protein, which is described as protein DNA interaction stabilizing loop. This mutant is also characterized to cause loss of function [180] due to its specific location near the zinc binding region. Thus, the patient carried two exclusively distributed p53 mutations in high frequency with a certain tissue signature. Structurally analyzed, the two mutations are both located at protein stabilizing regions of p53, which can result in disturbed protein function.

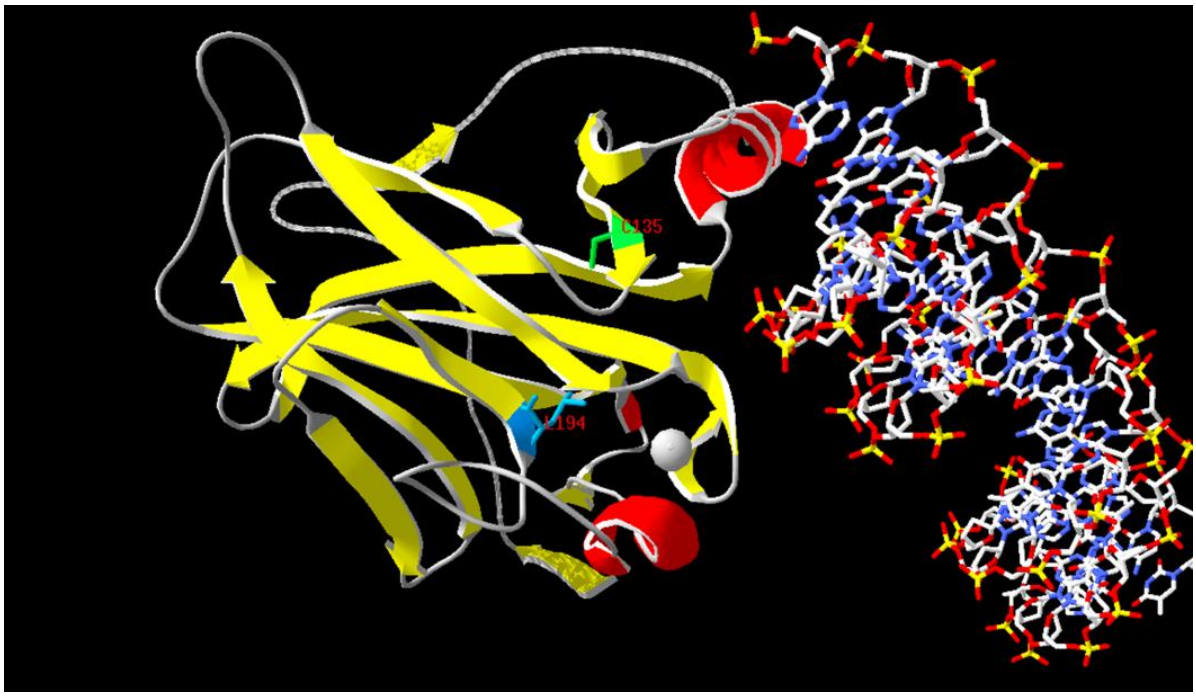

Figure 33: The two different functional TP53 mutations quantified using ddPCR in the patient. The mutation at codon L194R localized in L2 loop (labeled blue) which supports L3 loop occurred mainly in peritoneal tumor masses. The C135Y mutation in S2' β-sheet at loop-helix-sheet motif (labeled green) was shown to be a thermosensitive mutation. PDB ID: 4HJE [160].Structures were created using Swiss-PdbViewer v4.1[161].

Measuring the proliferation index depending on two different p53 signatures

In order to assess the dependence of tumor cell proliferation on the two different TP53 mutations, the proliferation index of tumor cells was determined using IF nuclear Ki67 staining in ovarian as well as peritoneal tumor tissues and embedded ascites cells.

The ovarian and peritoneal tumor tissues contained approximately 60-70% tumor cells and about 20% immune cells. Among all tissues, 0.2-11% of tumor cells was proliferating. Only the peritoneal tumor mass located in the ligamentum falciforme consisted of mostly fat cells and very few tumor cells (8%) with a high proliferation rate of 89%.

Discussion

We determined the characteristics of $CD45^+/EpCAM^+$ cells in an HGSOC patient based on IF staining and micro-bead assisted single cell isolation. As possible origin of such double positive cells a fusion of a macrophage with a tumor cell, was discussed [142]. Our results showed that in ascites of this patient proliferating $CD45^+/EpCAM^+$ double positive cells were present in substantial numbers, also weakly positive for CD14, CD16, and CD44, and only few double positive cells were positive for nuclear p53 expression (i.e. p53 signature, indicative for a functionally mutated TP53 gene).

Mutation analysis of mRNA by a functional yeast assay and subsequent sequencing of mRNA isolated from ovarian and peritoneal masses revealed two different TP53 mutations in this patient (data not shown). The further mutation analysis with patient materials exhibited a unique distribution of two independent TP53 mutations. Mutation analysis using ddPCR revealed two different functional TP53 mutations in this patient, one exclusively in the ovarian tumor mass and the other exclusively in ascites tumor cells and tumor masses obtained from the peritoneal cavity, respectively. In the ovarian tumor mass exclusively a missense C135Y mutation in exon 5 was present, whereas in ascites and peritoneal implants exclusively another missense mutation, L194R in exon 6, was present (Fig. 32). A DNA and RNA sequencing study focused on heterogeneity of advanced serious adenocarcinoma revealed two different independent TP53 missense mutations; P278L and I195N, occurring at distinct tumor locations including the ovary and the peritoneum [177]. The authors suggested that either the occurrence of independent mutations can be a consequence of two individually developing carcinomas or very early branched subclones, developed as consequence of parallel tumor progression model presented decades ago [173]. From our results, we conclude that the patient carries not only a high frequency of unusual cell populations, but also exhibit development of two independent tumors in the peritoneal cavity, distinguishable in their TP53 mutational signature. Furthermore, we infer that the two different mutations and the presence of unusual cell populations are not related to each other, because none of these two mutations were detected in these double positive cells. This suggests that either $CD45^+/EpCAM^+$ cells are not of cancerous origin or most of them lost the TP53 mutation during chromosomal consolidation after cell fusion. However, in filtered

larger cell aggregates, isolated from the ascites, nearly 100 percent of the alleles were L194R mutated (Fig. 32). Furthermore, Ki-67 staining (together with CD45, EpCAM), a nuclear proliferation marker, revealed that some double positive cells as well as tumor and immune cells proliferate. We found that the proliferation index was similar among almost all analyzed tissues, indicating that two independent p53 mutations do not affect proliferation.

Acknowledgement

I want to thank Univ.-Prof. Robert Zeillinger, Ph.D. for giving me the opportunity to work in his group and to acquire extensive research experiences.

My thanks and appreciations go to my supervisor Dietmar Pils, Ph.D. for his support at every step of my work and specially for allowing me to work independently and also as part of the team. He has shared his great knowledge and supported me by facing up to new challenges.

A special thanks to my supervisors and advisors Katharina Auer, MSc and Mag. Anna Bachmayr-Heyda for accompanying me during my master thesis. They have motivated me anytime with their encouraging feedbacks and helpful advises.

I am very grateful to all members of 'Molonc' group for their willingness to help and for their assistance.

Finally, special thanks to my family for their support, patience and understanding.

Summary

At advanced stages, serous ovarian carcinomas are characterized by excessive ascites formation and aggressive tumor spread, predominantly within the peritoneal cavity. It is still not fully understood to which extend ascites contributes to tumor progression and spread to the peritoneum. However, it is known that ascites is able to affect the tumor development by creating a cancer associated inflammatory milieu. It contains heterogeneous cell populations including e.g. two types of tumor cells (single cells and spheroids) and different types of immune cells, as well as other cell populations, such as reactive mesothelial cells and cancer-associated fibroblasts. In addition, a wide variety of immune-modulatory factors such as cytokines, chemokines and tumor growth factors are present at various concentrations in malignant ascites. This complexity of different cells and immune-modulators represents the tumor microenvironemnt in ascites and can affect ovarian tumor progression by different mechanisms. First, overexpression of immune-modulatory factors was shown to be involved in maintaining an immunosuppressive milieu in ascites. Second, immune cell accumulation in malignant ascites is mostly associated with pro-tumor signal activations, e.g. tumor cell escape from immune system.

Tumor-associated macrophages (TAMs) were identified as one of the most abundant cells in ascites. In addition, they were found to be a very heterogeneous population, since up to five phenotypically distinct subpopulations of monocytes and macrophages were described in several studies. Moreover, TAMs were shown to participate in sustained chronic inflammation, as well as in metastatic spread of ovarian tumor cells in the peritoneal cavity. One purpose of this project was to characterize the immune cell content of ascites, particularly which types of monocytes and macrophages are present in ascites of high grade serous ovarian cancer (HGSOC) patients, using multicolor immunofluorescence (IF) staining on formalin-fixed paraffin-embedded ascites cell blocks.

Two different patterns of tumor spread in the peritoneum of HGSOC patients have been proposed by us. One spread type, referred to as miliary is defined by a wide spread of numerous small millet sized implants, whereas the other, the non-miliary one is characterized by the presence of few, big, exophytically growing implants. Thus, the second aim was to evaluate the inflammatory milieu in malignant ascites based on the immune cell content and their modulation in relation to the different

metastatic spread types. For this purpose comprehensive cytokine, chemokine and tumor growth factor measurements were carried out in ascites and sera from HGSOC patients and their modulatory impact was estimated related to the immune cell content in ascites.

The IF analysis revealed that both immune and tumor cell frequencies were different in ascites of patients with the metastatic spread types. Further measurements of immuno-modulatory factors (cytokines, chemokines and tumor growth factors) analyzed by dimensionally reduction methods indicated that the two metastatic spread types differ in their immune cell composition, macrophage differentiation and inflammatory responses in ascites. In addition, human tumor growth factor analysis revealed significant associations between different metastatic spread types and angiogenesis activation in the peritoneal cavity. We conclude that miliary and non-miliary metastatic spread types in the peritoneum can be explained by different inflammatory conditions in the peritoneal cavity. Furthermore, differentiation of macrophages in the peritoneum and proangiogenic cytokines in ascites could be considered as main factors in development of the two different metastatic spread types.

An additional small side-project was evolved as unusual cell populations, co-expressing the pan-leucocyte cell marker CD45 and epithelial cell surface marker (EpCAM), were observed in ascites of a HGSOC patient. We aimed to characterize the phenotype of these $CD45^+/EpCAM^+$ double positive cells and performed further multicolor IF stainings with different tumor cell and immune cell markers, including CD14, CD16, CD44, pan-cytokeratin (Ck8, Ck18, and Ck19) and Ki67. For a final proof of the cancerous origin of the double positive cells, TP53 mutation analysis was undertaken by using digital droplet PCR (ddPCR) of isolated cells. Mutation analysis of the cells from ovarian masses, peritoneal masses and ascites revealed two different functional TP53 mutations, distributed uniquely over tissue origins, one exclusively in the ovarian tumor mass and the other exclusively in ascites tumor cells and tumor masses obtained from the peritoneal cavity. We concluded that this unique distribution of two different TP53 mutations in different tumor tissues indicates development of two independent carcinomas in the peritoneal cavity of the patient.

Zusammenfassung

Das ovarialkarzinom in fortgeschrittenen Stadien ist durch eine erhöhte Aszitesbildung und durch aggressive Metastasierung im Peritoneum gekennzeichnet. Es bleibt aber unklar, ob exzessive Aszitesbildung in der Peritonealhöhle zur Krebsprogression und zur Metastasierung aktiv beiträgt. Es ist bekannt, dass der Aszites und eine mögliche entzündliche Reaktion im Aszites bei der Krebsentwicklung eine Rolle spielt. Aszites enthält verschiedene Zellpopulationen, bestehend aus u.a. zwei verschiedene Tumorzellpopulationen (einzelnen Tumorzellen und Tumorzellaggregate, „Spheroide“), verschiedenen Immunzellpopulationen und anderen Zelltypen u.a., (reaktive) Mesothelzellen und tumor-assozierte Fibroblasten. Zusätzlich sind in malignem Aszites eine Reihe von immunmodulierenden Faktoren wie Zytokine, Chemokine und Tumorwachstumsfaktoren in verschiedenen Konzentrationen enthalten. Dieser komplexe Aszitesinhalt aus verschiedenen Zellen und Immunmodulatoren stellen für den Tumor ein spezifisches Microenvironment dar, das die Krebsprogression beeinflussen kann. Erstens wurde gezeigt, dass die Überexpression von immunmodulierenden Faktoren im Aszites ein immunsuppressives Milieu aufrechterhält. Zweitens sind Immunzellansammlung im malignen Aszites meistens mit einer pro-tumor Signalaktivierung verbunden, wie zum Beispiel, der „Escape“-Mechanismus der Tumorzellen vor immunologischer Überwachung. Monozyten und deren Abkömmlinge, insbesondere tumor-assoziierte Makrophagen gehören zu den häufigsten Zellen im Aszites. Bis zu fünf phänotypisch unterschiedliche Subpopulationen von Monozyten und Makrophagen wurden charakterisiert. Das zeigt die Heterogenität dieser Zellpopulationen. Weitere Studien mit tumorassoziierten Makrophagen haben gezeigt, dass sie bei der Erhaltung einer chronischen Entzündungen bei Krebserkrankung beteiligt sind und auch bei der Metastasierung von Ovarialkarzinomzellen in der Bauchhöhle eine Rolle spielen. Ein Ziel des Projektes war, Immunzellen, insbesondere Monozyten und Makrophagen, im Aszites von Patientinnen mit schlecht differenzierten, serösen Ovarialkarzinomen mit Hilfe von Multicolor- immunfluoreszenzfärbungen (IF) auf formalin-fixierten und im paraffin-eingebetteten Aszites-Zellblöcken zu charakterisieren.

Wir haben kürzlich zwei unterschiedliche Metastasierungmuster im Peritoneum von Patientinnen mit schlecht differenzierten, serösen Ovarialkarzinomen definiert. Das

eine, ‚miliary', ist durch viele, weit verbreitete, hirsegroße Metastasen charakterisiert, während das andere ‚non-miliary' sich durch wenige, größere Metastasen auszeichnet. Ein weiteres Ziel des Projektes war daher, den Entzündungsablauf im malignen Aszites, basierend auf Zellkonzentratinen und deren Modulierung mittels Zyto/Chemokinen im Zusammenhang mit verschiedenen Metastasierungsmustern zu bestimmen. Dafür wurden viele Zytokine, Chemokine sowie auch Tumorwachstumsfaktoren im Aszites und Serum von Patientinnen gemessen.
Die IF Analysen zeigten Unterschiede im Aszites von Patientinen mit verschiedenen Metastasierungsmustern. Weitere Analysen von immunmodulierenden Faktoren mittels Dimensionsreduktionsmethoden zeigten, dass sich die zwei Metastasierungsmuster auch aufgrund ihrer Immunzellzusammensetzung, der Makrophagendifferenzierung und der Entzündungsparameter im Aszites unterscheiden lassen. Außerdem weisen Messungen der Tumorwachstumsfaktoren auf einen Zusammenhang zwischen den zwei Metastasierungsmustern und Angiogenesesignalwegen hin. Wir folgern daraus, dass sich die ‚miliary'- und ‚non-miliary' Metastasierungstypen auch aufgrund unterschiedlicher Entzündungsreaktionen im Aszites entwickelt haben. Diese Unterschiede wurden in den verschiedenen Zusammensetzungen von Immunzellen, Tumorzellen und immunmodulierenden Faktoren deutlich.

Ein zusätzliches Nebenprojekt wurde durchgeführt, da in einer der Patientinnen unübliche Zellen entdeckt wurden. Diese Zellen exprimierten sowohl den Leukocyten Marker CD45 als auch EpCAM, ein Marker für Epithelzellen. Der Phänotyp dieser $CD45^{+}/EpCAM^{+}$ doppelpositiver Zellen wurde dann mittels IF mit verschiedenen Markern (wie CD14, CD16, CD44, pan-Zytokeratinen (Ck8, Ck18, and Ck19) und Ki67) charakterisiert. Um den Ursprung dieser Zellen zu bestimmen, wurde ddPCR auf zwei verschiedene TP53 Mutationen durchgeführt. Das Ergebnis war, dass die Patientin zwei unabhängige funktionelle TP53 Mutation trägt. Die eine kommt ausschließlich in der Ovarialtumormasse, die andere nur in der Peritonealtumormasse und im Aszites vor. Wir glauben, dass die Verteilung der zwei unterschiedlichen Mutationen auf zwei unabhängig voneinander entstandenen Karzinomen im Peritonealraum dieser Patientin hindeuten, welche vermutlich aus prämalignen Zellen des oberen Eileiters entstanden.

Curriculum Vitae

Personal Data

Name	Nyamdelger Sukhbaatar
Academic title	BSc
Address	Leegasse 1/22, 1140 Vienna, Austria
E-Mail	nyamdelger732@yahoo.com
Date of Birth	31.07.1983
Place of Birth	Arkhangai, Mongolia
Marital status	married
Citizenship	Mongolia

Education

09/2014-01/2015	Master thesis at the Molecular Oncology Group – Department of Obstetrics and Gynaecology at the Medical University of Vienna. The General Hospital of Vienna, Währinger Gürtel 18-20, 1090 Vienna, Austria Supervision by Univ.-Prof. Dr. Robert Zeillinger and Dietmar Pils, Ph.D. Master thesis: “Characterization of immune cell populations in ascites from patients with serous epithelial ovarian cancer”
10/2012-02/2015	Master studies of biology, specialization in cell biology with subsidiary subject molecular medicine, University of Vienna
24/06/2012	Attainment of BSc
10/2008-07/2012	Bachelor studies of molecular biology, University of Vienna
10/2003-02/2008	Studies of pharmacy, University of Leipzig
10/2002-07/2003	„Studienkolleg Sachsen“ - Preparation for study, University of Leipzig
10/2001-06/2002	Language course: German as a Foreign Language
09/1999-05/2001	Mongolian National University of Medical Sciences
09/1990-06/1999	Primary school Mongolia

Language skills	Mongolian (native), German (fluent), English (excellent)

Software skills	Microsoft office, 'R', Swiss PDB viewer, 'CellProfiler', 'ImageJ'
Publications	Anna Bachmayr-Heyda, Agnes Reiner, Katharina Auer, **Nyamdelger Sukhbaatar**, Stefanie Aust, Thomas Bachleitner-Hofmann, Ildiko Mesteri, Thomas W. Grunt, Robert Zeillinger, Dietmar Pils. **Correlation of circular RNA abundance with proliferation – exemplified with colorectal and ovarian cancer, idiopathic lung fibrosis, and normal human tissues.** Sci Rep, 2015, 5: 8057.
	Katharina Auer, Anna Bachmayr-Heyda, Stefanie Aust, **Nyamdelger Sukhbaatar**, Agnes Teresa Reiner, Christoph Grimm, Reinhard Horvat, Robert Zeillinger, Dietmar Pils. **Peritoneal Tumor Spread in Serous Ovarian Cancer - Epithelial Mesenchymal Status and Outcome.** Manuscript in preparation.
	Nyamdelger Sukhbaatar, Anna Bachmayr-Heyda, Katharina Auer, Martin Stöger, Simon Deycmar, Stefanie Aust, Reinhard Horvat, Robert Zeillinger, Dietmar Pils. **Two Different, Mutually, Exclusively Distributed TP53 Mutations in Ovarian and Peritoneal Implants of a Serous Ovarian Cancer Patient.** Manuscript in preparation.

References

1. Jemal A, Bray F, Center MM, Ferlay J, Ward E, Forman D: **Global cancer statistics**. *CA: a cancer journal for clinicians* 2011, **61**(2):69-90.
2. Prat J, Oncology FCoG: **Staging classification for cancer of the ovary, fallopian tube, and peritoneum**. *International journal of gynaecology and obstetrics: the official organ of the International Federation of Gynaecology and Obstetrics* 2014, **124**(1):1-5.
3. Forman D: **Cancer Incidence and Mortality in Europe - GLOBOCAN 2008**. *Eur J Cancer* 2011, **47**:S24-S24.
4. Ferlay J, Soerjomataram I, Dikshit R, Eser S, Mathers C, Rebelo M, Parkin DM, Forman D, Bray F: **Cancer incidence and mortality worldwide: Sources, methods and major patterns in GLOBOCAN 2012**. *International journal of cancer Journal international du cancer* 2015, **136**(5):E359-386.
5. Longuespee R, Boyon C, Desmons A, Vinatier D, Leblanc E, Farre I, Wisztorski M, Ly K, D'Anjou F, Day R *et al*: **Ovarian cancer molecular pathology**. *Cancer metastasis reviews* 2012, **31**(3-4):713-732.
6. Romero I, Bast RC, Jr.: **Minireview: human ovarian cancer: biology, current management, and paths to personalizing therapy**. *Endocrinology* 2012, **153**(4):1593-1602.
7. Hennessy BT, Coleman RL, Markman M: **Ovarian cancer**. *Lancet* 2009, **374**(9698):1371-1382.
8. Badgwell D, Bast RC, Jr.: **Early detection of ovarian cancer**. *Disease markers* 2007, **23**(5-6):397-410.
9. Viezens L, Schaefer C, Beyerlein J, Hansen-Algenstaedt N, Thietje R: **Response**. *Journal of neurosurgery Spine* 2013, **19**(2):265-266.
10. Auersperg N, Wong AS, Choi KC, Kang SK, Leung PC: **Ovarian surface epithelium: biology, endocrinology, and pathology**. *Endocrine reviews* 2001, **22**(2):255-288.
11. Rescigno P, Cerillo I, Ruocco R, Condello C, De Placido S, Pensabene M: **New hypothesis on pathogenesis of ovarian cancer lead to future tailored approaches**. *BioMed research international* 2013, **2013**:852839.
12. Ohman AW, Hasan N, Dinulescu DM: **Advances in tumor screening, imaging, and avatar technologies for high-grade serous ovarian cancer**. *Frontiers in oncology* 2014, **4**:322.
13. Liao J, Qian F, Tchabo N, Mhawech-Fauceglia P, Beck A, Qian Z, Wang X, Huss WJ, Lele SB, Morrison CD *et al*: **Ovarian cancer spheroid cells with stem cell-like properties contribute to tumor generation, metastasis and chemotherapy resistance through hypoxia-resistant metabolism**. *PloS one* 2014, **9**(1):e84941.
14. Carmignani CP, Sugarbaker TA, Bromley CM, Sugarbaker PH: **Intraperitoneal cancer dissemination: mechanisms of the patterns of spread**. *Cancer metastasis reviews* 2003, **22**(4):465-472.
15. Bell DA: **Origins and molecular pathology of ovarian cancer**. *Modern pathology : an official journal of the United States and Canadian Academy of Pathology, Inc* 2005, **18 Suppl 2**:S19-32.
16. Malpica A, Deavers MT, Lu K, Bodurka DC, Atkinson EN, Gershenson DM, Silva EG: **Grading ovarian serous carcinoma using a two-tier system**. *Am J Surg Pathol* 2004, **28**(4):496-504.
17. Koshiyama M, Matsumura N, Konishi I: **Recent concepts of ovarian carcinogenesis: type I and type II**. *BioMed research international* 2014, **2014**:934261.
18. Roth LM: **Two-tier grading system for ovarian epithelial cancer: has its time arrived?** *Am J Surg Pathol* 2007, **31**(8):1285-1287.
19. Oncology FCoG: **Current FIGO staging for cancer of the vagina, fallopian tube, ovary, and gestational trophoblastic neoplasia**. *International journal of gynaecology and obstetrics: the official organ of the International Federation of Gynaecology and Obstetrics* 2009, **105**(1):3-4.
20. Clark TG, Stewart ME, Altman DG, Gabra H, Smyth JF: **A prognostic model for ovarian cancer**. *Br J Cancer* 2001, **85**(7):944-952.

21. Yoshihara K, Tajima A, Yahata T, Kodama S, Fujiwara H, Suzuki M, Onishi Y, Hatae M, Sueyoshi K, Fujiwara H *et al*: **Gene expression profile for predicting survival in advanced-stage serous ovarian cancer across two independent datasets**. *PloS one* 2010, **5**(3):e9615.
22. Cancer Genome Atlas Research N: **Integrated genomic analyses of ovarian carcinoma**. *Nature* 2011, **474**(7353):609-615.
23. Gilks CB, Prat J: **Ovarian carcinoma pathology and genetics: recent advances**. *Human pathology* 2009, **40**(9):1213-1223.
24. Brenton JD, Stingl J: **Stem cells: Anatomy of an ovarian cancer**. *Nature* 2013, **495**(7440):183-184.
25. Reade CJ, McVey RM, Tone AA, Finlayson SJ, McAlpine JN, Fung-Kee-Fung M, Ferguson SE: **The fallopian tube as the origin of high grade serous ovarian cancer: review of a paradigm shift**. *Journal of obstetrics and gynaecology Canada : JOGC = Journal d'obstetrique et gynecologie du Canada : JOGC* 2014, **36**(2):133-140.
26. Erickson BK, Conner MG, Landen CN, Jr.: **The role of the fallopian tube in the origin of ovarian cancer**. *American journal of obstetrics and gynecology* 2013, **209**(5):409-414.
27. Vaughan S, Coward JI, Bast RC, Jr., Berchuck A, Berek JS, Brenton JD, Coukos G, Crum CC, Drapkin R, Etemadmoghadam D *et al*: **Rethinking ovarian cancer: recommendations for improving outcomes**. *Nat Rev Cancer* 2011, **11**(10):719-725.
28. Piek JM, van Diest PJ, Zweemer RP, Jansen JW, Poort-Keesom RJ, Menko FH, Gille JJ, Jongsma AP, Pals G, Kenemans P *et al*: **Dysplastic changes in prophylactically removed Fallopian tubes of women predisposed to developing ovarian cancer**. *The Journal of pathology* 2001, **195**(4):451-456.
29. Shield K, Ackland ML, Ahmed N, Rice GE: **Multicellular spheroids in ovarian cancer metastases: Biology and pathology**. *Gynecologic oncology* 2009, **113**(1):143-148.
30. Karst AM, Drapkin R: **The new face of ovarian cancer modeling: better prospects for detection and treatment**. *F1000 medicine reports* 2011, **3**:22.
31. Wertel I, Nowicka A, Rogala E, Kotarski J: **Peritoneal immune system in patients with advance epithelial ovarian cancer**. *Int Rev Immunol* 2011, **30**(2-3):87-101.
32. Sodek KL, Murphy KJ, Brown TJ, Ringuette MJ: **Cell-cell and cell-matrix dynamics in intraperitoneal cancer metastasis**. *Cancer metastasis reviews* 2012, **31**(1-2):397-414.
33. Cannistra SA, Kansas GS, Niloff J, DeFranzo B, Kim Y, Ottensmeier C: **Binding of ovarian cancer cells to peritoneal mesothelium in vitro is partly mediated by CD44H**. *Cancer research* 1993, **53**(16):3830-3838.
34. Zoller M: **CD44: can a cancer-initiating cell profit from an abundantly expressed molecule?** *Nat Rev Cancer* 2011, **11**(4):254-267.
35. Kipps E, Tan DS, Kaye SB: **Meeting the challenge of ascites in ovarian cancer: new avenues for therapy and research**. *Nat Rev Cancer* 2013, **13**(4):273-282.
36. Clark R, Krishnan V, Schoof M, Rodriguez I, Theriault B, Chekmareva M, Rinker-Schaeffer C: **Milky spots promote ovarian cancer metastatic colonization of peritoneal adipose in experimental models**. *The American journal of pathology* 2013, **183**(2):576-591.
37. Michailova KN UK: **The milky spots of the peritoneum and pleura: structure, development and pathology**. *Biomedical Reviews* 2004(15):47-66.
38. Hagiwara A, Takahashi T, Sawai K, Taniguchi H, Shimotsuma M, Okano S, Sakakura C, Tsujimoto H, Osaki K, Sasaki S *et al*: **Milky spots as the implantation site for malignant cells in peritoneal dissemination in mice**. *Cancer research* 1993, **53**(3):687-692.
39. Nieman KM, Kenny HA, Penicka CV, Ladanyi A, Buell-Gutbrod R, Zillhardt MR, Romero IL, Carey MS, Mills GB, Hotamisligil GS *et al*: **Adipocytes promote ovarian cancer metastasis and provide energy for rapid tumor growth**. *Nature medicine* 2011, **17**(11):1498-1503.
40. Nagy JA, Herzberg KT, Dvorak JM, Dvorak HF: **Pathogenesis of malignant ascites formation: initiating events that lead to fluid accumulation**. *Cancer research* 1993, **53**(11):2631-2643.
41. Balkwill F: **Cancer and the chemokine network**. *Nat Rev Cancer* 2004, **4**(7):540-550.

42. Barton DP, Cai A, Wendt K, Young M, Gamero A, De Cesare S: **Angiogenic protein expression in advanced epithelial ovarian cancer**. *Clinical cancer research : an official journal of the American Association for Cancer Research* 1997, **3**(9):1579-1586.
43. Matte I, Lane D, Laplante C, Rancourt C, Piche A: **Profiling of cytokines in human epithelial ovarian cancer ascites**. *American journal of cancer research* 2012, **2**(5):566-580.
44. Grivennikov SI, Greten FR, Karin M: **Immunity, inflammation, and cancer**. *Cell* 2010, **140**(6):883-899.
45. Del Prete A, Allavena P, Santoro G, Fumarulo R, Corsi MM, Mantovani A: **Molecular pathways in cancer-related inflammation**. *Biochemia medica* 2011, **21**(3):264-275.
46. Lin EY, Pollard JW: **Role of infiltrated leucocytes in tumour growth and spread**. *British journal of cancer* 2004, **90**(11):2053-2058.
47. Mantovani A, Allavena P, Sica A, Balkwill F: **Cancer-related inflammation**. *Nature* 2008, **454**(7203):436-444.
48. Balkwill FR, Mantovani A: **Cancer-related inflammation: common themes and therapeutic opportunities**. *Seminars in cancer biology* 2012, **22**(1):33-40.
49. Gavalas NG, Karadimou A, Dimopoulos MA, Bamias A: **Immune response in ovarian cancer: how is the immune system involved in prognosis and therapy: potential for treatment utilization**. *Clinical & developmental immunology* 2010, **2010**:791603.
50. Dunn GP, Old LJ, Schreiber RD: **The three Es of cancer immunoediting**. *Annual review of immunology* 2004, **22**:329-360.
51. Hanahan D, Weinberg RA: **Hallmarks of cancer: the next generation**. *Cell* 2011, **144**(5):646-674.
52. Colotta F, Allavena P, Sica A, Garlanda C, Mantovani A: **Cancer-related inflammation, the seventh hallmark of cancer: links to genetic instability**. *Carcinogenesis* 2009, **30**(7):1073-1081.
53. de Visser KE, Eichten A, Coussens LM: **Paradoxical roles of the immune system during cancer development**. *Nat Rev Cancer* 2006, **6**(1):24-37.
54. Qian BZ, Pollard JW: **Macrophage diversity enhances tumor progression and metastasis**. *Cell* 2010, **141**(1):39-51.
55. Gajewski TF, Schreiber H, Fu YX: **Innate and adaptive immune cells in the tumor microenvironment**. *Nature immunology* 2013, **14**(10):1014-1022.
56. Charbonneau B, Goode EL, Kalli KR, Knutson KL, Derycke MS: **The immune system in the pathogenesis of ovarian cancer**. *Critical reviews in immunology* 2013, **33**(2):137-164.
57. Janeway CAJ, Paul Travers, Mark Walport, and Mark J Shlomchik: **Basic Concepts in Immunology**. In: *Immunobiology. Volume 5*, edn. New York: Garland Science; 2001: 28-29.
58. Mantovani A, Savino B, Locati M, Zammataro L, Allavena P, Bonecchi R: **The chemokine system in cancer biology and therapy**. *Cytokine & growth factor reviews* 2010, **21**(1):27-39.
59. Sauer K, Cooke MP: **Regulation of immune cell development through soluble inositol-1,3,4,5-tetrakisphosphate**. *Nature reviews Immunology* 2010, **10**(4):257-271.
60. Janeway CAJ, Paul Travers, Mark Walport, and Mark J Shlomchik: **The Humoral Immune Response**. In: *Immunobiology. Volume 5*, edn. New York: Garland Science; 2001: 390-392.
61. Janeway CA, Jr., Medzhitov R: **Innate immune recognition**. *Annual review of immunology* 2002, **20**:197-216.
62. Nielsen JS, Nelson BH: **Tumor-infiltrating B cells and T cells: Working together to promote patient survival**. *Oncoimmunology* 2012, **1**(9):1623-1625.
63. Luster AD: **The role of chemokines in linking innate and adaptive immunity**. *Current opinion in immunology* 2002, **14**(1):129-135.
64. Wertel I, Polak G, Bednarek W, Barczynski B, Rolinski J, Kotarski J: **Dendritic cell subsets in the peritoneal fluid and peripheral blood of women suffering from ovarian cancer**. *Cytometry Part B, Clinical cytometry* 2008, **74**(4):251-258.

65. Melichar B, Freedman RS: **Immunology of the peritoneal cavity: relevance for host-tumor relation**. *International journal of gynecological cancer : official journal of the International Gynecological Cancer Society* 2002, **12**(1):3-17.
66. Murphy MA, Trabert B, Yang HP, Park Y, Brinton LA, Hartge P, Sherman ME, Hollenbeck A, Wentzensen N: **Non-steroidal anti-inflammatory drug use and ovarian cancer risk: findings from the NIH-AARP Diet and Health Study and systematic review**. *Cancer causes & control : CCC* 2012, **23**(11):1839-1852.
67. Negus RP, Stamp GW, Hadley J, Balkwill FR: **Quantitative assessment of the leukocyte infiltrate in ovarian cancer and its relationship to the expression of C-C chemokines**. *The American journal of pathology* 1997, **150**(5):1723-1734.
68. Mahdavi A, Pejovic T, Nezhat F: **Induction of ovulation and ovarian cancer: a critical review of the literature**. *Fertility and sterility* 2006, **85**(4):819-826.
69. Gerber SA, Rybalko VY, Bigelow CE, Lugade AA, Foster TH, Frelinger JG, Lord EM: **Preferential attachment of peritoneal tumor metastases to omental immune aggregates and possible role of a unique vascular microenvironment in metastatic survival and growth**. *The American journal of pathology* 2006, **169**(5):1739-1752.
70. Loercher AE, Nash MA, Kavanagh JJ, Platsoucas CD, Freedman RS: **Identification of an IL-10-producing HLA-DR-negative monocyte subset in the malignant ascites of patients with ovarian carcinoma that inhibits cytokine protein expression and proliferation of autologous T cells**. *Journal of immunology* 1999, **163**(11):6251-6260.
71. Colvin EK: **Tumor-associated macrophages contribute to tumor progression in ovarian cancer**. *Frontiers in oncology* 2014, **4**:137.
72. Mutsaers SE: **Mesothelial cells: their structure, function and role in serosal repair**. *Respirology* 2002, **7**(3):171-191.
73. Bachmayr-Heyda A, Aust S, Heinze G, Polterauer S, Grimm C, Braicu EI, Sehouli J, Lambrechts S, Vergote I, Mahner S *et al*: **Prognostic impact of tumor infiltrating CD8+ T cells in association with cell proliferation in ovarian cancer patients--a study of the OVCAD consortium**. *BMC cancer* 2013, **13**:422.
74. Curiel TJ, Coukos G, Zou L, Alvarez X, Cheng P, Mottram P, Evdemon-Hogan M, Conejo-Garcia JR, Zhang L, Burow M *et al*: **Specific recruitment of regulatory T cells in ovarian carcinoma fosters immune privilege and predicts reduced survival**. *Nature medicine* 2004, **10**(9):942-949.
75. Rodriguez GC, Haisley C, Hurteau J, Moser TL, Whitaker R, Bast RC, Jr., Stack MS: **Regulation of invasion of epithelial ovarian cancer by transforming growth factor-beta**. *Gynecologic oncology* 2001, **80**(2):245-253.
76. Santin AD, Hermonat PL, Ravaggi A, Bellone S, Roman JJ, Smith CV, Pecorelli S, Radominska-Pandya A, Cannon MJ, Parham GP: **Phenotypic and functional analysis of tumor-infiltrating lymphocytes compared with tumor-associated lymphocytes from ascitic fluid and peripheral blood lymphocytes in patients with advanced ovarian cancer**. *Gynecologic and obstetric investigation* 2001, **51**(4):254-261.
77. Dong HP, Elstrand MB, Holth A, Silins I, Berner A, Trope CG, Davidson B, Risberg B: **NK- and B-cell infiltration correlates with worse outcome in metastatic ovarian carcinoma**. *American journal of clinical pathology* 2006, **125**(3):451-458.
78. Sica A, Allavena P, Mantovani A: **Cancer related inflammation: the macrophage connection**. *Cancer letters* 2008, **267**(2):204-215.
79. Hagemann T, Wilson J, Burke F, Kulbe H, Li NF, Pluddemann A, Charles K, Gordon S, Balkwill FR: **Ovarian cancer cells polarize macrophages toward a tumor-associated phenotype**. *Journal of immunology* 2006, **176**(8):5023-5032.
80. Torroella-Kouri M, Silvera R, Rodriguez D, Caso R, Shatry A, Opiela S, Ilkovitch D, Schwendener RA, Iragavarapu-Charyulu V, Cardentey Y *et al*: **Identification of a subpopulation of macrophages in mammary tumor-bearing mice that are neither M1 nor M2 and are less differentiated**. *Cancer research* 2009, **69**(11):4800-4809.

81. Schmieder A, Michel J, Schonhaar K, Goerdt S, Schledzewski K: **Differentiation and gene expression profile of tumor-associated macrophages**. *Seminars in cancer biology* 2012, **22**(4):289-297.
82. Chittezhath M, Dhillon MK, Lim JY, Laoui D, Shalova IN, Teo YL, Chen J, Kamaraj R, Raman L, Lum J *et al*: **Molecular profiling reveals a tumor-promoting phenotype of monocytes and macrophages in human cancer progression**. *Immunity* 2014, **41**(5):815-829.
83. Goswami S, Sahai E, Wyckoff JB, Cammer M, Cox D, Pixley FJ, Stanley ER, Segall JE, Condeelis JS: **Macrophages promote the invasion of breast carcinoma cells via a colony-stimulating factor-1/epidermal growth factor paracrine loop**. *Cancer research* 2005, **65**(12):5278-5283.
84. Murdoch C, Muthana M, Coffelt SB, Lewis CE: **The role of myeloid cells in the promotion of tumour angiogenesis**. *Nat Rev Cancer* 2008, **8**(8):618-631.
85. Riboldi E, Porta C, Morlacchi S, Viola A, Mantovani A, Sica A: **Hypoxia-mediated regulation of macrophage functions in pathophysiology**. *International immunology* 2013, **25**(2):67-75.
86. Pollard JW: **Tumour-educated macrophages promote tumour progression and metastasis**. *Nat Rev Cancer* 2004, **4**(1):71-78.
87. Wyckoff JB, Wang Y, Lin EY, Li JF, Goswami S, Stanley ER, Segall JE, Pollard JW, Condeelis J: **Direct visualization of macrophage-assisted tumor cell intravasation in mammary tumors**. *Cancer research* 2007, **67**(6):2649-2656.
88. Condeelis J, Pollard JW: **Macrophages: obligate partners for tumor cell migration, invasion, and metastasis**. *Cell* 2006, **124**(2):263-266.
89. Hagemann T, Robinson SC, Thompson RG, Charles K, Kulbe H, Balkwill FR: **Ovarian cancer cell-derived migration inhibitory factor enhances tumor growth, progression, and angiogenesis**. *Molecular cancer therapeutics* 2007, **6**(7):1993-2002.
90. Duluc D, Corvaisier M, Blanchard S, Catala L, Descamps P, Gamelin E, Ponsoda S, Delneste Y, Hebbar M, Jeannin P: **Interferon-gamma reverses the immunosuppressive and protumoral properties and prevents the generation of human tumor-associated macrophages**. *International journal of cancer Journal international du cancer* 2009, **125**(2):367-373.
91. Wang X, Zhao X, Wang K, Wu L, Duan T: **Interaction of monocytes/macrophages with ovarian cancer cells promotes angiogenesis in vitro**. *Cancer science* 2013, **104**(4):516-523.
92. Melichar B, Savary CA, Patenia R, Templin S, Melicharova K, Freedman RS: **Phenotype and antitumor activity of ascitic fluid monocytes in patients with ovarian carcinoma**. *International journal of gynecological cancer : official journal of the International Gynecological Cancer Society* 2003, **13**(4):435-443.
93. Szaflarska A, Baj-Krzyworzeka M, Siedlar M, Weglarczyk K, Ruggiero I, Hajto B, Zembala M: **Antitumor response of CD14+/CD16+ monocyte subpopulation**. *Experimental hematology* 2004, **32**(8):748-755.
94. Schmidl C, Renner K, Peter K, Eder R, Lassmann T, Balwierz PJ, Itoh M, Nagao-Sato S, Kawaji H, Carninci P *et al*: **Transcription and enhancer profiling in human monocyte subsets**. *Blood* 2014, **123**(17):e90-99.
95. Takaishi K, Komohara Y, Tashiro H, Ohtake H, Nakagawa T, Katabuchi H, Takeya M: **Involvement of M2-polarized macrophages in the ascites from advanced epithelial ovarian carcinoma in tumor progression via Stat3 activation**. *Cancer science* 2010, **101**(10):2128-2136.
96. Allavena P, Chieppa M, Bianchi G, Solinas G, Fabbri M, Laskarin G, Mantovani A: **Engagement of the mannose receptor by tumoral mucins activates an immune suppressive phenotype in human tumor-associated macrophages**. *Clinical & developmental immunology* 2010, **2010**:547179.
97. Robinson-Smith TM, Isaacsohn I, Mercer CA, Zhou M, Van Rooijen N, Husseinzadeh N, McFarland-Mancini MM, Drew AF: **Macrophages mediate inflammation-enhanced metastasis of ovarian tumors in mice**. *Cancer research* 2007, **67**(12):5708-5716.

98. Kulbe H, Chakravarty P, Leinster DA, Charles KA, Kwong J, Thompson RG, Coward JI, Schioppa T, Robinson SC, Gallagher WM *et al*: **A dynamic inflammatory cytokine network in the human ovarian cancer microenvironment**. *Cancer research* 2012, **72**(1):66-75.
99. Kulbe H, Thompson R, Wilson JL, Robinson S, Hagemann T, Fatah R, Gould D, Ayhan A, Balkwill F: **The inflammatory cytokine tumor necrosis factor-alpha generates an autocrine tumor-promoting network in epithelial ovarian cancer cells**. *Cancer research* 2007, **67**(2):585-592.
100. Lewis CE, Pollard JW: **Distinct role of macrophages in different tumor microenvironments**. *Cancer research* 2006, **66**(2):605-612.
101. Zhang W, Tian J, Hao Q: **HMGB1 combining with tumor-associated macrophages enhanced lymphangiogenesis in human epithelial ovarian cancer**. *Tumour biology : the journal of the International Society for Oncodevelopmental Biology and Medicine* 2014, **35**(3):2175-2186.
102. Janeway CAJ, Paul Travers, Mark Walport, and Mark J Shlomchik: **The Recognition of Antigen**. In: *Immunobiology. Volume 5*, edn. New York; 2001: 99-103.
103. Dinarello CA: **Proinflammatory cytokines**. *Chest* 2000, **118**(2):503-508.
104. Mantovani A: **The chemokine system: redundancy for robust outputs**. *Immunology today* 1999, **20**(6):254-257.
105. Murphy PM, Baggiolini M, Charo IF, Hebert CA, Horuk R, Matsushima K, Miller LH, Oppenheim JJ, Power CA: **International union of pharmacology. XXII. Nomenclature for chemokine receptors**. *Pharmacological reviews* 2000, **52**(1):145-176.
106. Matsushima KYT, Etsuko Toda, Francis Shand, Ueha aS: **Chemokines in inflammatory and immune diseases**. *Inflammation and Regeneration* 2011, **31**(1):11-22.
107. Janeway CAJ, Paul Travers, Mark Walport, and Mark J Shlomchik: **The Recognition of Antigen**. In: *Immunobiology. Volume 5*, edn. New York: Garland Science; 2001: 103-111.
108. Matsukawa A, Hogaboam CM, Lukacs NW, Kunkel SL: **Chemokines and innate immunity**. *Reviews in immunogenetics* 2000, **2**(3):339-358.
109. Landskron G, De la Fuente M, Thuwajit P, Thuwajit C, Hermoso MA: **Chronic inflammation and cytokines in the tumor microenvironment**. *Journal of immunology research* 2014, **2014**:149185.
110. Matsuoka I, Oda T, Seno S: **The Effect of Oxygen Tension on Tetrazolium Reduction by Respiratory Enzyme Systems of Tissue Culture Cells**. *Acta medicinae Okayama* 1963, **17**:221-230.
111. Allavena P, Germano G, Marchesi F, Mantovani A: **Chemokines in cancer related inflammation**. *Experimental cell research* 2011, **317**(5):664-673.
112. Witsch E, Sela M, Yarden Y: **Roles for growth factors in cancer progression**. *Physiology* 2010, **25**(2):85-101.
113. Hanahan D, Weinberg RA: **The hallmarks of cancer**. *Cell* 2000, **100**(1):57-70.
114. Laoui D, Van Overmeire E, De Baetselier P, Van Ginderachter JA, Raes G: **Functional Relationship between Tumor-Associated Macrophages and Macrophage Colony-Stimulating Factor as Contributors to Cancer Progression**. *Frontiers in immunology* 2014, **5**:489.
115. Mantovani A, Schioppa T, Porta C, Allavena P, Sica A: **Role of tumor-associated macrophages in tumor progression and invasion**. *Cancer metastasis reviews* 2006, **25**(3):315-322.
116. Yigit R, Figdor CG, Zusterzeel PL, Pots JM, Torensma R, Massuger LF: **Cytokine analysis as a tool to understand tumour-host interaction in ovarian cancer**. *Eur J Cancer* 2011, **47**(12):1883-1889.
117. Lu D, Kuhn E, Bristow RE, Giuntoli RL, 2nd, Kjaer SK, Shih Ie M, Roden RB: **Comparison of candidate serologic markers for type I and type II ovarian cancer**. *Gynecologic oncology* 2011, **122**(3):560-566.
118. Clendenen TV, Arslan AA, Lokshin AE, Liu M, Lundin E, Koenig KL, Berrino F, Hallmans G, Idahl A, Krogh V *et al*: **Circulating prolactin levels and risk of epithelial ovarian cancer**. *Cancer causes & control : CCC* 2013, **24**(4):741-748.

119. Mills GB, May C, Hill M, Campbell S, Shaw P, Marks A: **Ascitic fluid from human ovarian cancer patients contains growth factors necessary for intraperitoneal growth of human ovarian adenocarcinoma cells**. *The Journal of clinical investigation* 1990, **86**(3):851-855.
120. Carpenter AE, Jones TR, Lamprecht MR, Clarke C, Kang IH, Friman O, Guertin DA, Chang JH, Lindquist RA, Moffat J *et al*: **CellProfiler: image analysis software for identifying and quantifying cell phenotypes**. *Genome biology* 2006, **7**(10):R100.
121. Stewart S, Ivy MA, Anslyn EV: **The use of principal component analysis and discriminant analysis in differential sensing routines**. *Chemical Society reviews* 2014, **43**(1):70-84.
122. Centurion S: **STATGRAPHICS® Centurion XVI User Manual**. In., vol. 64-bit edition V16.2.04 edn. United States of America: StatPoint Technologies, Inc; 2009.
123. Yaari G, Bolen CR, Thakar J, Kleinstein SH: **Quantitative set analysis for gene expression: a method to quantify gene set differential expression including gene-gene correlations**. *Nucleic acids research* 2013, **41**(18):e170.
124. Woopen H, Pietzner K, Richter R, Fotopoulou C, Joens T, Braicu EI, Mellstedt H, Mahner S, Lindhofer H, Darb-Esfahani S *et al*: **Overexpression of the epithelial cell adhesion molecule is associated with a more favorable prognosis and response to platinum-based chemotherapy in ovarian cancer**. *Journal of gynecologic oncology* 2014, **25**(3):221-228.
125. Sillanpaa S, Anttila MA, Voutilainen K, Tammi RH, Tammi MI, Saarikoski SV, Kosma VM: **CD44 expression indicates favorable prognosis in epithelial ovarian cancer**. *Clinical cancer research : an official journal of the American Association for Cancer Research* 2003, **9**(14):5318-5324.
126. Ross JS, Sheehan CE, Williams SS, Malfetano JH, Szyfelbein WM, Kallakury BV: **Decreased CD44 standard form expression correlates with prognostic variables in ovarian carcinomas**. *American journal of clinical pathology* 2001, **116**(1):122-128.
127. Kulbe H, Hagemann T, Szlosarek PW, Balkwill FR, Wilson JL: **The inflammatory cytokine tumor necrosis factor-alpha regulates chemokine receptor expression on ovarian cancer cells**. *Cancer research* 2005, **65**(22):10355-10362.
128. Singh R, Stockard CR, Grizzle WE, Lillard JW, Jr., Singh S: **Expression and histopathological correlation of CCR9 and CCL25 in ovarian cancer**. *International journal of oncology* 2011, **39**(2):373-381.
129. Johnson EL, Singh R, Singh S, Johnson-Holiday CM, Grizzle WE, Partridge EE, Lillard JW, Jr.: **CCL25-CCR9 interaction modulates ovarian cancer cell migration, metalloproteinase expression, and invasion**. *World journal of surgical oncology* 2010, **8**:62.
130. Epelman S, Lavine KJ, Randolph GJ: **Origin and functions of tissue macrophages**. *Immunity* 2014, **41**(1):21-35.
131. Sica A, Schioppa T, Mantovani A, Allavena P: **Tumour-associated macrophages are a distinct M2 polarised population promoting tumour progression: potential targets of anti-cancer therapy**. *Eur J Cancer* 2006, **42**(6):717-727.
132. Markowska A, Lubin J, Madry R, Markowska J: **Development of antiangiogenic therapies for ovarian cancer**. *European journal of gynaecological oncology* 2013, **34**(4):303-306.
133. Sallinen H, Heikura T, Koponen J, Kosma VM, Heinonen S, Yla-Herttuala S, Anttila M: **Serum angiopoietin-2 and soluble VEGFR-2 levels predict malignancy of ovarian neoplasm and poor prognosis in epithelial ovarian cancer**. *BMC cancer* 2014, **14**:696.
134. Wang L, Liu X, Wang H, Wang S: **Correlation of the expression of vascular endothelial growth factor and its receptors with microvessel density in ovarian cancer**. *Oncology letters* 2013, **6**(1):175-180.
135. Wimberger P, Chebouti I, Kasimir-Bauer S, Lachmann R, Kuhlisch E, Kimmig R, Suleyman E, Kuhlmann JD: **Explorative investigation of vascular endothelial growth factor receptor expression in primary ovarian cancer and its clinical relevance**. *Gynecologic oncology* 2014, **133**(3):467-472.
136. Wendel M, Galani IE, Suri-Payer E, Cerwenka A: **Natural killer cell accumulation in tumors is dependent on IFN-gamma and CXCR3 ligands**. *Cancer research* 2008, **68**(20):8437-8445.

137. Chen G, Goeddel DV: **TNF-R1 signaling: a beautiful pathway**. *Science* 2002, **296**(5573):1634-1635.
138. Allavena P, Mantovani A: **Immunology in the clinic review series; focus on cancer: tumour-associated macrophages: undisputed stars of the inflammatory tumour microenvironment**. *Clinical and experimental immunology* 2012, **167**(2):195-205.
139. Gordon S, Martinez FO: **Alternative activation of macrophages: mechanism and functions**. *Immunity* 2010, **32**(5):593-604.
140. Goustin AS, Leof EB, Shipley GD, Moses HL: **Growth factors and cancer**. *Cancer research* 1986, **46**(3):1015-1029.
141. Balkwill F, Charles KA, Mantovani A: **Smoldering and polarized inflammation in the initiation and promotion of malignant disease**. *Cancer cell* 2005, **7**(3):211-217.
142. Ramakrishnan M, Mathur SR, Mukhopadhyay A: **Fusion-derived epithelial cancer cells express hematopoietic markers and contribute to stem cell and migratory phenotype in ovarian carcinoma**. *Cancer research* 2013, **73**(17):5360-5370.
143. Hindson BJ, Ness KD, Masquelier DA, Belgrader P, Heredia NJ, Makarewicz AJ, Bright IJ, Lucero MY, Hiddessen AL, Legler TC *et al*: **High-throughput droplet digital PCR system for absolute quantitation of DNA copy number**. *Analytical chemistry* 2011, **83**(22):8604-8610.
144. Lane DP, Crawford LV: **T antigen is bound to a host protein in SV40-transformed cells**. *Nature* 1979, **278**(5701):261-263.
145. Linzer DI, Levine AJ: **Characterization of a 54K dalton cellular SV40 tumor antigen present in SV40-transformed cells and uninfected embryonal carcinoma cells**. *Cell* 1979, **17**(1):43-52.
146. Brosh R, Rotter V: **When mutants gain new powers: news from the mutant p53 field**. *Nat Rev Cancer* 2009, **9**(10):701-713.
147. Hollstein M, Hergenhahn M, Yang Q, Bartsch H, Wang ZQ, Hainaut P: **New approaches to understanding p53 gene tumor mutation spectra**. *Mutation research* 1999, **431**(2):199-209.
148. Olivier M, Hollstein M, Hainaut P: **TP53 mutations in human cancers: origins, consequences, and clinical use**. *Cold Spring Harbor perspectives in biology* 2010, **2**(1):a001008.
149. Muller PA, Vousden KH: **Mutant p53 in cancer: new functions and therapeutic opportunities**. *Cancer cell* 2014, **25**(3):304-317.
150. Petitjean A, Achatz MI, Borresen-Dale AL, Hainaut P, Olivier M: **TP53 mutations in human cancers: functional selection and impact on cancer prognosis and outcomes**. *Oncogene* 2007, **26**(15):2157-2165.
151. Canadillas JM, Tidow H, Freund SM, Rutherford TJ, Ang HC, Fersht AR: **Solution structure of p53 core domain: structural basis for its instability**. *Proceedings of the National Academy of Sciences of the United States of America* 2006, **103**(7):2109-2114.
152. Friedler A, DeDecker BS, Freund SM, Blair C, Rudiger S, Fersht AR: **Structural distortion of p53 by the mutation R249S and its rescue by a designed peptide: implications for "mutant conformation"**. *Journal of molecular biology* 2004, **336**(1):187-196.
153. Wong KB, DeDecker BS, Freund SM, Proctor MR, Bycroft M, Fersht AR: **Hot-spot mutants of p53 core domain evince characteristic local structural changes**. *Proceedings of the National Academy of Sciences of the United States of America* 1999, **96**(15):8438-8442.
154. Cho Y, Gorina S, Jeffrey PD, Pavletich NP: **Crystal structure of a p53 tumor suppressor-DNA complex: understanding tumorigenic mutations**. *Science* 1994, **265**(5170):346-355.
155. Kitayner M, Rozenberg H, Kessler N, Rabinovich D, Shaulov L, Haran TE, Shakked Z: **Structural basis of DNA recognition by p53 tetramers**. *Molecular cell* 2006, **22**(6):741-753.
156. Ho WC, Fitzgerald MX, Marmorstein R: **Structure of the p53 core domain dimer bound to DNA**. *The Journal of biological chemistry* 2006, **281**(29):20494-20502.
157. Bullock AN, Fersht AR: **Rescuing the function of mutant p53**. *Nat Rev Cancer* 2001, **1**(1):68-76.
158. Bullock AN, Henckel J, Fersht AR: **Quantitative analysis of residual folding and DNA binding in mutant p53 core domain: definition of mutant states for rescue in cancer therapy**. *Oncogene* 2000, **19**(10):1245-1256.

159. May E, Lasne C, Prives C, Borde J, May P: **Study of the functional activities concomitantly retained by the 115,000 Mr super T antigen, an evolutionary variant of simian virus 40 large T antigen expressed in transformed rat cells**. *Journal of virology* 1983, **45**(3):901-913.
160. Chen Y, Zhang X, Dantas Machado AC, Ding Y, Chen Z, Qin PZ, Rohs R, Chen L: **Structure of p53 binding to the BAX response element reveals DNA unwinding and compression to accommodate base-pair insertion**. *Nucleic acids research* 2013, **41**(17):8368-8376.
161. Guex Nicolas AD, Manuel C. Peitsch , & Torsten Schwede: **Swiss-PdbViewer**. In. Edited by (SIB) SIoB, v4.1 edn; 2012.
162. Joerger AC, Ang HC, Fersht AR: **Structural basis for understanding oncogenic p53 mutations and designing rescue drugs**. *Proceedings of the National Academy of Sciences of the United States of America* 2006, **103**(41):15056-15061.
163. Scian MJ, Stagliano KE, Deb D, Ellis MA, Carchman EH, Das A, Valerie K, Deb SP, Deb S: **Tumor-derived p53 mutants induce oncogenesis by transactivating growth-promoting genes**. *Oncogene* 2004, **23**(25):4430-4443.
164. Muller PA, Vousden KH: **p53 mutations in cancer**. *Nature cell biology* 2013, **15**(1):2-8.
165. Olivier M, Petitjean A, Marcel V, Petre A, Mounawar M, Plymoth A, de Fromentel CC, Hainaut P: **Recent advances in p53 research: an interdisciplinary perspective**. *Cancer gene therapy* 2009, **16**(1):1-12.
166. Guimaraes DP, Hainaut P: **TP53: a key gene in human cancer**. *Biochimie* 2002, **84**(1):83-93.
167. Giaccia AJ, Kastan MB: **The complexity of p53 modulation: emerging patterns from divergent signals**. *Genes & development* 1998, **12**(19):2973-2983.
168. Leroy B, Anderson M, Soussi T: **TP53 mutations in human cancer: database reassessment and prospects for the next decade**. *Human mutation* 2014, **35**(6):672-688.
169. Petitjean A, Mathe E, Kato S, Ishioka C, Tavtigian SV, Hainaut P, Olivier M: **Impact of mutant p53 functional properties on TP53 mutation patterns and tumor phenotype: lessons from recent developments in the IARC TP53 database**. *Human mutation* 2007, **28**(6):622-629.
170. Forbes SA, Bindal N, Bamford S, Cole C, Kok CY, Beare D, Jia M, Shepherd R, Leung K, Menzies A *et al*: **COSMIC: mining complete cancer genomes in the Catalogue of Somatic Mutations in Cancer**. *Nucleic acids research* 2011, **39**(Database issue):D945-950.
171. Feki A, Irminger-Finger I: **Mutational spectrum of p53 mutations in primary breast and ovarian tumors**. *Critical reviews in oncology/hematology* 2004, **52**(2):103-116.
172. Lang GA, Iwakuma T, Suh YA, Liu G, Rao VA, Parant JM, Valentin-Vega YA, Terzian T, Caldwell LC, Strong LC *et al*: **Gain of function of a p53 hot spot mutation in a mouse model of Li-Fraumeni syndrome**. *Cell* 2004, **119**(6):861-872.
173. Ahmed AA, Etemadmoghadam D, Temple J, Lynch AG, Riad M, Sharma R, Stewart C, Fereday S, Caldas C, Defazio A *et al*: **Driver mutations in TP53 are ubiquitous in high grade serous carcinoma of the ovary**. *The Journal of pathology* 2010, **221**(1):49-56.
174. Brachova P, Thiel KW, Leslie KK: **The consequence of oncomorphic TP53 mutations in ovarian cancer**. *International journal of molecular sciences* 2013, **14**(9):19257-19275.
175. Kang HJ, Chun SM, Kim KR, Sohn I, Sung CO: **Clinical relevance of gain-of-function mutations of p53 in high-grade serous ovarian carcinoma**. *PloS one* 2013, **8**(8):e72609.
176. Kim SA, Yoon JA, Kang MJ, Choi YM, Chae SJ, Moon SY: **An efficient and reliable DNA extraction method for preimplantation genetic diagnosis: a comparison of allele drop out and amplification rates using different single cell lysis methods**. *Fertility and sterility* 2009, **92**(2):814-818.
177. Hoogstraat M, de Pagter MS, Cirkel GA, van Roosmalen MJ, Harkins TT, Duran K, Kreeftmeijer J, Renkens I, Witteveen PO, Lee CC *et al*: **Genomic and transcriptomic plasticity in treatment-naive ovarian cancer**. *Genome research* 2014, **24**(2):200-211.
178. Walker DR, Bond JP, Tarone RE, Harris CC, Makalowski W, Boguski MS, Greenblatt MS: **Evolutionary conservation and somatic mutation hotspot maps of p53: correlation with p53 protein structural and functional features**. *Oncogene* 1999, **18**(1):211-218.

179. Dearth LR, Qian H, Wang T, Baroni TE, Zeng J, Chen SW, Yi SY, Brachmann RK: **Inactive full-length p53 mutants lacking dominant wild-type p53 inhibition highlight loss of heterozygosity as an important aspect of p53 status in human cancers**. *Carcinogenesis* 2007, **28**(2):289-298.
180. Jordan JJ, Inga A, Conway K, Edmiston S, Carey LA, Wu L, Resnick MA: **Altered-function p53 missense mutations identified in breast cancers can have subtle effects on transactivation**. *Molecular cancer research : MCR* 2010, **8**(5):701-716.

References

Supplements

1. Concentrations of total **16 tumor growth factors** are compared between miliary and non-miliary metastatic spread types **in ascites**.

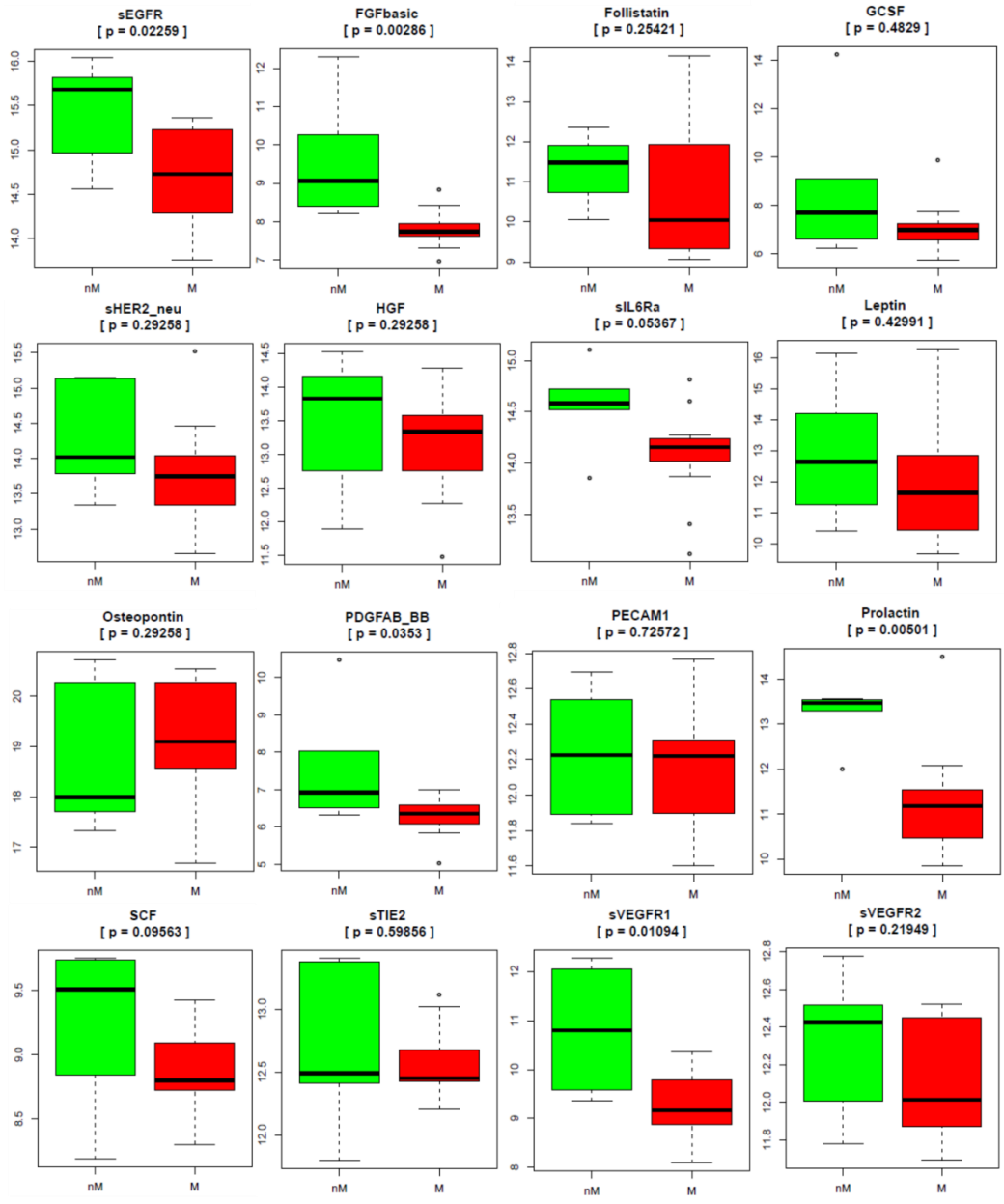

2. Comparison of **40 different cytokine and chemokine** concentrations **in ascites** between miliary and non-miliary metastatic spread types. ►

Supplements

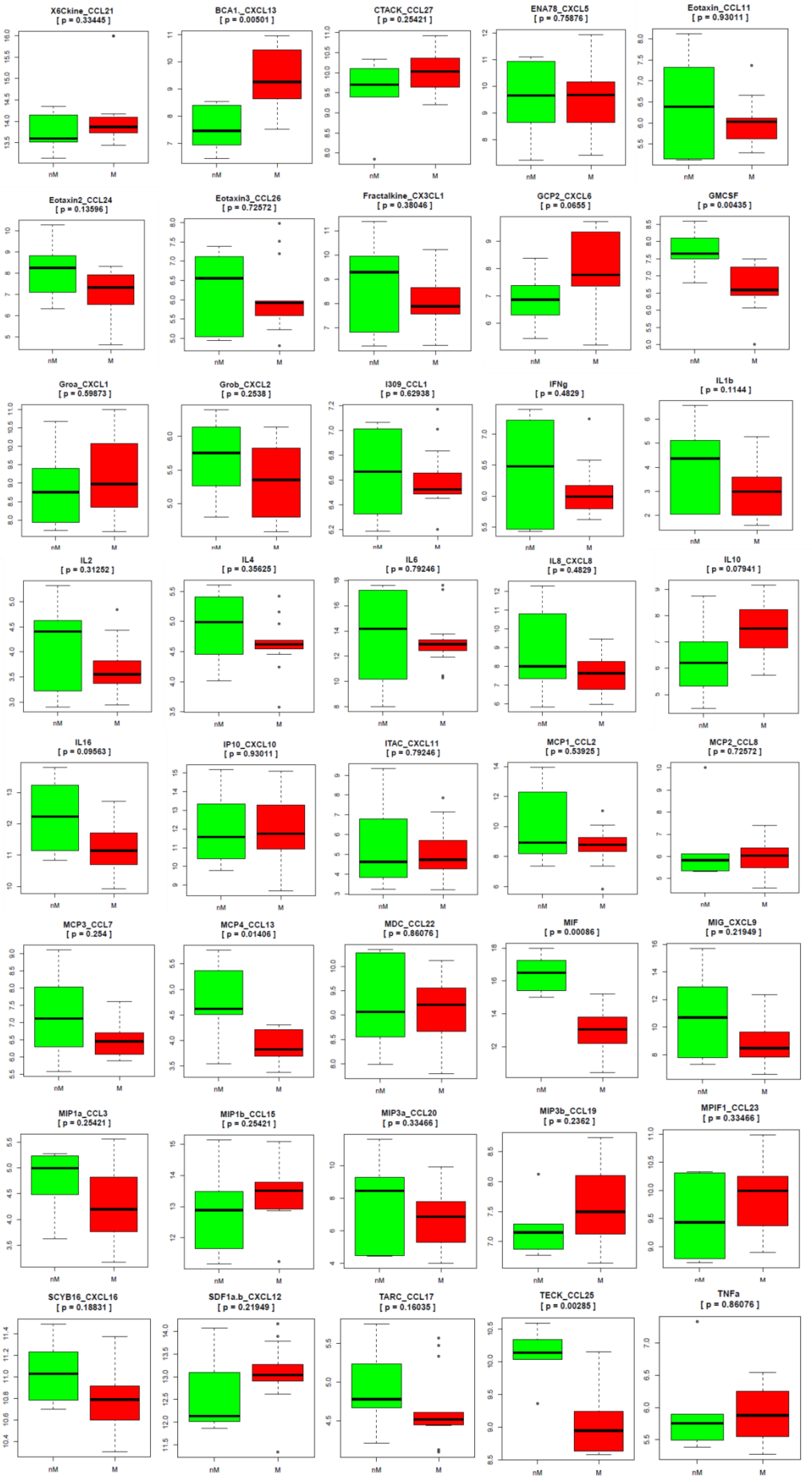

3. Concentrations of total **16 tumor growth factors** are compared between miliary and non-miliary metastatic spread types **in patient sera**.

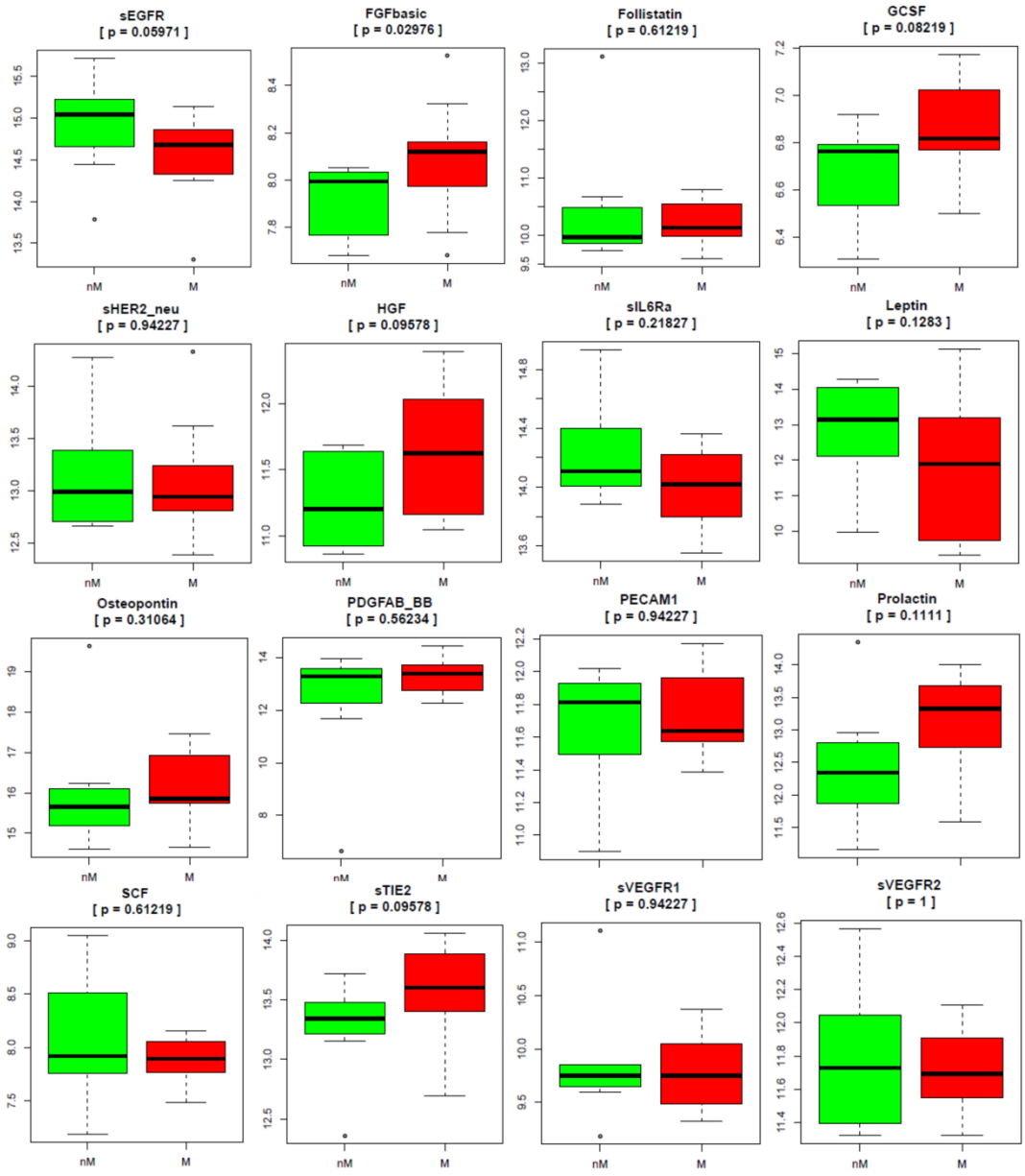

4. Comparison of **40 different cytokine and chemokine** concentrations **in patient sera** between miliary and non-miliary metastatic spread types. ►

Supplements